Fatigue of Masonry Walls with Carbon Fiber Reinforced Polymers (CFRP) Applied Externally for Out-of-Plane Loads

A Thesis

Presented to

the Faculty of California Polytechnic State University

San Luis Obispo, California

In partial fulfillment

of the Requirements for the Degree

Master of Science in Architecture with a Specialization in Architectural Engineering

by

Joseph Louis Williams

August 2009

COMMITTEE MEMBERSHIP

TITLE: for	Fatigue of Masonry Walls with CFRP Applied Externally Out-of-Plane Loads
AUTHOR:	Joseph Louis Williams
DATE SUBMITTED:	August 27, 2009
COMMITTEE CHAIR:	James Mwangi, Ph.D., S.E.
COMMITTEE MEMBER:	Craig Baltimore, Ph.D., S.E.
COMMITTEE MEMBER:	Ravi Kanitkar, S.E.
COMMITTEE MEMBER:	Kevin Dong, S.E.

ABSTRACT

Fatigue of Masonry Walls with CFRP Applied Externally for Out-of-Plane Loads

Joseph Louis Williams

This master's thesis presents an investigation on the effects of fatigue on fiber-reinforced polymers (FRP) when applied to masonry walls subjected to out-of-plane loading. The project aims to provide further research and add to the general testing database of FRP enhanced masonry. An introduction to the problems and solutions associated with unreinforced masonry is discussed along with a literature review on previous testing done in the field of FRP enhanced masonry. The investigation on the effects of fatigue on FRP when applied to masonry walls subjected to out-of-plane loading is performed through experimental testing. A total of four wall specimens (6 ft x 4 ft x 8 in) were constructed. One of the specimens was left unreinforced and used as a baseline for testing while the remaining three specimens were reinforced with carbon fiber reinforced polymer (CFRP) strips designed to take the out-of-plane loads capable of creating the cracking moment in the unreinforced wall. The material testing, construction of the test specimens, and CFRP application are all presented in this thesis.

With the use of an oscillating shake table to generate the out-of-plane loading, the walls were fixed at the base and cantilevered from the shake table. By determining the frequency and amplitude that generated the cracking moment in the baseline unreinforced wall, the remaining three CFRP reinforced walls were tested at the same frequency and amplitude. The results from the testing of the three CFRP reinforced walls are presented along with time histories showing the shake table displacement and wall's tip displacement versus time. In general, fatigue of masonry walls reinforced with CFRP strips can be managed as long as the out-of-plane reinforcement has sufficient strength and development length. Additional findings were made as a result from the testing. The development length of a vertical CFRP strip can be increased by adding a horizontal CFRP strips near the critical section and surface damage to CFRP may have severe consequences.

ACKNOWLEDGEMENTS

I would like to thank Karl Gillette from Edge Structural Composites for generously donating all the CFRP materials used in the experimental testing for my thesis. I would also like to thank the people who helped with the construction and/or testing of the masonry walls: Scott Williams, Blake Williams, Doug Williams, Chris Taylor, and Hunter Kett. I would also like to thank my future employer, Crosby Group, for providing me with a scholarship used to purchase some materials for my thesis. I would like to thank Scott and Andrea Williams for providing me with any additional costs of materials used for my thesis. A special thank you goes to Ray Ward, the Architecture Shop Technician for providing me with all the computer programs used during testing as well as for helping me with the moving and demolition of the test walls. Finally, I would like to thank my advisors, James Mwangi, Craig Baltimore, Ravi Kanitkar, Kevin Dong, and Deborah Wilhelm for their help with the development and review of my thesis.

TABLE OF CONTENTS

LIST OF TABLES

LIST OF FIGURES

LIST OF NOMENCLATURE

A = amplitude, in

A_g = gross cross-sectional area of masonry, in^2

a = acceleration, ft/sec^2

b = width of section, in

b_{FRP} = width of FRP strip, in

c = distance from extreme compression fiber to the neutral axis, in

d = distance from extreme compression fiber to centroid of tension reinforcement, in

E_m = modulus of elasticity of masonry in compression, psi

f = frequency, hertz

F_b = allowable compressive stress available to resists flexure only, psi

F_v = allowable shear stress in masonry, psi

f_b = calculated compressive stress in masonry due to flexure only, psi

f_{FRPu} = FRP capacity in terms of force per unit width as tested or reported by the manufacture, lbs/in

f'_g = specified compressive strength of grout, psi

f'_m = specified compressive strength of masonry, psi

f'_{mortar} = specified compressive strength of mortar, psi

F_p = force due to acceleration of ground motion, lb

f_r = modulus of rupture, psi

f'_{CMU} = specified compressive strength of CMU, psi

f_v = calculated shear stress in masonry, psi

h = height of wall, in

I_{cr} = moment of inertia of cracked cross-sectional area of a member, in^4

I_{eff} = effective moment of inertia, in^4

I_g = moment of inertia of gross cross-sectional area of a member, in^4

j = ratio of distance between centroid of flexural compressive forces and centroid of tensile forces to depth d, in/in

k = stiffness, lb/in

m = mass, lb-sec^2/ft

M = maximum moment at the section under consideration, lb · ft

M_a = maximum moment in member due to applied loading for which deflection is computed, lb · ft

M_{cr} = nominal cracking moment strength, lb · ft

M_n = nominal moment strength, lb · ft

P = axial load, lb

S_g = section modulus of gross sectional area of a member, in^3

t = nominal thickness of member, in

t = time, sec

T_{FRP} = total capacity of FRP strip, lbs

V = shear force, lb

x = displacement, in

ω = angular frequency, rad/sec

ω_n = natural angular frequency, rad/sec

ε_{FRP} = Strain in FRP, in/in

ε_m = Strain in masonry, in/in

LIST OF TERMS

Fatigue: the tendency of a material to break under repeated stress

FRP: fiber reinforced polymers

CFRP: carbon fiber reinforced polymers

Development Length: The minimum length of reinforcement extending beyond the critical section required to develop the design strength of the reinforcement

GFRP: glass fiber reinforced polymers

Table Displacement: The horizontal displacement measured at the base of the shake table

Tip Displacement: The horizontal displacement measured at the top of a wall

URM: unreinforced or under-reinforced masonry

CMU: concrete masonry unit

MSJC: Masonry Standards Joint Committee Code

1.0 PURPOSE

This Master's thesis investigates the effects of fatigue (the tendency of a material to break under repeated stress) on carbon fiber-reinforced polymers (CFRP) when applied to masonry walls subjected to out-of-plane loading. In order to determine the fatigue effects on CFRP and masonry, experiments were performed on specimens of masonry walls with CFRP under simulated forces comparable to those experienced by walls exposed to out-of-plane loads. The simulating force was provided through the use of an oscillating shake table.

Currently, information and experimental testing relevant to fatigue of FRP applied to masonry are scarce. This project aims to provide further research and add to the general testing database of CFRP enhanced masonry.

2.0 INTRODUCTION

Unreinforced and under-reinforced masonry (URM) walls are highly susceptible to failure due to extreme out-of-plane loading as well as failure due to fatigue from out-of-plane loads. Out-of-plane loading on walls can occur when high wind loads, seismic loads, or blast loads arise, causing brittle failure of masonry walls, which may in turn cause detriment to lives and the collapse of masonry structures (Carney and Myers 2003).

Some possible solutions to strengthening URM walls for out-of-plane loading include the following:

- Adding rebar and epoxy grout into vertical drilled holes in URM walls
- Adding an adjacent reinforced concrete wall tied to the existing URM walls
- Adding externally bonded strips fiber reinforced polymers (FRP) to the existing URM walls (U.S. Department of Air Force 2000)

For many cases, adding externally bonded strips of FRP offers the most practical solution for strengthening URM walls. URM walls strengthened with FRP provide high strength for bending and high modulus of elasticity for deflection without introducing added weight to the structure. In addition, using FRP versus other methods to strengthen URM walls reduces both installation cost and down time of the occupied structure while under construction (Hamilton and Dolan 2001).

3.0 BACKGROUND

Fiber reinforced polymers (FRP) are made up of thousands strands of fibers woven together into a fabric. Two main types of FRP are available: glass fiber reinforced polymers (GFRP) and carbon fiber reinforced polymers (CFRP), both of which can be seen in Figure A and Figure B.

Figure A: Glass Fiber Reinforced Polymers[1]

Source: Edge Structural Composites 2003 B

Figure B: Carbon Fiber Reinforced Polymers[1]

Source: Edge Structural Composites 2003 C

[1] Edge Structural Composites
21811 8th St East
Sonoma, CA 95476, USA

The strengths of both GFRP and CFRP vary among proprietors, but generally, CFRP boasts higher tensile strengths and a higher modulus of elasticity than GFRP. Unfortunately, CFRP tends to cost more than GFRP.

The material properties of GFRP and CFRP also vary depending on orientation of the fibers making up the FRP fabric, known as the weave pattern. The two types of FRP weave patterns are unidirectional and bidirectional. A unidirectional FRP has material strength in only one direction parallel to the orientation of fibers, while a bidirectional FRP has material strength in two orthogonal directions.

FRP is applied to masonry using epoxy resins. Epoxy resins are manufactured by FRP proprietors and vary in material properties such as strength, viscosity, bond strength, and cure time. Before the FRP can be applied to masonry, the masonry surface must be prepared. In order to prepare the masonry for the FRP installation, the surface must be cleaned form all contaminants and then lightly roughened with a wire brush or sand blasted. Applying FRP to a prepared masonry surface follows five steps, which may also vary among proprietors (HJ3 Composite Technologies 2001 A). The five steps in the application process are as follows:

1. Apply a primer coat to the prepared masonry surface.
2. Apply a coat of epoxy resin to the still-tacky primed surface.
3. Press the dry or saturated FRP fabric onto the surface without trapping air bubbles.
4. Apply a final coat of epoxy resin on top of the fabric.

5. Apply paint or a protective coating, if desired, while the final resin coat is still tacky.

After the application of the FRP is complete, the final product should cure for ample time, sufficient to completely harden the FRP to the touch. The time in which the epoxy resins cure depends upon the product and the ambient conditions. The cure can last anywhere from 1 to 6 hours. Once the product has been applied, the FRP should not be disturbed for a minimum of 24 hours (QuakeWrap 2008 A).

4.0 LITERATURE REVIEW

The following literature review discusses published experimental research that applies to fiber reinforced polymers (FRP), masonry, and/or out-of-plane loading on masonry walls.

A substantial amount of experimental research has been conducted in the field of applying FRP to unreinforced masonry (URM) to resist out-of-plane loads. In 2001, S. A. Hamoush et al. performed tests on fifteen concrete masonry unit (CMU) wall panels (4 ft x 6 ft x 8 in). Twelve panels were assembled with fiber-reinforcing systems attached to the tension side, and three control panels were left without external reinforcement. Two configurations of external reinforcement were tested. The first reinforcement configuration consisted of two layers of FRP webbing, and the second configuration consisted of vertical and horizontal bands of unidirectional fiber composites. Two methods of surface preparation were tested: sand blasting and wire brushing. Three wall panels were tested for each variable. Each wall panel was tested with a uniformly distributed load applied by airbags. Failure loads, strains in the FRP, out-of-plane deformations, and failure modes were recorded. The tests showed that the flexural strength of masonry walls can be increased if the shear failure is controlled (Hamoush, McGinley, Mlakar, Scott, and Murray 2001).

S. A. Hamoush et al. performed further experimental research in 2002 to build on the findings from their 2001 research. The next set of experiments evaluated the out-of-plane shear strength for masonry walls and the influence of the area of externally bonded

FRP composites on the shear strength of the system. Eighteen CMU wall panels (3 ft x 2 ft x 8 in) were tested for static out-of-plane loads under four-point loading. Nine of the walls were reinforced with two layers of glass fiber reinforced polymers (GFRP) on the tension side of the wall, and the other nine were reinforced with only one layer of GFRP on the tension side. The variables evaluated included three layout configurations and two reinforcement ratios. The failure load, mid-span deflection, and failure modes were all recorded. The tests showed that the out-of-plane shear strength of the CMU walls was constant over all the variables tested. Hamoush concluded that the MSJC code-defined shear strengths may not be as conservative as assumed based on the measured shear strength of the masonry wall specimens (Hamoush, McGinley, Mlakar, Terro 2002).

H. R. Hamilton also performed experimental research on out-of-plane CMU walls with FRP in 2001. Six URM walls (four 6 ft and two 15 ft 4 in tall) were tested in out-of-plane flexure up to capacity. The walls were strengthened with GFRP composite composed of unidirectional glass fabric with an epoxy matrix. The composite was applied to the surface of the masonry using the same epoxy with the fibers oriented perpendicular to the bed joints. General flexural strength design equations from the 1999 MSJC were compared with the results of the testing. Hamilton's experiments found that the equations over-predicted the actual capacity of the test specimens by no more than 20% (Hamilton and Dolan 2001).

While limited experimental research has been conducted on fatigue of FRP applied to masonry, some research has been conducted on the fatigue behavior of

reinforced concrete with FRP. In 2005, Gussenhoven and Breña performed experimental research on the fatigue behavior of reinforced concrete beams strengthened with different FRP laminate configurations. Thirteen concrete beams with carbon fiber reinforced polymer (CFRP) were tested under repeated loads to investigate their fatigue behavior. The beams were strengthened using different thicknesses and widths of CFRP laminates to identify the parameters that would generate different failure modes. Two main fatigue failure modes were identified through testing: fatigue of the steel reinforcement with debonding of the composite laminate and fatigue fracture of the concrete layer below the tension reinforcing steel, also called concrete peel off. The testing results indicate that peak stresses applied to the reinforcing steel in combination with carbon FRP laminate configuration are the main parameters that affect the controlling failure modes (Gussenhoven and Breña 2005). Although Gussenhoven's experiments were performed on reinforced concrete, the testing results might provide a prediction of a possible failure mode that could be expected in experimental research on FRP enhanced masonry. Debonding of the composite laminate would most likely fail FRP enhanced masonry.

5.0 EXPERIMENT

An experiment was conducted to investigate the effects of fatigue on carbon fiber reinforced polymer (CFRP) when applied to masonry walls. This experiment consisted of the testing of four 6ft x 4ft x 8in cantilevered CMU walls: one unreinforced masonry (URM) wall and three walls reinforced with CFRP strips applied to each side of the wall. Surface preparations and FRP application were practiced per the manufacturer's specifications.

The flexural demands on the cantilevered walls determined CFRP reinforcement. This flexural demand was equivalent to the nominal cracking moment strength (M_{cr}) of the URM wall. M_{cr} is the moment at which the wall begins to crack and therefore would engage the FRP reinforcement. The cracking moment of the URM wall was used as the design moment for the FRP reinforcement. The design moment for the FRP reinforcement of the three testing walls used the same maximum moment induced into each wall.

In order to load the walls out of plane, the Pegasus (model # 5622A) shake table, as seen in Figure C, was used to induce the necessary cracking moment for each wall.

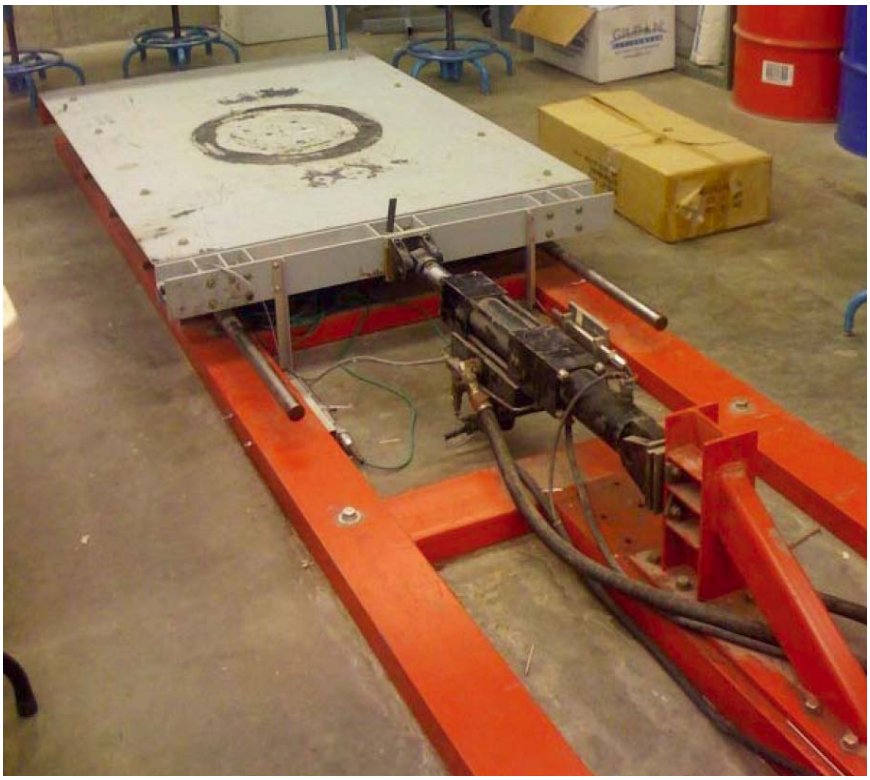

Figure C: Pegasus Shake Figure model # 6622A

Source: Author Photo

The Pegasus shake table is located in the Seismic Lab of the Architectural Engineering Department at California Polytechnic University (Cal Poly), San Luis Obispo, CA.

Each wall was subjected to a sinusoidal oscillation for 5,000 cycles or until failure, due to fatigue. Both the displacement at the top of the wall and the table displacement were measured for the duration of all tests. Both the wall's tip deflection and the table displacement were recorded on a computer for the duration of each test.

5.1 Hypothesis

When an out-of-plane moment is applied to the masonry wall, one side of the wall will be subjected to compression stresses while the other side will have tension stresses. On the tension side of the wall, the externally bonded FRP will experience these tension stresses due to strain compatibility. The critical section of FRP under tension, where failure is expected to occur, is at the mortar joint above the first course of CMU where the section has less moment capacity and the demand is the highest (see Figure D).

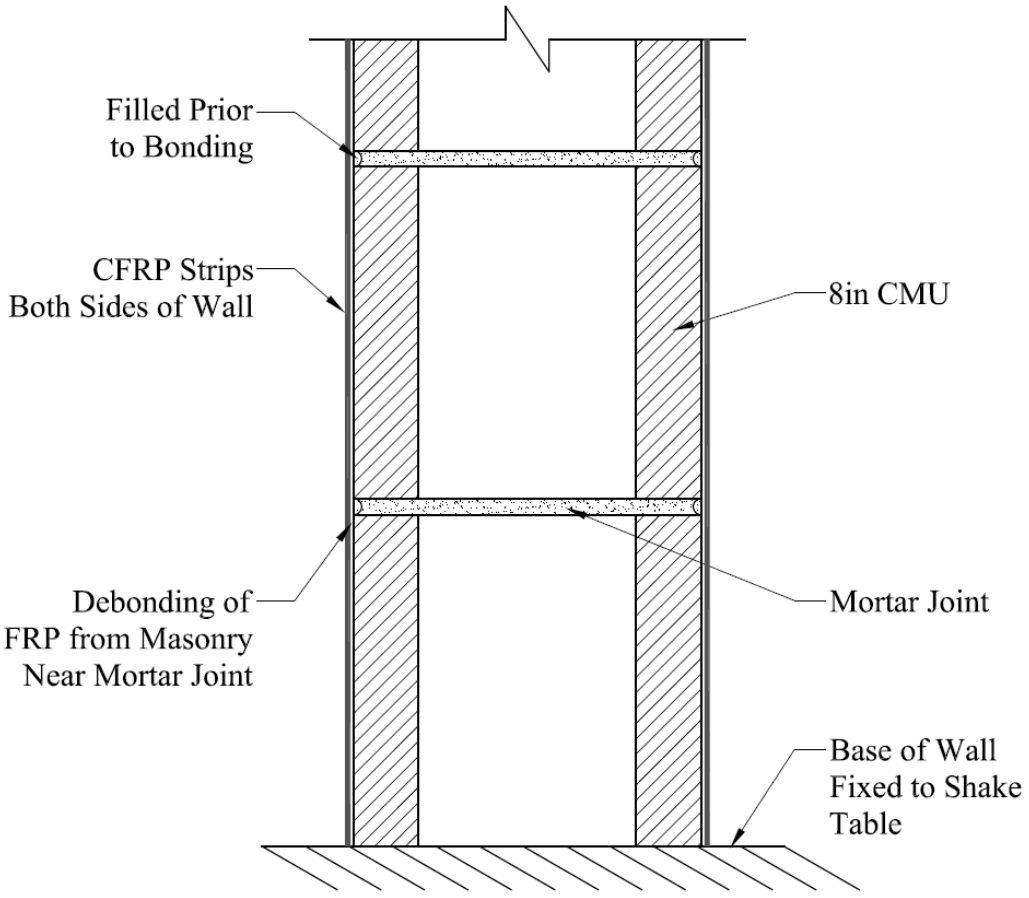

Figure D: Vertical Section of CMU Wall of Suspected Failure at Mortar Joint

Source: Author Diagram

Since the applied moment is highest at the base, the wall will crack at the mortar joint above the first course of CMU when the applied moment reaches the wall's cracking moment. When the wall begins to crack at the mortar joint, the FRP will engaged and will be stressed in tension. The stressed FRP strip will elongate causing the epoxy resin to crack. Under repeated stressing, the FRP strips will continue to elongate and begin to debond from the masonry around the mortar joint. Over a long period of loading and unloading, the FRP will continue to debond and crack causing the masonry wall to lose strength and may even fail due to fatigue.

5.2 Equipment Verification

Before testing of the masonry walls began, the calibration of the Pegasus shake table was verified. In order to verify the calibration of the Pegasus, a LED Based Linear Displacement Sensor (Banner L-Gage model # Q50BVU, see Appendix A for product specifications) was installed to record the displacement of the shake table. The shake table was cycled at different frequencies with 0.5 inch amplitude, the same amplitude used for testing the walls (see section 5.8 Estimation of Wall Loading Input Function).

The input frequency and amplitude of the table were compared to the output frequency and amplitude recorded to investigate any variation in results. The input frequencies and amplitude matched the output with less than 1% difference for frequencies ranging from 0.1 to 10 hertz. When running the table at frequencies greater than 10 hertz, there was a significant drop in amplitude. This drop in amplitude is due to the fact that the shake table does not have sufficient capacity to run at high frequencies with 0.5 inch amplitude.

Although there was a discrepancy in verification results at table frequencies greater than 10 hertz, the table was still adequate for the testing of the masonry walls. The shake table was adequate for testing with a 0.5 inch amplitude because it was determined that accelerations capable of generating the cracking moment of the wall could be achieved with frequencies less than 10 hertz.

5.3 Testing Set Up

Figure E and Figure F show schematics of how each wall was attached to the shake table.

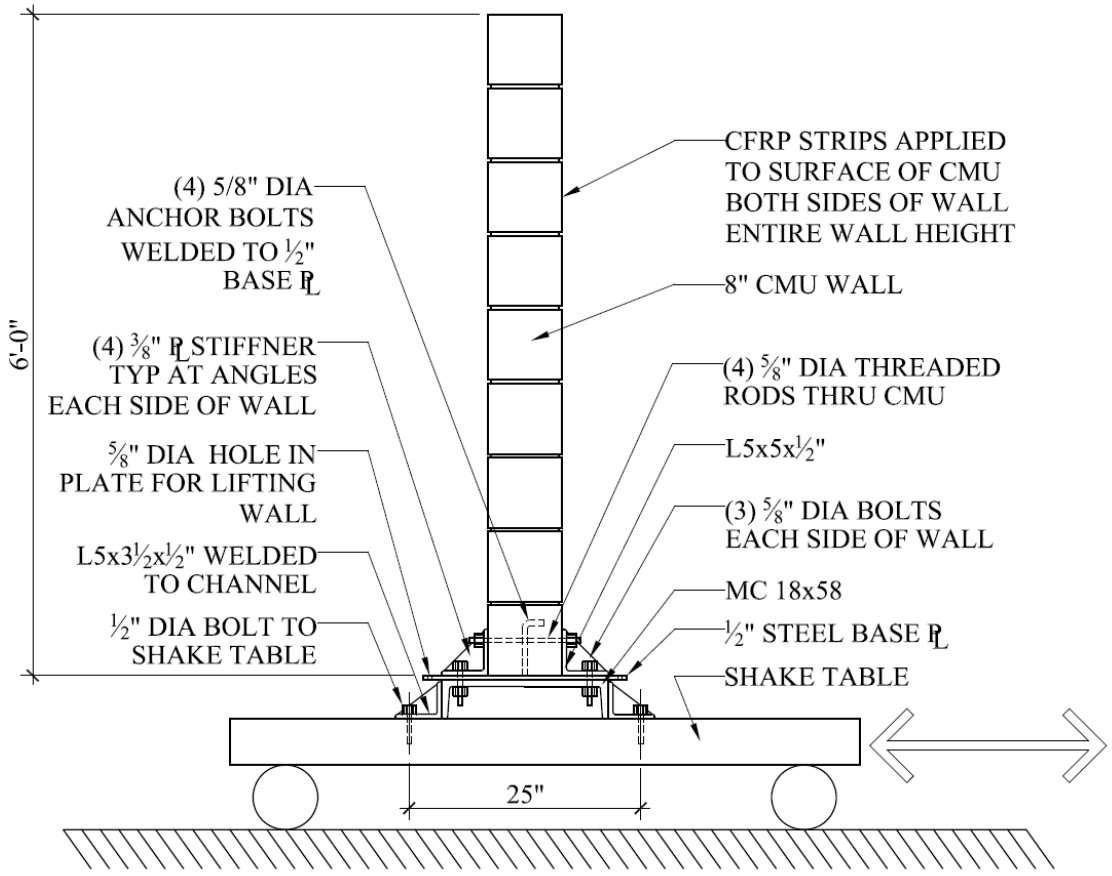

Figure E: Side View of CMU Cantilever Wall Testing Schematic

Source: Author Diagram

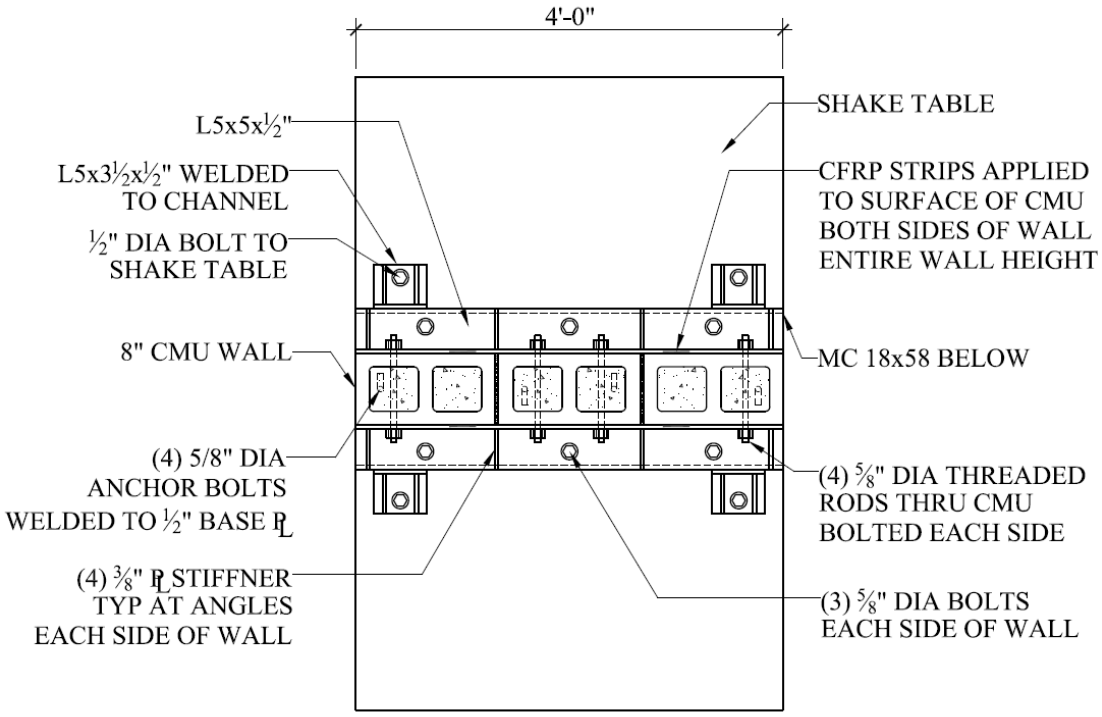

Figure F: Plan View of CMU Cantilever Wall Testing Schematic

Source: Author Diagram

Each wall was constructed on ½" steel plate prefabricated with anchor bolts. The cells of each CMU were fully grouted and cured for 28 days. The walls were then lifted with a forklift onto the shake table. The forks on the forklift were positioned so that they straddled the wall on both sides. Chains were then attached to the holes in the ½" steel plate base beneath the walls, shown in Figure E, and then wrapped around the forklift's forks. The walls were then lifted and positioned into place atop the metal channel on the shake table. Next, metal angles were bolted snug against each side of the wall and to the metal channel. Steel angles welded to the metal channel were then bolted to the shake table.

5.4 Materials

Except as noted below, all materials were either donated or purchased from the manufacturer. The following lists materials used to complete the experiment:

- 8" CMU (f'_{CMU} = 1900 psi) – Purchased from Air Vol Block, Inc., San Luis Obispo, CA
- Mortar (Quikrete Mason Mix Type S Mortar) – Purchased from Air Vol Block
- Grout (Coarse) – Donated by Cal Poly
- CFRP (Velacarb 335 U) – Donated by Edge Structural Composites, Sonoma, CA (Edge Structural Composites 2003 A)
- Epoxy Resin (Veloxx LR) – Donated by Edge Structural Composites, Sonoma, CA (Edge Structural Composites 2003 F)
- ½" Steel Plate – Purchased from Premier Steel, Anaheim, CA
- Steel Angles (L5x5x½ & L5x3.5x½)– Purchased from Premier Steel, Anaheim, CA
- Steel channel (MC18x58) – Purchased from Premier Steel, Anaheim, CA
- General tools used for building provided by the College of Architecture and Environmental Design (CAED) Support Shop at Cal Poly, San Luis Obispo, CA

5.4.1 Material Testing and Properties

In order to determine the strengths and properties of the materials used for the wall construction, four tests were performed. The following is a list of the four tests performed and the material property that was determined:

- Grout Cylinder Test – used to determine the grout compression strength (f'_g)
- Mortar Cube Test – used to determine the mortar compression strength (f'_{mortar})
- Prism Test – used to determine the masonry assemblage compression strength (f'_m)
- Modulus of Rupture Test – used to determine the modulus of rupture (tension strength) of the masonry assemblage (f_r)

The procedure and results for each of the test are given in this section.

5.4.1.1 Grout Cylinder Test

In order to determine the grout compression strength, grout cylinder tests were performed on samples of the grout used to construct the walls. The grout mix design used for testing was in accordance with MSJC recommendations for Grout Proportions by Volume for coarse grout and shown in Table A (MSJC 2008).

Table A: Coarse Grout Proportions by Volume per MSJC

Coarse Grout Proportions by Volume Used for Testing			
Grout Type	Cement	Aggregate	
		Coarse	Fine
Coarse	1	1.5	2.625

The dry ingredients were placed in a concrete mixer and were mixed together. Water was added until the mix achieved a consistency that had an 10 inch slump. Three samples of the coarse grout mix were then prepared per ASTM C1019. The samples were placed in 6 inch diameter by 12 high plastic cylinder molds. The grout cylinders

were allowed to dry cure for 28 days in order to reach ultimate strength. The grout samples are shown in Figure G.

Figure G: Grout Cylinder Samples

Source: Author Photo

Once the samples were released from their molds, the ultimate compressive strength was determined for each sample using the Forney Testing Machine (model # 00-50-106) shown in Figure H.

Figure H: Forney Testing Machine used for Grout Cylinder Test

Source: Author Photo

Each grout cylinder was placed in Forney Testing Machine where the cylinders were subjected to axial load. The axial load was increased until the cylinders crushed, shown in Figure I.

Figure I: Crushed Grout Cylinder

Source: Author Photo

The ultimate load that crushed the cylinders was then recorded and the ultimate stress, f'_g, was calculated by dividing the ultimate load by the area of the cylinder. The results from the grout cylinder tests are presented in Table B.

Table B: Results from Grout Cylinder Test

Results from Grout Cylinder Test			
Cylinder #	Ultimate Load, P (lbs)	Area = π(dia.)^2/4, A (in^2)	f'_g = P/A (psi)
1	119000	28.27	4209
2	96000	28.27	3395
3	116000	28.27	4103

The mean grout compressive strength from the three tests was, f'_g = 3902 psi. This mean f'_g from testing is comparable to the mean f'_g tabulated in Table C-8 of the

MSJC. The MSJC gives three mean grout compressive strengths from three different tests as follows: f'_g = 3106 psi, 4145 psi, and 5455 psi (MSJC 2008). The f'_g = 3902 psi from testing is between the acceptable compression strengths in the MSJC.

5.4.1.2 Mortar Cube Test

In order to determine the mortar compression strength, mortar cube tests were performed on samples of the mortar used to construct the walls. The mortar cube test, per ASTM C109/C109M, required the preparation of 2 in x 2 in x 2 in samples of mortar that were tested for their ultimate compressive strength. The mortar mix used for testing was Quikrete Mason Mix Type S Mortar. The mortar mix was mixed with the specified quantity of water per the Quikrete specifications. Three samples of the type S mortar were prepared and placed in 2 inch mortar cube molds made out of plywood. The mortar cubes were allowed to dry cure for 28 days. The mortar cubes are shown in Figure J.

Figure J: Mortar Cubes

Source: Author Photo

Once the samples were released from their plywood molds, the ultimate compressive strength was determined for each sample using the Riehle Universal Testing Machine (model # FS-3600) shown in Figure K.

Figure K: Riehle Universal Testing Machine used for Mortar Cube Test
Source: Author Photo

Each mortar cube was placed in Riehle Universal Testing machine where the cubes were subjected to axial load. The axial load was increased until the cubes crushed, shown in Figure L.

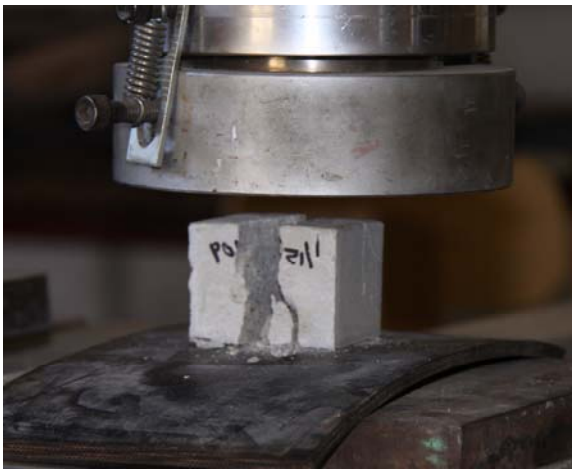

Figure L: Crushed Mortar Cube

Source: Author Photo

The ultimate load at which the mortar cubes crushed was then recorded and the ultimate stress, f'_{mortar}, was calculated by dividing the ultimate load by the area of the cube. The results from the mortar cube test are presented in Table C.

Table C: Results from Mortar Cube Test

Results from Mortar Cube Test			
Cube #	Ultimate Load, P (lbs)	Area = 2 in x 2 in, A (in^2)	$f'_{mortar} = P/A$ (psi)
1	9350	4	2338
2	9950	4	2488
3	10800	4	2700

The mean mortar compressive strength from the three tests was, $f'_{mortar} = 2508$ psi.

5.4.1.3 Prism Test.

In order to determine the compression strength of the masonry assemblage, prism tests were performed on masonry prisms constructed with samples of the CMU, mortar, and grout used to construct the walls. Three prisms were constructed, per ASTM C1314, using 8" x 8" x 16" CMU's, three courses high, bonded with Type S mortar, and then fully grouted with the course grout. The masonry prisms were allowed to dry cure for 28 days, after the grout was placed, in order to reach ultimate strength. In order to have enough prisms for the modulus of rupture test, the prisms were cut in half vertically using a wet cutting masonry saw. One half of each of the three prisms was used for the prism test and the other half was saved to be used for the modulus of rupture test, discussed later.

The ultimate compressive strength for each half prism was determined using the Riehle Universal Testing Machine (model # FS-3600) shown in Figure M.

Figure M: Riehle Universal Testing Machine used for Prism Test

Source: Author Photo

Each prism was placed in Riehle Universal Testing machine where the prisms were subjected to axial load. The axial load was increased until the prisms crushed, shown in Figure N.

Figure N: Crushed Masonry Prism

Source: Author Photo

The ultimate load at which the prisms crushed were then recorded, and the ultimate stress, f'_m, was calculated by dividing the ultimate load by the area of the prism. The results from the prism test are presented in Table D.

Table D: Results from Prism Test

Results from Prism Test			
Prism #	Ultimate Load, P (lbs)	Area = $7^5/_8$ in x $7^5/_8$ in, A (in^2)	$f'_m = P/A$ (psi)
1	94000	58.14	1617
2	89000	58.14	1531
3	82500	58.14	1419

The mean compressive strength from the three prism tests was, f'_m = 1522 psi. This mean f'_m from testing is very comparable to that tabulated in Table 2 of the MSJC. For a CMU with compressive strength equal to 1900 psi, with Type S mortar, and fully grouted, the MSJC gives a f'_m equal to 1500 psi. Therefore the f'_m from testing is only 1.47% higher than that tabulated in the MSJC.

5.4.1.4 Modulus of Rupture Test

In order to determine the modulus of rupture of the masonry assemblage, the Modulus of Rupture Test was performed per ASTM C1072 on three specimens of the masonry prisms. The Modulus of Rupture Test was conducted by applying an eccentric axial load (P) to the masonry prism as shown in Figure O.

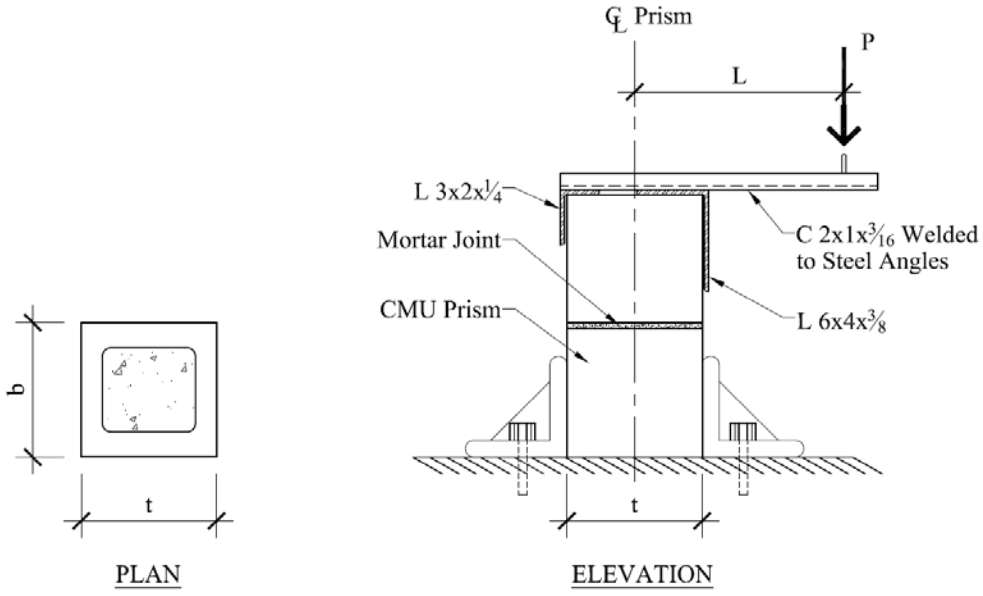

Figure O: Modulus of Rupture Test Schematic

Source: Author Diagram

The eccentric load causes the prism to be under combined axial and bending stresses. Once the modulus of rupture is reached in the prism, the prism fails in flexure. The modulus of rupture (f_r) for the masonry assemblage can then be calculated by determining the flexural stress in the prism at the applied failure load. The flexural stress in the prism is given by the combined stress equation from ASTM C1072:

$$f_r = \frac{6PL}{bt^2} - \frac{P}{bt} \qquad \text{Eq. 1}$$

where P is the applied load

L is the distance from the center line of the prism to the load point

b is the width of the prism section

t is the thickness of the prism section

In equation 1, the flexural stress is calculated by summing the stress due the axial load with the stress due to the moment caused by eccentric loading. It is noted that tension stress is taken to be positive, hence the negative sign in front of the axial term in equation 1.

Three of the masonry prisms left over from the prism test were then cut down with a wet cutting masonry saw so that the prisms were two CMU's high. The prisms were then subjected to the eccentric axial load with the use of the Riehle Universal Testing Machine (model # FS-3600) shown in Figure P.

Figure P: Riehle Universal Testing Machine used for Modulus of Rupture Test
Source: Author Photo

Figure N shows the masonry prism placed in the testing machine. The bottom coarse of the prism was fixed to the base of the machine. An apparatus was created by welding a steel channel to the top of two angles, and was then clammed to the top of the prism in order to apply the eccentric load. The eccentric axial load was applied at a distance 8 inches from the edge of the prism. The applied load was increased until the prisms failed in flexure, shown in Figure Q.

Figure Q: Prism Failing in Flexure

Source: Author Photo

As seen above, the prism fails in flexure at the mortar joint where the applied eccentric load induces the cracking moment in the prism section. The ultimate load at which each prism failed was recorded and the modulus of rupture was calculated using Equation 1. The results from the modulus of rupture test are presented in Table E.

Table E: Results form the Modulus of Rupture Test

Results from Modulus of Rupture Test					
Prism #	Ultimate Load P (lbs)	L (in)	width b (in)	Thickness t (in)	f_r (psi)
1	1865	11.81	7.625	7.625	266
2	2175	11.81	7.625	7.625	310
3	1820	11.81	7.625	7.625	260

The mean modulus of rupture from the three tests was, f_r = 280 psi, and was used to determine the cracking moment of the URM wall for the experiment. The modulus of rupture from testing is much higher than that tabulated in Table 3.1.8.2.1 in the MSJC. The MSJC gives an allowable f_r equal to 200 psi, parallel to bed joints for fully grouted hollow units, with type S mortar, in a running bond (MSJC 2008). Therefore, the f_r from testing is 40% higher than that tabulated in the MSJC.

5.5 CFRP Design

The design of the CFRP strengthening system was based on the strength design approach, allowed by the Masonry Standards Joint Committee (MSJC 2008). The strength design approach is very practical for FRP design since FRP suppliers provide ultimate tensile strength for their composite system as part of their manufacturer product information. The ultimate tensile strength can be used in limiting the amount of reinforcing used as well as capacity prediction.

5.5.1 Strength Equations for FRP Design

Before discussing the out-of-plane CFRP design for the URM walls, the derivation for the nominal moment capacity for masonry reinforced with FRP is shown. The derivation is a simplified analytical method based on the following five assumptions:

- Linear stain distribution through the full depth of the wall
- Small deformations
- No tensile strength in the masonry block
- No slip between the FRP and the masonry wall
- Plane sections remain plane (Hamoush, McGinley, Mlakar, and Terro 2002)

To derive the strength equations for the flexural design of the FRP enhanced masonry walls, a free body diagram of the cross section of the masonry wall was analyzed. Figure R is a labeled cross section of a masonry wall reinforced with FRP.

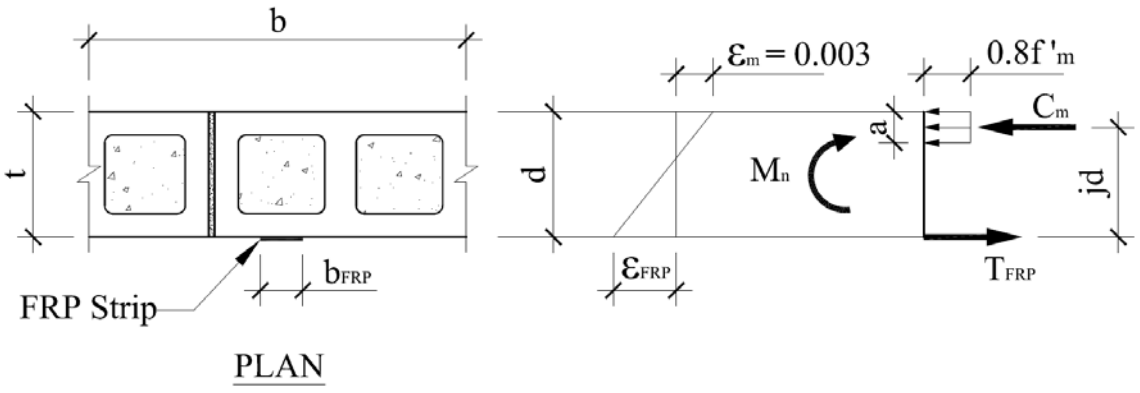

Figure R: Derivation of Strength Equations for FRP Reinforcements

Source: Author Diagram

The stress-strain relationship of the FRP was considered to be linear elastic, while the stress-strain relationship of the masonry is modeled as an idealized uniform stress block. The maximum stress in the idealized stress block was taken to be 80% of f'_m based on the equation 3-28 in the MSJC (MSJC 2008). The ultimate compression strain in the masonry was assumed to be 0.003.

Displayed on the right side of Figure R, are the internal wall forces, at capacity, for a CMU wall externally reinforced with FRP. Because of the small thickness of the FRP relative to the thickness of the wall, the effective depth d will be taken as equal to the specified wall thickness t (d = t). The effective width, b corresponds to the spacing of the FRP reinforcing along the length of the wall. It shall be noted that the effective flange width is limed due to shear lag. Based of the MSJC, the spacing of reinforcement shall be limited to 6 times the nominal wall thickness, or 72 inches maximum (MSJC 2008).

By summing the moments created by the internal wall forces to zero at the compression resultant force, C_m, the equation for predicting the flexural capacity of the wall section is as follows:

$$M_n = T_{FRP}\left(d - \frac{a}{2}\right) \quad \text{Eq. 2}$$

$$a = \frac{T_{FRP}}{0.8 f'_m b} \quad \text{Eq. 3}$$

where M_n is the nominal moment capacity in flexural bending

T_{FRP} is the FRP strip capacity

a is the depth of the equivalent stress block for masonry in compression

The strip capacity can also be expressed as:

$$T_{FRP} = b_{FRP}\left(f_{FRPu}\right) \quad \text{Eq. 4}$$

where b_{FRP} is the width of the FRP strip

f_{FRPu} is the FRP capacity in terms of force per unit width

Equations 2, 3 and 4 are used to determine a reinforced section's nominal moment capacity. In order for these equations to be used for design, there needs to be an estimate of the width of the FRP strip (b_{FRP}). To estimate b_{FRP}, the moment arm (jd) between the internal compression and tension forces must be assumed. For tension controlled sections (where the FRP fails in tension before the masonry crushes), it is assumed that j ranges from 0.9 to 0.95. Therefore, b_{FRP} can be estimated using equation 5.

$$b_{FRP} = \frac{M_n}{jd f_{FRPu}} \quad \text{Eq. 5}$$

Once the width of the FRP strips is estimated, the nominal moment capacity on the masonry section under consideration can be determined using equations 2, 3, and 4. If the nominal moment capacity is greater than the design moment, then the section is adequate.

5.5.2 Nominal Cracking Moment

In order to determine the required CFRP reinforcement for the walls, the moment (M_a) must be determined. The applied moment for the experiment was based on the cracking moment (M_{cr}) of the wall. Therefore M_a is equal to M_{cr}. To determine M_{cr} of the wall, the modulus of rupture (f_r) was determined based by experimental testing discussed in section 5.4.1.4. The modulus of rupture normal to the bed joint for full grouted CMU's with Type S mortar was determined to be, $f_r = 280$ psi. Assuming tension being positive and the masonry wall remains elastic until cracking occurs, the cracking moment was determined using the equation:

$$f_r = \frac{M_{cr}}{s_g} - \frac{P}{A_g} \qquad \text{Eq. 6}$$

where P is the dead load of the wall (estimated at 10 psf per in of masonry)

A_g is the gross cross-section area of the masonry wall

S_g is the section modulus of gross sectional area of the masonry wall

Eq. 6 is the combined stress equation for a member undergoing elastic bending and compression. Solving Eq. 6 for M_{cr}, the results are as follows:

$$M_{cr} = S_g\left(\frac{P}{A_g} + f_r\right)$$

$$M_{cr} = \frac{(48in)\times(7.625in)^2}{6}\left[\frac{1920lbs}{(48in)\times(7.625in)} + 280\,psi\right]\left(\frac{1\,ft}{12in}\right) = \boldsymbol{11{,}053\ lb\cdot ft}$$

The cracking moment for the unreinforced wall is 11,053 lbs-ft. This moment will be the maximum applied moment the walls will undergo during the fatigue test and will be used to size the CFRP reinforcement for the experiment reinforced walls.

5.5.3 Flexural Design of CFRP for Experiment

The product information for the VELA-CARB 335 CFRP, used in the experiment, was provided by Edge Structural Composites and is shown in Figure S.

VELA-CARB 335U

VelaCarb 335U is a Pan based dry, unidirectional carbon fiber fabric that is field-impregnated with **Veloxx LR** laminating resin to create a carbon fiber reinforced polymer (CFRP) laminate. **VelaCarb** fabrics are produced under ISO 9002 standards.

VelaCarb 335U is a patented, ICBO/ICC-ES approved (ER #5836) part of the FiberBond™ Strengthening System, a highly engineered product for strengthening concrete and masonry structures.

For most applications **VelaCarb 335U** is a proven cost effective alternative to traditional strengthening techniques.

General information		
Color	Black	
Primary Fiber Direction	0° (unidirectional)	
Flame Spread Index (1) [ASTM E84]	25 (Class 1)	
Typical Fiber Properties		
Fabric areal weight density	9.8 oz/yd^2	335 g/m^2
Fabric thickness per ply (2)	0.00689 in^2 per in	1.75 cm^2 per m
Tensile Strength	650,000 psi	4,480 MPa
Modulus of Elasticity	34x10^6 psi	234,400 MPa
Elongation at Break	1.9%	1.9%
Cured Laminate Properties for Design		
Average thickness per ply	0.023 in	0.584 mm
Tensile Strength (3) [ASTM D3039]	150,000 psi	1,035 MPa
Modulus of Elasticity [ASTM D3039]	10.1 x 10^6 psi	70,000 N/mm^2
Elongation at Break (3) [ASTM D3039]	1.5%	1.5%
Strength per unit width [per ply]	3450 lbs/in	600 kN/m
Shear Bond Strength [Concrete failure]	680 psi	4-68 N/mm^2
Notes		
(1) Tests conducted on fully cured samples of VelaCarb 335U without a protective coating. (2) Fabric thickness is based on the area of fibers. (3) Properties are statistically based and can be used for design without further reductions		

Figure S: VELA-CARB 335U Product Information

Source: Edge Structural Composites 2003 A

As seen in the Figure Q, the ultimate strength per unit width (f_{FRPu}) for the VELA-CARB 335U is 3450 lbs/in. This value was used in determining the required CFRP reinforcement for the flexural strengthening of the URM walls for the experiment.

In order to design the CFRP, the width of CFRP (b_{FRP}) required was estimated. To estimate b_{FRP}, the moment arm between the internal compression and tension forces is jd, where j was assumed to be 0.93. By using Equation 5, the width of CFRP required to withstand the wall's cracking moment was determined as follows.

$$b_{FRP} = \frac{M_{cr}}{j d f_{FRPu}} = \frac{11053\,lb \cdot ft}{0.93 \times 7.625in \times 3450lb/in} \times \frac{12in}{ft} = \mathbf{5.42\,in}$$

The required width of FRP was determined to be 5.42 inches. If two equally spaced, 3 inch strips of FRP were used, then the total width would be 6 inches, which is greater than 5.42 inches. Therefore, the wall section's nominal moment capacity was checked assuming two 3 inch strips CFRP. To determine the nominal moment capacity of the wall, equations 2, 3, and 4 were combined as follows.

$$M_n = b_{FRP}\, f_{FRPu}\left(d - \frac{b_{FRP}\, f_{FRPu}}{2\left(0.8 f'_m\, b\right)} \right) \qquad \text{Eq. 7}$$

Using the Equation 7, the nominal moment capacity of the 4 ft wide, 8 inch CMU wall reinforced with two 3 inch strips of VELA-CARB 335U is:

$$M_n = (2 \times 3in)(3450\,lbs/in)\left(7.625\,in - \frac{(2 \times 3in)(3450\,lbs/in)}{2(0.8 \times 1522\,psi \times 48\,in)} \right) \times \frac{1\,ft}{12in} = \mathbf{12{,}843\,lb \cdot ft}$$

Since the M_n for two 3 inch strips is equal to 12,843 lb-ft and is greater than 11,053 lb ft, the applied M_{cr}, the section is deemed adequate. Therefore, the three reinforced CMU walls that will be tested will be reinforced as shown in Figure T.

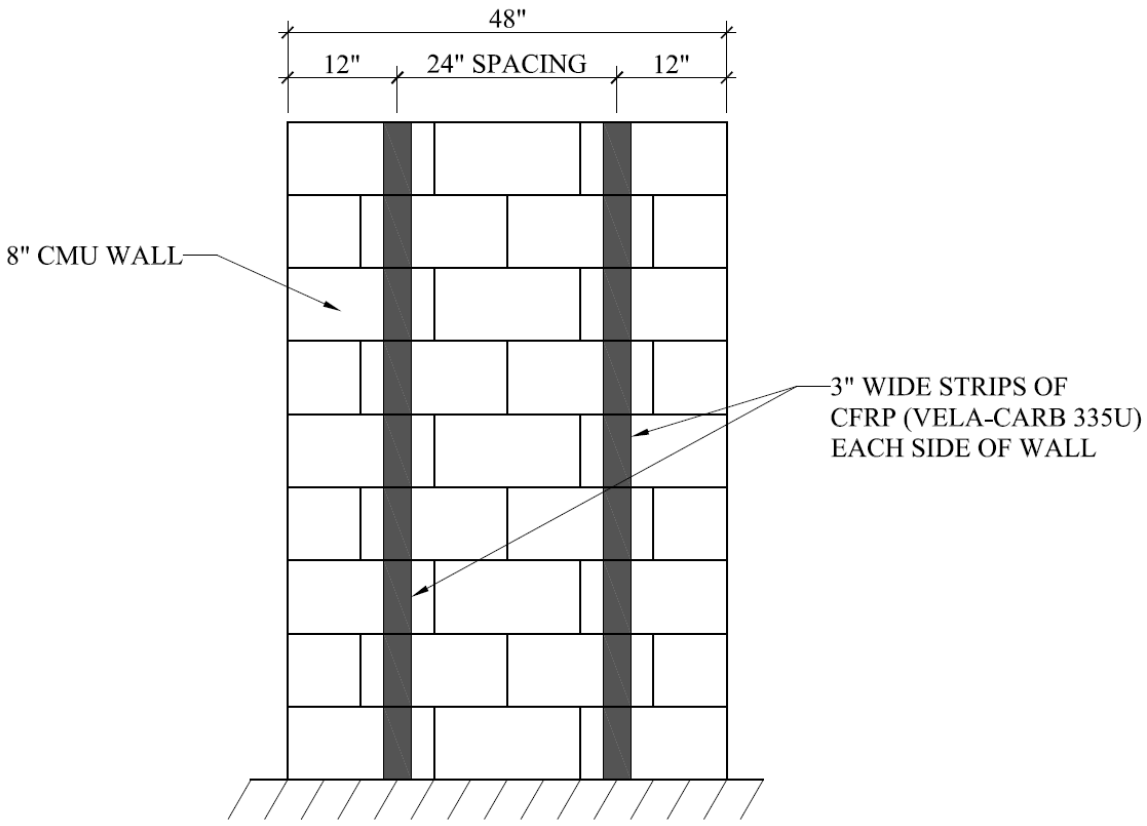

Figure T: Wall Elevation of CFRP Reinforcement Configuration

Source: Author Diagram

The two CFRP strips will be spaced evenly at a 24” on each side of the walls. The spacing is typical of standard vertical wall reinforcement and meets the shear lag requirements previously discussed. Both strips are placed the full height of the wall to ensure that the walls have the same out of plane stiffness for the entire wall height.

5.6 Wall Construction

In this section, a detailed procedure of the masonry wall construction of the test specimens is described. It is noted that all four of the wall test specimens were constructed with the same materials and labor. The masonry construction techniques used to construct the walls are typical of that practiced in the masonry industry.

5.6.1 Base Plate Preparation

Prior to laying the first course of CMU, $^{5}/_{8}$ inch diameter anchor bolts were fastened to the ½ inch steel base plates as shown in Figure U.

Figure U: Base Plate with Anchor Bolts

Source: Author Photo

There were four anchor bolts spaced evenly for each wall that were welded to the steel base plates with a ½ inch fillet welds. The anchors were placed at the center line of the walls, and were designed to transfer the out of plane wall shear, in order to create a fixed condition at the first course during testing.

5.6.2 Laying CMU

In order to attach the first course of CMU, an all purpose construction adhesive (PL Premium) was used to bond the CMU's to the base plate. The adhesive provided a semi-fixed connection at the base of the walls prior to their grouting. The application of the adhesive, along with the final laying of the first course, is shown in Figure V.

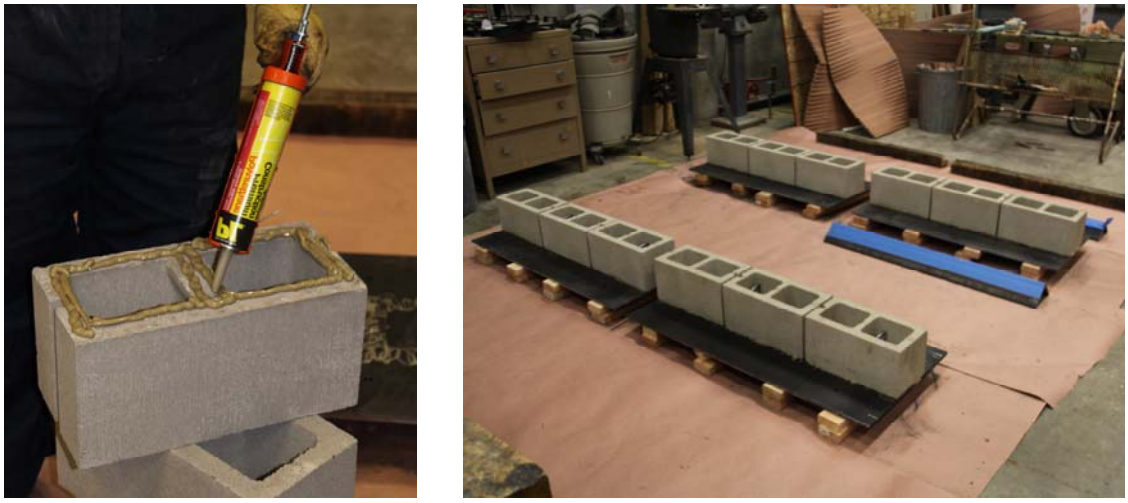

Figure V: Wall Construction - Laying First Course

Source: Author Photo

The picture on the left shows how the adhesive was applied generously to the underside of each CMU. The CMU's were then placed on the centerline of the steel

plates. After the first course was complete, the adhesive was allowed to sit for 24 hours prior to laying the next course of CMU.

Once the first course was secured, the remaining 8 courses were laid. Batches of mortar were made with Quikrete Mason Mix Type S Mortar. The mortar was then applied to the bed joint as shown in Figure W.

Figure W: Application of Mortar to CMU

Source: Author Photo

With the use of a mason's trowel, the mortar was applied evenly over the entire top side of a course of CMU's as shown above. The next course of CMU's was then placed atop the mortar bed joint as shown in Figure X.

Figure X: Laying a course of CMU

Source: Author Photo

Each CMU was carefully set atop bed joint and positioned into place by tapping the top and sides of the CMU with the mason trowel. The vertical mortar head joints were created by adding mortar to the ends of the CMU's prior to positioning them on the bed joint. In order to ensure the walls were kept to the proper dimensions during construction, all mortar joints between the CMU's were measured to be $^{3}/_{8}$", and with the use of a level, all CMU's were leveled in and out of plane of the wall. The process of laying the mortar and CMU's continued until the walls reached their full height of nine courses. At this point the mortar was allowed to cure for seven days in order to gain strength.

5.6.3 Grouting Walls

Prior to grouting the walls, threaded rods were added at the base of each wall as shown in Figure Y.

Figure Y: Threaded Rods at Base of Walls

Source: Author Photo

In order to create a fixed end condition with the wall to the shake table during testing, threaded rods were used to create a fixed base connection at the base of the wall. With the use of the metal angles as a template, four holes were drilled into the bottom course and threaded rods were put through the walls.

The grout was mixed in accordance to the proportions in Table A titled "Coarse Grout Proportions by Volume per MSJC." Once the grout was fully mixed, the grout was placed in accordance with the MSJC. A trough was positioned over the walls and the grout was placed with a five gallon bucket, as shown in Figure Z.

Figure Z: Grouting the CMU Walls

Source: Author Photo

The five gallon buckets were filled with grout, lifted above the wall, and poured into the CMU cells. This process continued until the grout reached the top of the cells. Once the walls were fully grouted, the grout was then consolidated in accordance with the MSJC, section 3.5 E. The consolidation was achieved with the use of a concrete electric vibrator as shown in Figure AA.

Figure AA: Consolidating Grout

Source: Author Photo

The electric vibrator was placed at the bottom the cells and set for ten seconds. Then the vibrator was lifted out of the cells at a rate of three inches per second. With the use of the vibrator, the grout was ensured to be consolidated at the full height of the wall. This was very important to ensure that there were no weak points in the wall and the cracking moment for the wall was the same over the full height.

5.7 CFRP Installation

The installation process of the VELA-CARB 335U CFRP reinforcement was performed to the manufacture's specifications and recommendations. Three of the four test specimen walls were reinforced with two 3 inch strips as previously designed. The following steps were performed for each of the three walls in order to install the CFRP:

- Surface Preparation
- Cut carbon fabric strips to required width
- Primer surface with epoxy
- Saturate carbon fabric with epoxy
- Apply strips to wall

5.7.1 Surface Preparation

Before the CFRP could be applied to the walls, the surface between the CFRP and the masonry was prepared. In order for the CFRP to completely adhere to the masonry, the surface was abraded to smooth out all irregularities and remove any contaminants. First, the mortar joints were made smooth with the use of an electric grinder as seen in Figure BB.

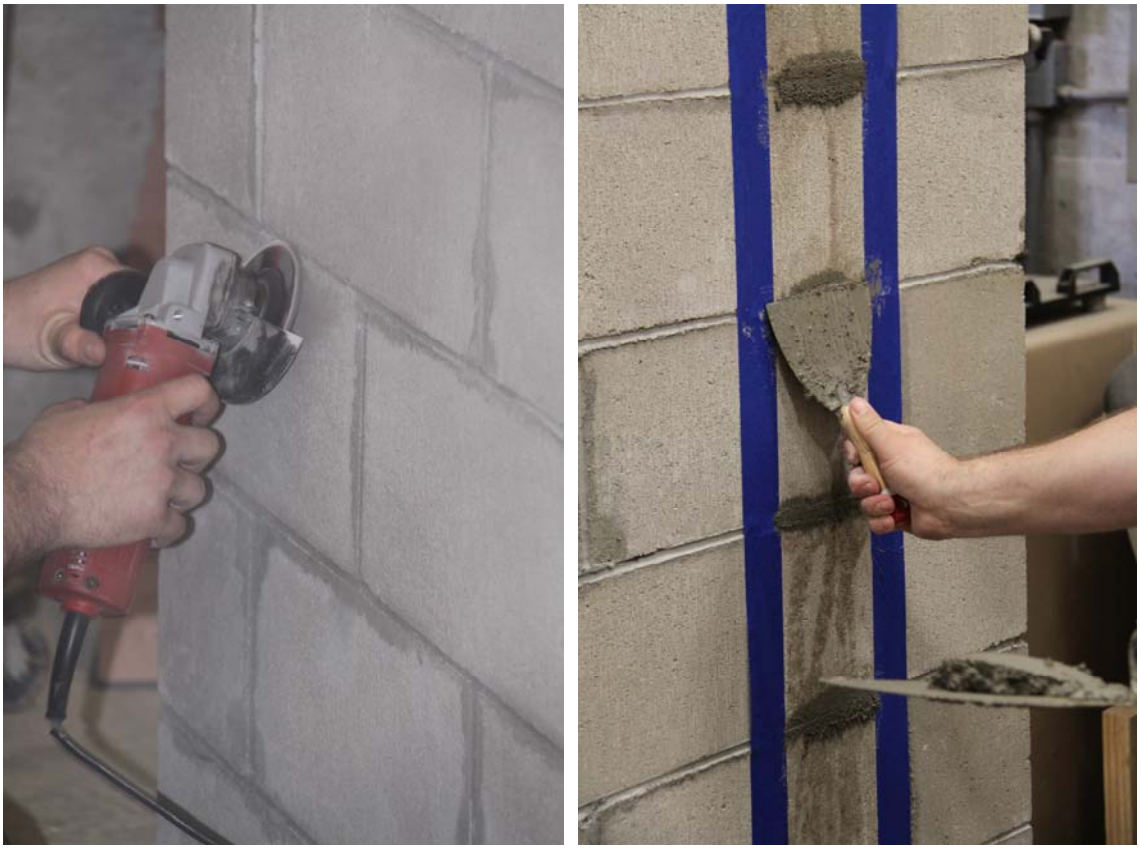

Figure BB: Surface Preparation for CFRP Installation

Source: Author Photo

After the surface was made smooth, all the mortar beds were filled in with mortar so the CFRP would be in complete contact with the masonry wall. Once the mortar had cured for 24 hours, the surface was then cleaned and roughened with a coarse wire brush.

5.7.2 Cutting Fabric

The design for the CFRP fabric was determined to be two 3 inch strips for each side of the CFRP reinforced walls. Since the CFRP fabric is manufactured to be 24

inches wide, the material was cut into the required width prior to installation, as seen in Figure CC.

Figure CC: Cutting CFRP Fabric to Required Width

Source: Author Photo

The 24 inch wide roll of CFRP fabric was placed flat on a clean table away from the resins. With the use of a razor blade and a metal straight edge, the fabric was

carefully measured and cut into 3 inch strips. The 3 inch strips were then rolled up and safely stored until they were ready to be installed on the walls.

5.7.3 Primer Surface

In order to promote adhesion and prevent the masonry surface from drawing resin from the CFRP, an epoxy primer was applied to the masonry walls where the fabric was to be placed (shown in Figure DD).

Figure DD: Primer Surface of Masonry Prior to CFRP Application

Source: Author Photo

The primer used to prep the walls was the Veloxx LR, the same epoxy used to apply the CFRP strips. The primer was applied using a roller until the masonry surface was locally saturated.

5.7.4 Saturate Fabric

Once the walls were ready for the CFRP installation, the CFRP strips were saturated in Veloxx LR epoxy resin as shown in Figure EE.

Figure EE: Saturating CFRP Strips with Epoxy

Source: Author Photo

A batch of epoxy was prepared and placed in a small plastic container. The CFRP strips were then slowly pulled through the epoxy bath where they became saturated with

the laminating epoxy resin. Any extra epoxy was taken off the strips by gently pinching the strips between two fingers, as seen in Figure CC.

5.7.5 Apply Strips to Wall

The saturated strips of fabric were then applied to the primed masonry surface as seen in Figure FF.

Figure FF: Applying Fabric to Masonry Wall

Source: Author Photo

Starting at the top and working down towards the bottom of the wall, the fabric was carefully laid onto the surface making sure that the fibers in the fabric were straight vertically. At the base of the wall, where the first course of CMU meets the steel base plate, the CFRP strips were applied continuously to the base plate in order to increase the CFRP development length (the minimum length of CFRP reinforcement extending beyond the critical section required to develop the design strength of the CFRP reinforcement) under the first mortar joint. During the application process, precautions were taken to prevent air bubbles from becoming trapped under the fabric which would have prevented adhesion of the CFRP to the CMU wall.

After the fabric was applied to the walls, a final coat of epoxy was applied to the walls over the top of the fabric, as seen in Figure GG.

Figure GG: Applying a Final Coat of Epoxy Over CFRP Strips

Source: Author Photo

The final coat of epoxy was applied with the use of a roller. The roller also took out all the smaller air bubbles entrapped in the fabric and ensured that the fabric was completely adhered to the wall. During the cure of the epoxy, the fabric was checked to ensure that it was not sagging.

After the walls had been left for 24 hours, the masking tape was removed. The final product is shown in Figure HH.

Figure HH: Finalized CFRP Reinforced Test Specimens

Source: Author Photo

In Figure HH, it can be seen that the CFRP strips are evenly spaced at 24 inches on center and are aligned vertical. Also the CFRP strips were installed the full height of the walls and extended at the bottom of the walls where the strips were adhered to the steel base plate to give more development length at the base of the wall.

5.8 Estimation of Wall Loading Input Function

Each wall was loaded by the use of the shake table with a sinusoidal forcing function shown in Equation 8.

$$x(t) = \mathrm{A}\sin(\omega t) \qquad \text{Eq.8}$$

where x is the displacement of the shake table

t is time

A is the amplitude of the shake table

ω is the angular frequency of the shake table

The shake table amplitude used for testing was set at 0.5 inches. This decision was made to keep the wall from resonating at its natural frequency (shown in section 5.8.3) before the wall's cracking moment was achieved. At resonance, the dynamic amplification effects are very large for a low damped system, such as the masonry wall, and could create much larger forces in the walls than would have been anticipated. By choosing a larger amplitude for loading the walls, the cracking moment in the wall would occur at a frequency smaller than the natural frequency. This allows for a smaller dynamic amplification while still keeping the wall in a first mode response.

The angular frequency (ω) was estimated by calculating the frequency that would induce the nominal cracking moment (M_{cr}) into the unreinforced wall. To equate M_{cr} to the angular frequency and amplitude, the acceleration of the shake table required to induce the cracking moment into the walls was determined. By using the 0.5 inch displacement, the angular frequency that would produce the acceleration to create M_{cr} was determined.

5.8.1 Shake Table Acceleration

Next the acceleration required by the shake table to induce M_{cr} into the wall was established. The force, F_p generated by the shake table's acceleration is assumed to act at the effective height of the wall shown in Figure II. The effective wall height, for a first mode dominate cantilevered structure, can be assumed to act at 70% of the total wall height (Chopra 2001).

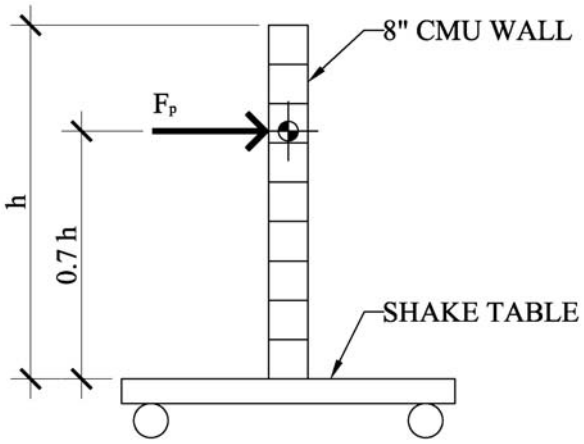

Figure II: Force, F_p Generated by Shake Table Acting at 0.7h of Wall

Source: Author Diagram

As the shake table accelerates, F_p is generated into the 8" CMU wall at a height of 4.2 feet from the base of the table. To determine the force F_p that generates M_{cr} into the wall, M_{cr} is divided by the moment arm to which F_p acts. Therefore F_p can be determined using Equation 9.

$$F_p = \frac{M_{cr}}{moment\ arm} \qquad \text{Eq. 9}$$

$$F_p = \frac{11{,}053\,lbs \cdot ft}{4.2\,ft} = \boldsymbol{2632\ lbs}$$

The shake table's acceleration was then calculated using Equation 10 below:

$$F_p = m\,a \qquad \text{Eq. 10}$$

where m is the mass of the CMU wall

a is the acceleration of the shake table

By solving Equation 10 for 'a', the required acceleration was calculated as follows:

$$a = \frac{F_p}{m} = \frac{2632\,lbs}{\left(\frac{1920\,lbs}{32.2\ ft/\sec^2}\right)} = \frac{2632\,lbs}{59.6\,lbs \cdot \sec^2/\,ft} = \boldsymbol{44.2\ ft/sec^2}$$

Therefore, it would take a maximum acceleration of 44.2 ft/sec^2, or 1.37g, for the unreinforced wall to reach its cracking moment. This acceleration of 1.37g was compared with the maximum acceleration used to design nonstructural components per ASCE 7-05, section 13.3.1. Using the USGS website and assuming the site was located at Cal Poly in San Luis Obispo, zip code 93407, it was determined that the site specific

spectral acceleration was equal to $S_{DS} = 0.861$. Using equation 13.3-1 from ASCE 7-05, the maximum acceleration for the wall was 0.34g. Therefore, the maximum acceleration required to crack the unreinforced cantilevered wall was 4 times greater than the value obtained using the provisions in ASCE 7-05.

5.8.2 Required Angular Frequency

The shake table's required angular frequency was determined using the relationship between the acceleration, frequency, and amplitude which is given in Equation 11 below:

$$a = A\omega^2 \qquad \text{Eq. 11}$$

By solving Equation 11 for ω, the required angular frequency was computed as follows:

$$\omega = \sqrt{\frac{a}{A}} = \sqrt{\frac{44.2\,ft/\sec^2 \times \frac{12\,in}{1\,ft}}{0.5\,in}} = \boldsymbol{32.6\ rad/sec}$$

By substituting the required angular frequency and 0.5 inch amplitude used to generate the cracking moment into the testing walls, the sinusoidal forcing function Equation 8 becomes:

$$x(t) = (0.5in)\,\sin(32.6t) \qquad \text{Eq. 12}$$

This sinusoidal forcing input function is only an estimation of the shake table's required motion that will create the cracking moment in the baseline unreinforced wall.

In actuality, the angular frequency that will cause the cracking moment is less than that predicted since dynamic amplification effects are not taken into account.

The input function that was used for testing the CFRP reinforced walls was determined by finding the frequency with 0.5 inch amplitude that would crack the unreinforced wall. This frequency was then used to test the three CFRP reinforced walls.

5.8.3 Natural Frequency

To check the assumption of using the 0.5 inch amplitude to avoid reaching resonance, the natural frequency of the wall was determined. The natural frequency was determined using Equation 13 below:

$$\omega_n = \sqrt{\frac{k}{m}} \qquad \text{Eq. 13}$$

where ω_n is the natural angular frequency of the CMU wall

k is the out-of-plane stiffness of the CMU wall

m is the mass of the CMU wall

Before determining the wall's natural frequency, the out-of-plane stiffness of the CMU wall was determined. The wall's stiffness was determined using Equation 14 below:

$$k = \frac{3 E_m I_g}{h^3} \qquad \text{Eq. 14}$$

where E_m is the modulus of elasticity of masonry equal to $900f'_m$ (MSJC 2008)

I_g is the moment of inertia of gross cross-sectional area of the wall

h is the wall height

Solving Equation 14 the stiffness of the cantilevered wall was determined as follows:

$$k = \frac{3 \times 900(1522\,psi)\dfrac{48in(7.625in)^3}{12}}{\left(6\,ft \times \dfrac{12\,in}{ft}\right)^3} = \mathbf{19{,}524}\,lbs/in$$

By substituting the stiffness and mass of the wall into Equation 13, the natural frequency of the wall was established.

$$\omega_n = \sqrt{\frac{19{,}524\,lbs/in}{59.6\,lbs \cdot \sec^2/ft} \times \frac{12in}{1\,ft}} = \mathbf{62.7}\,rad/\mathbf{sec}$$

Since the natural frequency of the wall (62.7 rad/sec) is greater than the required angular frequency that creates the cracking moment in the wall (32.6 rad/sec), the wall will reach the cracking moment before reaching resonance. Therefore, the dynamic amplification effects for the low damped wall will be much smaller than those if the wall was cycled under its natural frequency.

5.9 Wall Testing

Of the four walls tested, three were reinforced with CFRP strips and one was left unreinforced. The unreinforced baseline wall was tested to determine the shake table frequency that created the cracking moment in the unreinforced wall. The frequency that cracked the unreinforced wall was then used to cycle the other three CFRP reinforced walls.

Each wall was transported into the Seismic Lab and positioned onto the Pegasus shake table with the use of a forklift as shown in Figure JJ.

Figure JJ: Positioning Wall onto Shake Table with Forklift

Source: Author Photo

The forks on the forklift were positioned so that they straddled the wall on both sides. Metal chains were then wrapped around each fork and attached to two I-bolts, on each side of the wall, that were bolted the steel base plate beneath the wall. Each wall was carefully placed atop and fastened to the shake table as shown in Figure KK.

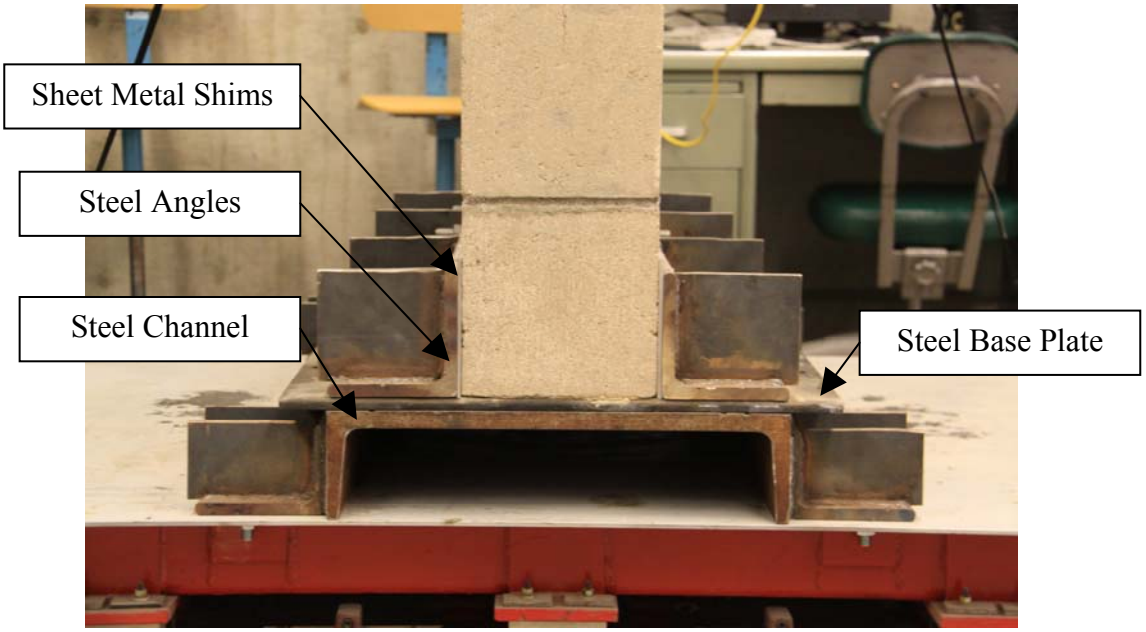

Figure KK: Wall to Table Connection

Source: Author Photo

Each wall was positioned on top of the steel channel attached to the shake table. Next, steel angles were placed on each side of the wall. Sheet metal shims were then placed between the wall and the metal angles to make up for any gaps. Once everything was in position, the wall was fastened to the steel channel with six $^{5}/_{8}$" diameter bolts extending from the steel angles all the way though the metal channel below the base plate. Last, hex nuts were placed on the four threaded rods which extended through the wall.

Gages were placed at the top of the wall and at the bottom of the shake table that monitored the wall's deflection during the testing process. The locations of the gages can be seen in Figure LL.

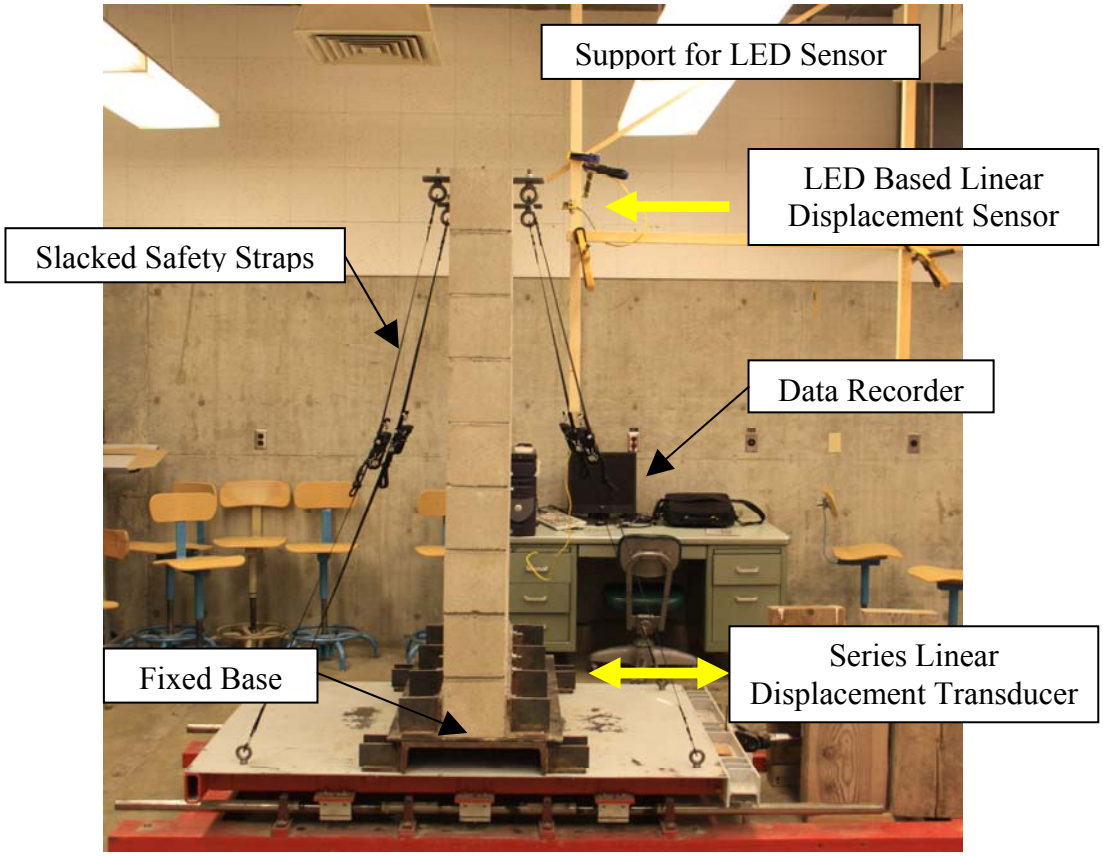

Figure LL: Measurement Instrumentation Set Up

Source: Author Photo

The tip displacement at the top of the wall was measured using an LED Based Linear Displacement Sensor (Banner L-Gage model # Q50BVU, see Appendix A for product specifications). The LED was hung from the ceiling by a truss as seen in Figure II. The table displacement was measured using a Series Linear Displacement Transducer (Transducers Direct series # TD590, see Appendix A for product specifications). The Series Linear Displacement Transducer was attached to the underside of the shake table.

Both deflection gages were wired to a laptop computer where the data was collected during the duration of each test.

Also it is noted, Figure II shows four cargo tie downs attached to the top of the wall and to the edges of the shake table. These tie downs were left slacked during testing and were used as a safety precaution to ensure that if the wall failed, it would not fall over.

5.9.1 Wall #1 – Unreinforced Baseline

The unreinforced baseline wall was the first to be tested. Figure MM shows the unreinforced wall fastened to the shake table prior to testing.

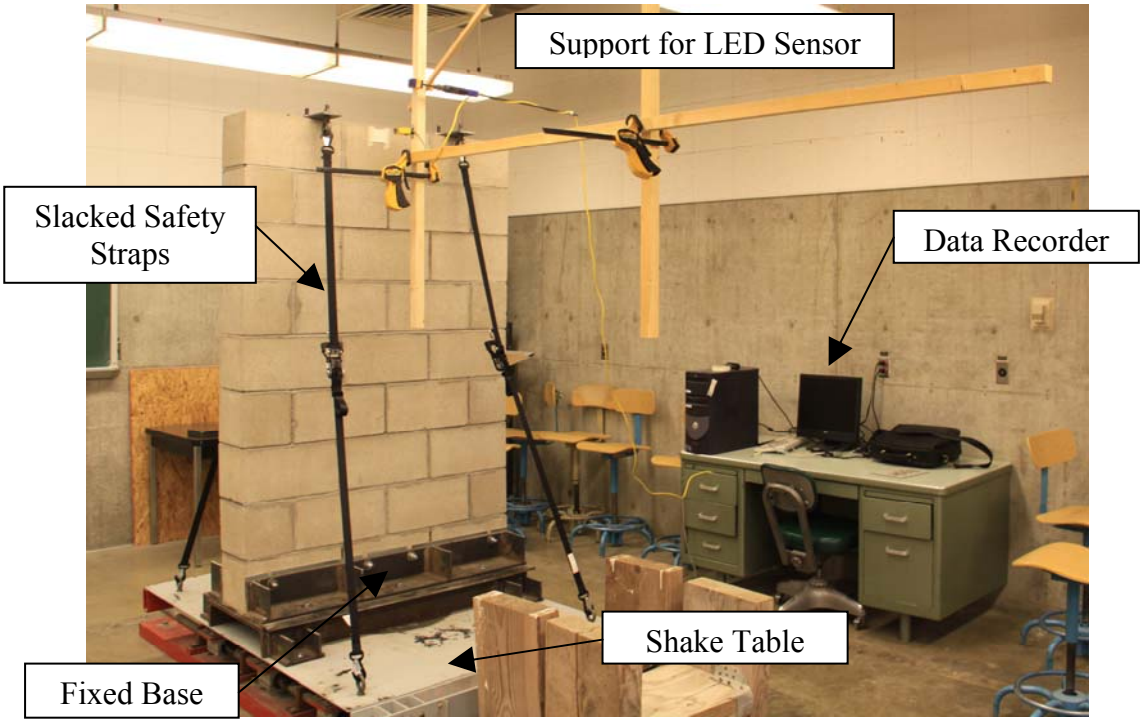

Figure MM: Wall #1 - Unreinforced Base Line Wall

Source: Author Photo

The test started by setting the oscillation amplitude of the shake table to 0.5 inches and the frequency (*f*) to 1 cycle per second or hertz (the frequency can be related to the angular frequency (ω) of the shake table, previously discussed, by $\omega = 2\pi f$). The frequency of the shake table was then increased while the amplitude of the oscillation stayed constant in order to determine the frequency that caused the unreinforced wall to fail. In order to ensure a slow change in frequency, the shake table frequency was increased at a rate of 0.1 hertz every 10 seconds.

Once the shake table frequency was increased to 3.4 hertz ($\omega = 21.4$ rad/sec), the wall failed. At this frequency, the induced moment in the wall had reached the wall's cracking moment, causing the wall to crack. The cracked wall section can be seen in Figure NN.

Figure NN: Cracked Unreinforced Baseline Wall #1

Source: Author Photo

The crack occurred just above the mortar joint of the first course of CMU and extended all the way through the entire wall section.

Comparing the shake table frequency that cracked the unreinforced wall with the angular frequency previously calculated there are larger differences than would be expected. It was calculated that with 0.5 inch shake table amplitude, the required angular frequency to crack the unreinforced wall was 32.6 rad/sec. The results from testing show that it only took an angular frequency of 21.4 rad/sec to crack the wall, making it a 34.4% decrease in frequency from what was expected. This difference in results is due to the dynamic amplification effects experienced under dynamic loading.

The unreinforced wall was used as a baseline to test the three CFRP reinforced walls. Knowing the frequency that generated the cracking moment in the unreinforced wall, it was assumed that this frequency of 3.4 hertz would generate the cracking moment for the walls reinforced with CRRP. Therefore, the frequency at which the unreinforced wall cracked was used as the input frequency for testing the CFRP reinforced walls.

5.9.2 Wall #2 – Reinforced with CFRP Strips

The second wall tested was the first of the three CFRP reinforced CMU walls. After being securely fastened to the table as previously described, the amplitude of the shake table was again set at 0.5 inches and the frequency was set at 1 hertz. In order to keep all testing procedures consistent, the frequency was increased slowly by 0.1 hertz every 10 seconds until the input frequency reached 3.4 hertz. At this point, the frequency was left alone while the table oscillated.

After the table had cycled 56 times, one of the CFRP strips had been scored by the sheet metal shims used to take the gap between the wall and the steel angle support (see Figure OO and Figure PP).

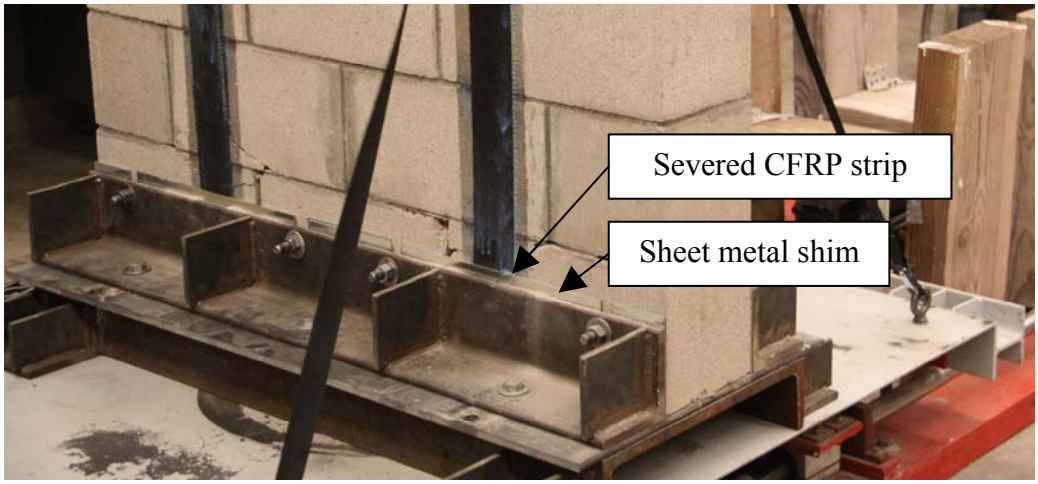

Figure OO: Wall #2 - CFRP Strip Scored by Metal Shim A

Source: Author Photo

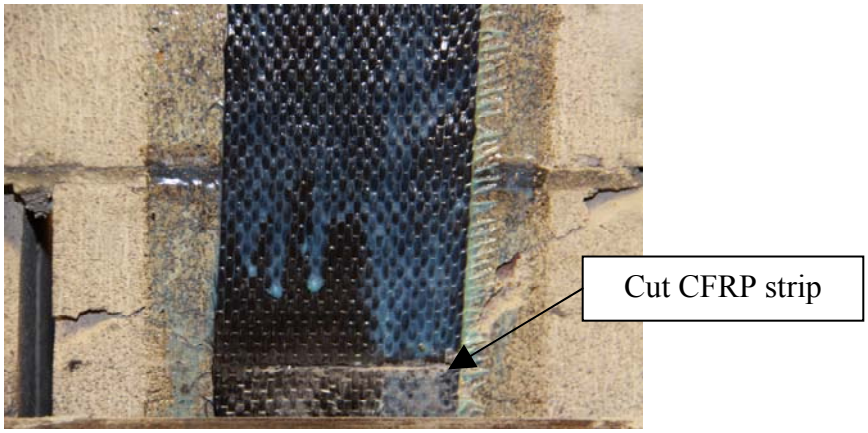

Figure PP: Wall #2 – CFRP Strip Scored by Metal Shim B

Source: Author Photo

The CFRP strip on the right side of the CMU wall, seen in Figure OO, was scored by the sharp edge of the metal shim. The scoring of CFRP strip caused the capacity of the strip to decrease. Figure PP shows the cut made straight across the CFRP strip after the metal shims had been removed. Once the CFRP strip failed, the wall fully cracked across the section at the first mortar joint. The cracking of the wall decreased the wall's stiffness, and thus, increased the tip displacement of the wall while the shake table was remained on. With the increased tip displacement, the other three CFRP strips that were still intact began to debond from the CMU wall. As the CFRP strips began to debond, spalling of the CMU occurred above and below the first mortar joint, as seen in Figure QQ.

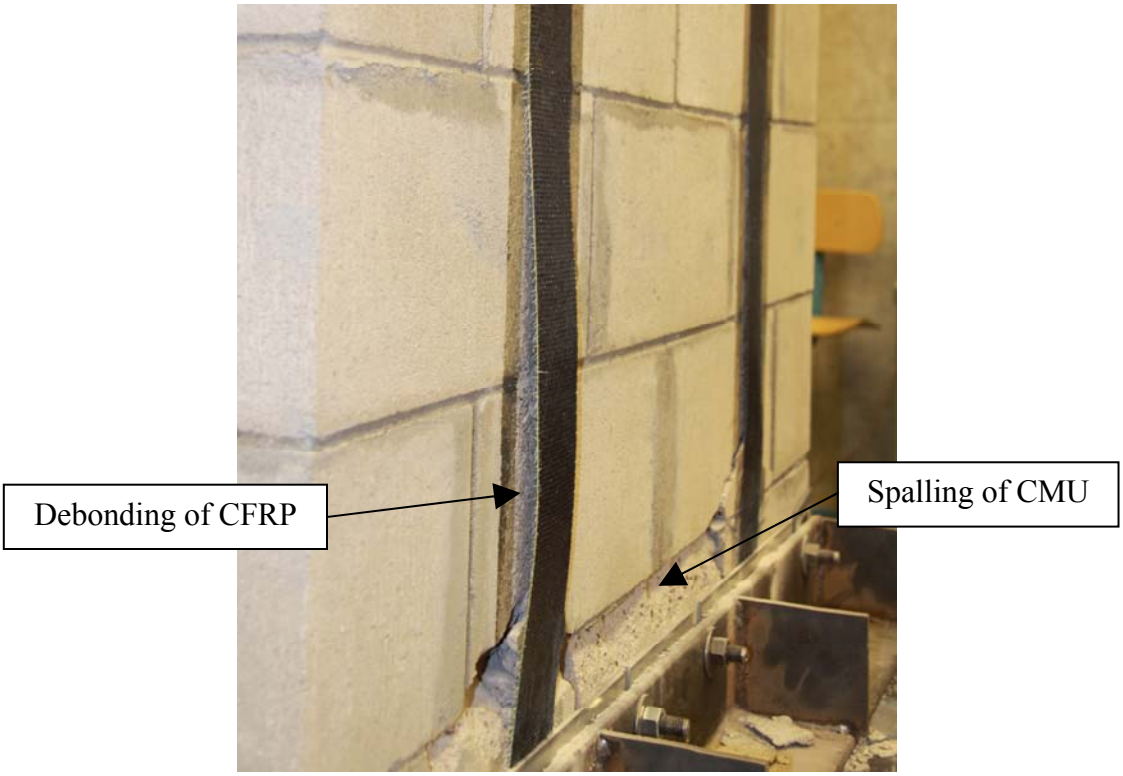

Figure QQ: Wall #2 – Debonding of CFRP strips and Spalling of CMU

Source: Author Photo

The CFRP strips started debonding about 3 to 4 inches above the mortar joint where out of plane shear cracks of the CMU reached the CFRP strips. The length of CFRP debonding slowly grew after more cycles until finally stopping as shown in Figure QQ.

Although one CFRP strip failed and the three others had partially debonded from the CMU wall, the wall continued to oscillate on the shake table for a total of 5000 cycles without completely falling over. Since the wall had cracked, but was still partially reinforced, the decrease in wall stiffness, in turn, decreased the forces the wall

experienced while oscillating at the same input amplitude and frequency. Thus the wall continued to rock back and forth at the first mortar joint.

5.9.3 Wall #3 – Reinforced with CFRP Strips

In order to prevent early failure of the CFRP strips by severing due to the metal shims, adjustments were made to the test set up for Wall #3. The metal shims in contact with the CFRP strips were bent over on the top side as shown in Figure RR.

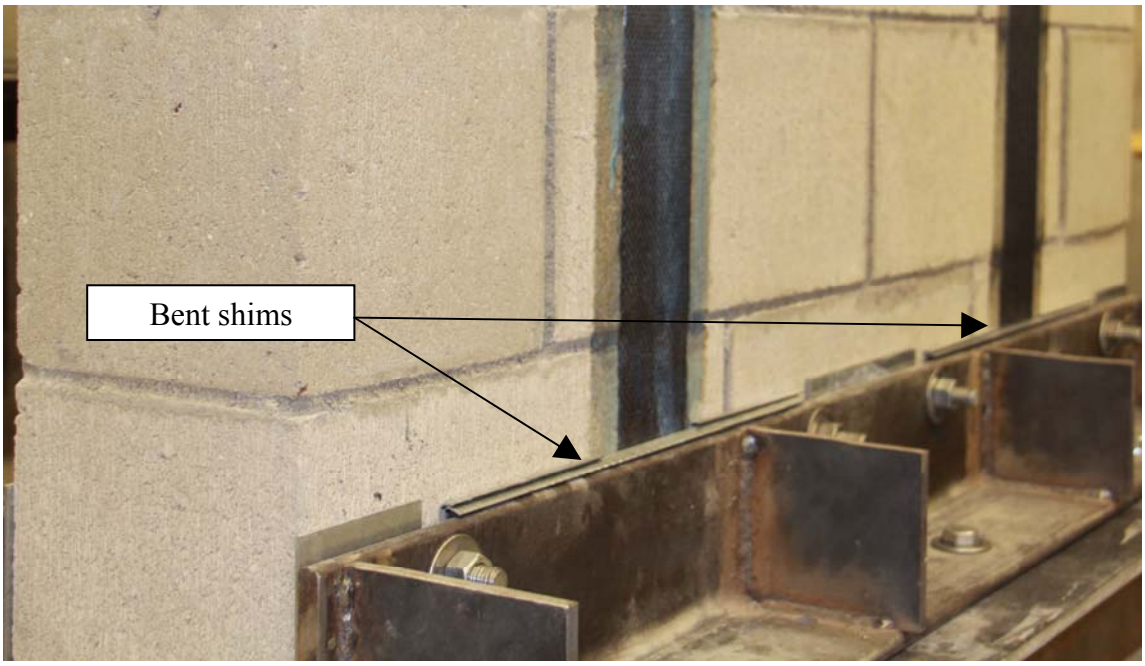

Figure RR: Wall #3 – Bent Shims to Prevent Cutting of CFRP Strips

Source: Author Photo

By bending the metal shims in contact with the CFRP strips, the sharp edge of the metal was moved away from contact with the CFRP. Also, to ensure that the rubbing of the shim against the CFRP would not affect the results, one piece, of the three metal

shims making up the gap between the wall and the support, was taken out at the area in contact with the CFRP.

After the wall had been secured to the shake table, the shake table amplitude was set to 0.5 inches and the frequency was slowly increased, just as in the previous test, until reaching the frequency of 3.4 hertz. At this point, the frequency was not changed while the table oscillated.

After 3 cycles, two CFRP strips had completely debonded from one side of the wall (see Figure SS) due to lack of adequate development length. At the instant the strips debonded, the wall's section cracked at the first mortar joint. The cargo tie downs were then engaged keeping the wall from completely falling over.

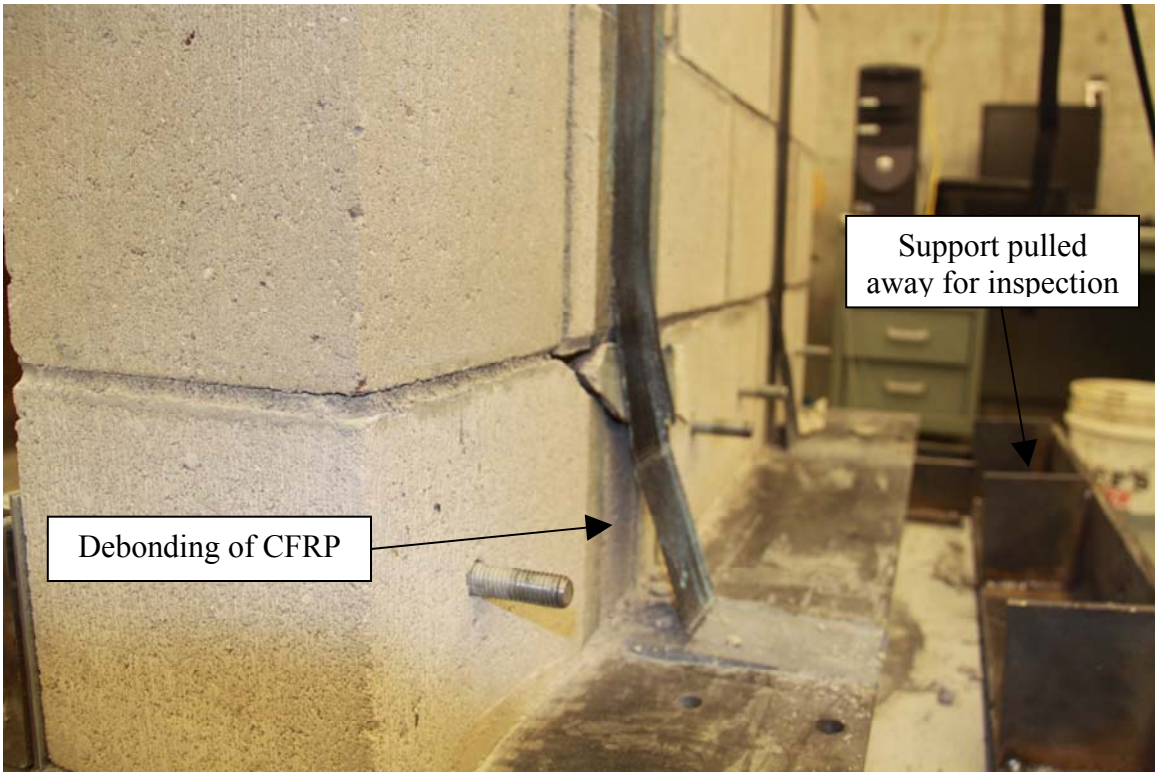

Figure SS: Wall #3 - CFRP Strips Debonded from CMU Wall

Source: Author Photo

The metal angle supports were pulled away from the wall for inspection of failure. It was determined that the CFRP strips were not able to develop at the 90 degree angle where the CMU meets the steel base plate. Due to the inadequate development length, the CFRP debonded from the first course of CMU and then sheared off from the steel base plate causing failure of the CMU wall.

5.9.4 Wall #4 – Reinforced with CFRP Strips

In order to prevent debonding of the CFRP strips below the first mortar joint, adjustments were made to the test set up for Wall #4. To increase the development

length of the CFRP strips, additional horizontal CFRP strips were added below the first mortar joint as shown in Figure TT.

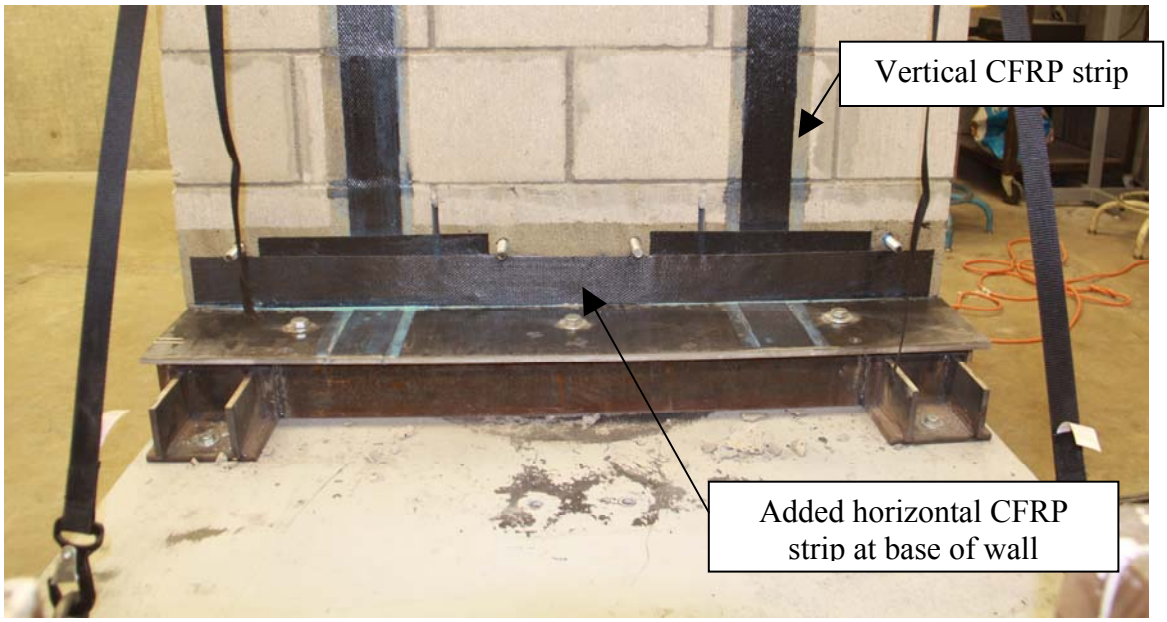

Figure TT: Wall #4 - Added CFRP to Increase Development Length at Base of Wall
Source: Author Photo

The additional CFRP added at the base of the wall used the same fabric and epoxy resin used to install the vertical strips of CFRP. Also, the additional CFRP was added in accordance with the same CFRP installation process as previously described. First a 14 inch wide by 5 inch tall piece of fabric was placed with the fiber orientation vertical at the base of each vertical strip. Next (1) 3 inch wide strip was placed at the base of each side of the wall with the fiber orientation horizontal to the wall. The theory behind placing additional CFRP in this orientation is that the first piece of fabric would be engaged at 45 degree angles from the point at which it meets the vertical strip. This piece

of fabric would then help develop the forces into the 3 inch wide strip placed at the bottom of the wall. Once the forces could be developed from the vertical CFRP reinforcement to the horizontal CFRP, the vertical strips would have sufficient development length to reach their capacity.

After the wall had been secured to the shake table, the shake table amplitude was set to 0.5 inches and the frequency was slowly increased, just as in the previous tests, until reaching the frequency of 3.4 hertz. At this point, the frequency was not changed while the table oscillated.

The wall was allowed to cycle for 24 minutes and 30 seconds at which the wall had cycled for 5000 cycles. After the 5000 cycles the wall showed no signs of failure or dramatic increase in tip deflection.

At this point, it was decided to increase the frequency of the shake table until the wall reached failure. By increasing the frequency, the demand on the wall would be increased as well. The frequency was increased 0.1 hertz every 60 seconds. When the table reached a frequency of 3.9 hertz, the wall underwent 3 cycles before failure. The wall had failed due to a tension failure of two of the four CFRP strips (see Figure UU).

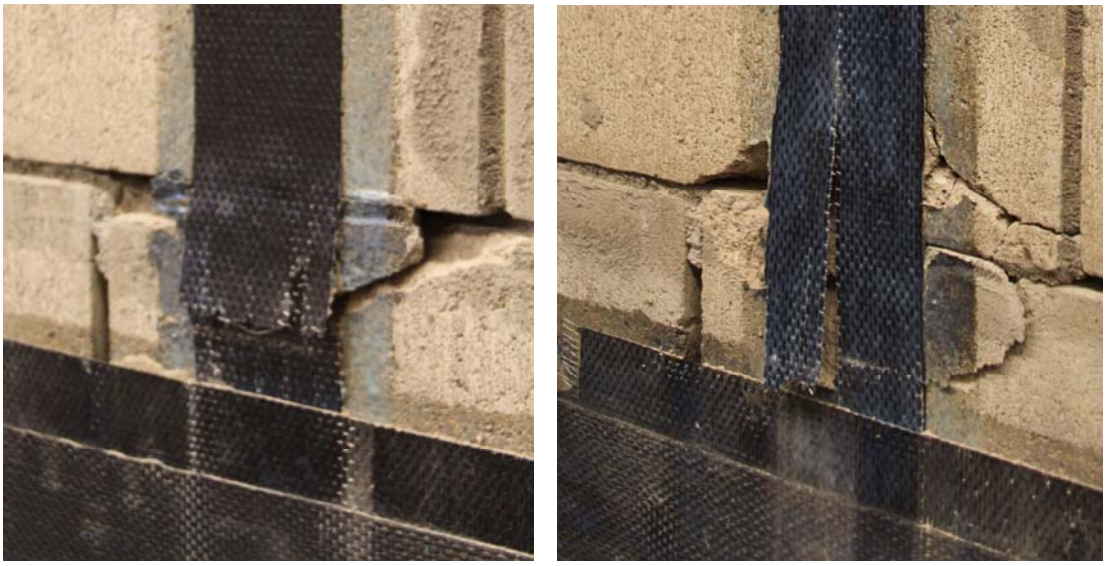

Figure UU: Wall #4 - Tension Failure of CFRP at a Table Frequency of 3.9 Hertz
Source: Author Photo

The tension failure of the CFRP strips occurred below the first mortar joint, between the metal angle support and the mortar joint. Having the CMU wall fail due to tension failure of the CFRP shows that the CFRP strips had sufficient development length to fully develop the forces in the CFRP generated by the shake table. At the point of CFRP failure, the wall then fully cracked, but did not completely fall over. The wall was still able to oscillate just as Wall #2 did after cracking of the wall.

5.10 Testing Results

After the completion of wall testing, the output from the shake table and tip displacements for each test were analyzed. Plots were made comparing the table displacement and tip displacement versus time for each test.

5.10.1 Wall #1 – Unreinforced Baseline

The unreinforced baseline wall was used to determine the frequency which induced the cracking moment into the wall. It was determined from testing that the wall cracked at an input frequency of 3.4 hertz. Figure VV shows the displacement versus time plot for the unreinforced baseline wall.

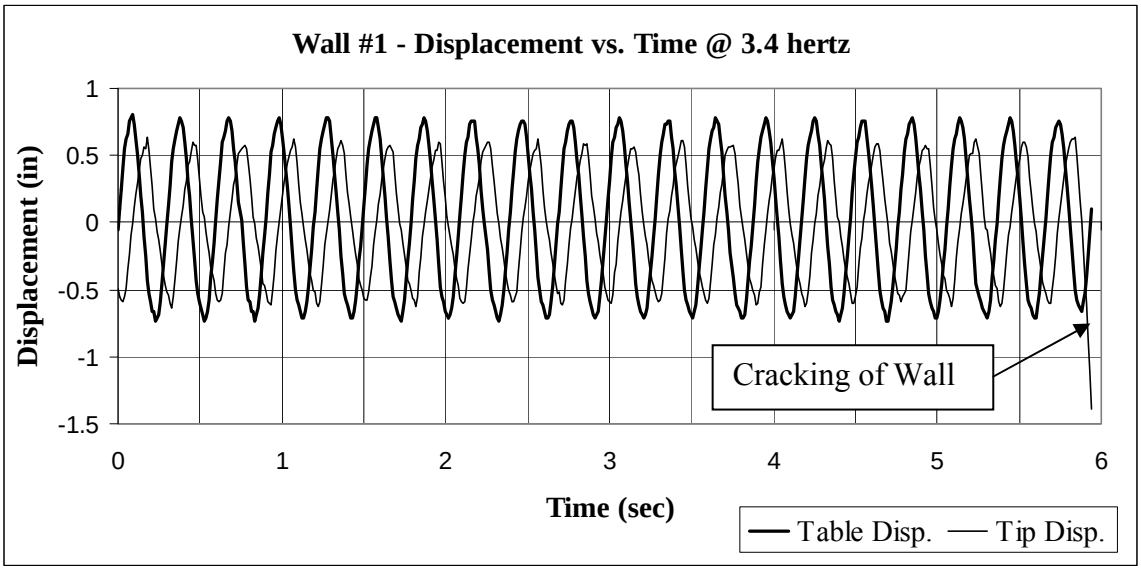

Figure VV: Wall #1 Displacement vs. Time Plot

Source: Author

This plot shows the actual table displacement with respect to time as well as the wall's displacement measured at the top of the wall (tip displacement) with respect to

time on the same plot at a shake table frequency of 3.4 hertz. The output frequency for the shake table was equal to 3.37 hertz and differing from the input frequency of 3.4 hertz by only 0.88%, therefore the same. It is noted that the input amplitude for the table was set to 0.5 inches, but this does not match up with the output. The output shows the shake table amplitude was equal to 0.75 inches. With the added weight of the wall and test setup (over 2000 pounds) atop the shake table, the table was not able to stop at exact 0.5 inch amplitude due to the large inertia forces created. This is due to the hydraulic pump powering the oscillation of the shake table not being large enough. Although the input and output amplitudes do not match up, this does not pose any problems with the test data. Since all the walls tested weigh the same and were cycled using the same amplitude, the output amplitude would be the same for all the tests.

The tip deflection at the top of the wall shows a single mode response to the sinusoidal oscillation. The maximum tip deflection at the top of the wall prior to the cracking of the wall was equal to 0.636 inches.

Using the displacement versus time data for the unreinforced baseline wall, a hysteresis plot was created comparing the wall force, F_p, with the tip deflection of the wall (see Figure WW).

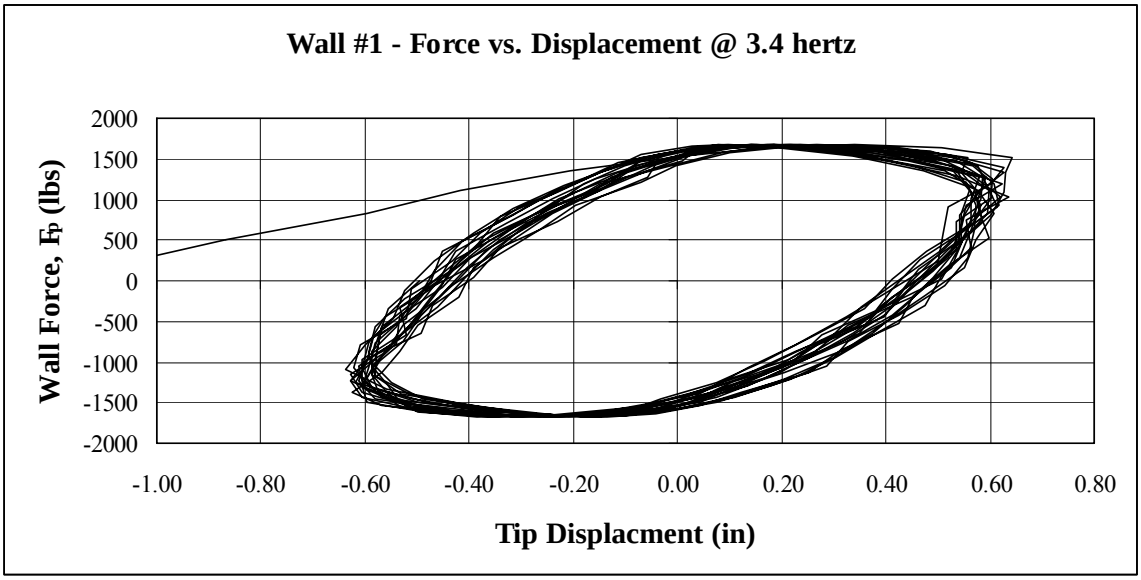

Figure WW: Wall #1 – Force vs. Displacement Hysteresis Plot

Source: Author

Figure WW shows F_p versus tip deflection as the wall cycled at a table frequency of 3.4 hertz until failure. The plot shows the wall behaved elastic until the wall fully cracked, at which point, the wall lost the majority of its original stiffness. This loss in stiffness can be seen in Figure WW as the tip deflection of the wall continued to increase as the wall force, F_p, decreased.

With a frequency of 3.37 hertz and amplitude of 0.75 inches, the maximum acceleration that generated the cracking moment into the wall was 28.02 ft/sec^2. The results for the baseline unreinforced wall will be used to compare with the results for the three walls reinforced with CFRP strips.

5.10.2 Wall #2 – Reinforced with CFRP Strips

Wall #2 was the first of three walls reinforced with CFRP strips. This wall was cycled at an input frequency of 3.4 hertz for 56 cycles until one of the CFRP strips was scored by a metal shim used in the test setup causing failure the strip. Figure XX, YY, and ZZ are a series of three plots showing the displacement versus time for wall #2 at 3.4 hertz.

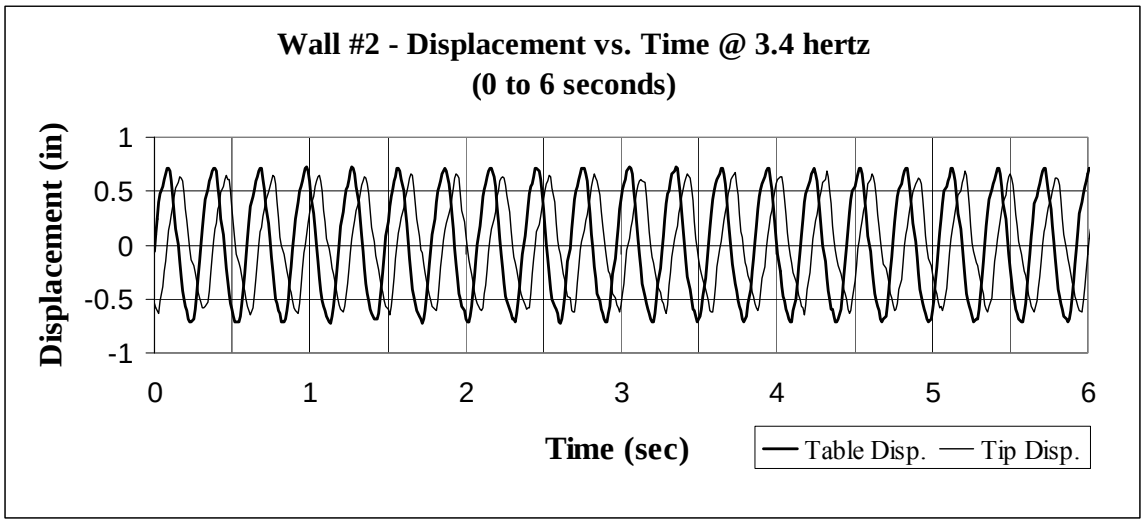

Figure XX: Wall#2 - Displacement vs. Time Plot A

Source: Author

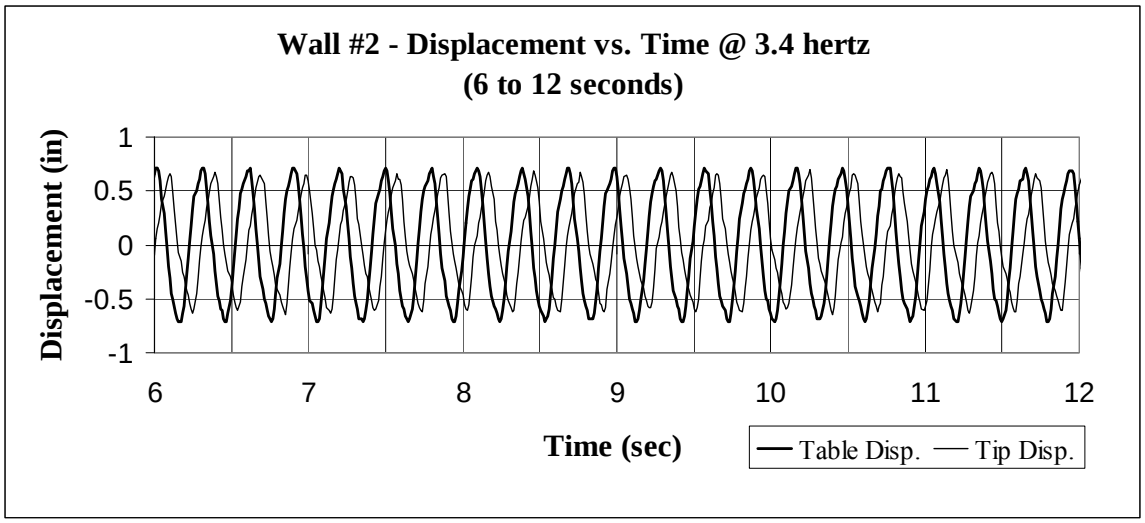

Figure YY: Wall#2 - Displacement vs. Time Plot B

Source: Author

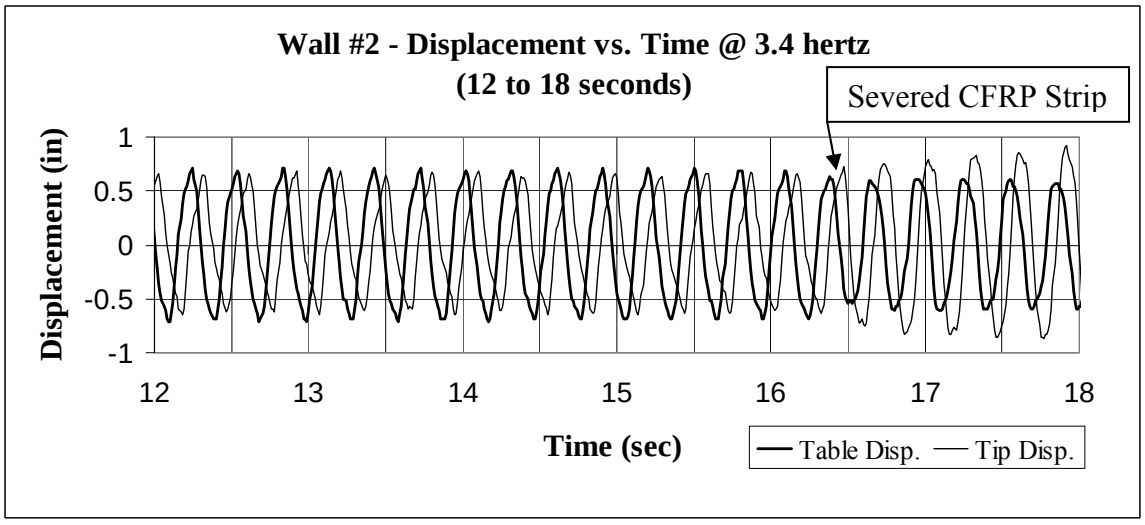

Figure ZZ: Wall#2 - Displacement vs. Time Plot C

Source: Author

The output frequency for the shake table was 3.37 hertz, almost the same as the output frequency for the baseline wall. Also, the output amplitude for wall #2 was 0.74

inches, only 0.01 inches less than the baseline wall. With an output frequency of 3.37 hertz and amplitude of 0.74 inches, the maximum acceleration the wall underwent was 27.68 ft/sec^2. This maximum acceleration is 1.21% less than the maximum acceleration that failed the baseline unreinforced wall.

The tip deflection measured at the top of wall #2 shows the same single mode response as seen in the baseline wall. The maximum tip deflection, prior to the failure CFRP strip, was 0.694 inches. This tip deflection is slightly larger than that of the baseline wall by 9.12%. The increase in tip deflection can possibly be due to the micro-cracking of the masonry near the base of the wall as the CFRP strips became engaged.

Using the displacement versus time data for the wall #2, a hysteresis plot was created comparing the wall force, F_p, with the tip deflection of the wall (see Figure AAA).

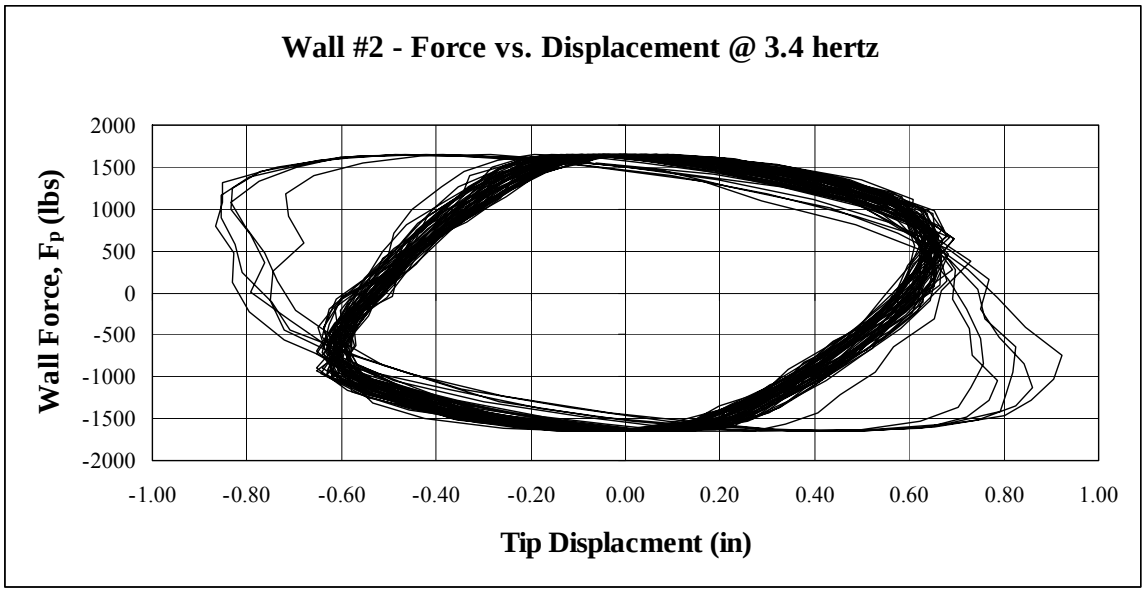

Figure AAA: Wall #2 – Force vs. Displacement Hysteresis Plot

Source: Author

Figure AAA shows F_p versus tip deflection as the wall cycled at a table frequency of 3.4 hertz for the same 18 seconds displayed in Figures XX, YY, and ZZ. Comparing Figure AAA to Figure WW, it is seen that the stiffness of wall #2 is slightly less than that of the elastic stiffness of wall #1. This is due to the fact that when the wall began to crack the CFRP became engaged. The plot also shows the post cracked wall behavior was also elastic, until the scoring of the CFRP strip by the metal shim caused failure to the strip, at which point, the wall lost stiffness. The loss in stiffness can be seen in Figure AAA by the flattening of the backbone curve of the hysteresis loop. Other than the fact that one of the CFRP strips lost strength and failed due to the scoring by a metal shim, wall #2 showed no loss in strength due to fatigue for the 56 cycles it underwent.

5.10.3 Wall #3 – Reinforced with CFRP Strips

The second of the three walls CFRP reinforced walls tested was wall #3. This wall only completed three cycles at an input frequency of 3.4 hertz prior to the complete debonding of two of the CFRP strips below the first mortar joint of the wall. Figure BBB and CCC are two plots showing the displacement versus time for wall #3 at 3.3 hertz and 3.4 hertz respectively.

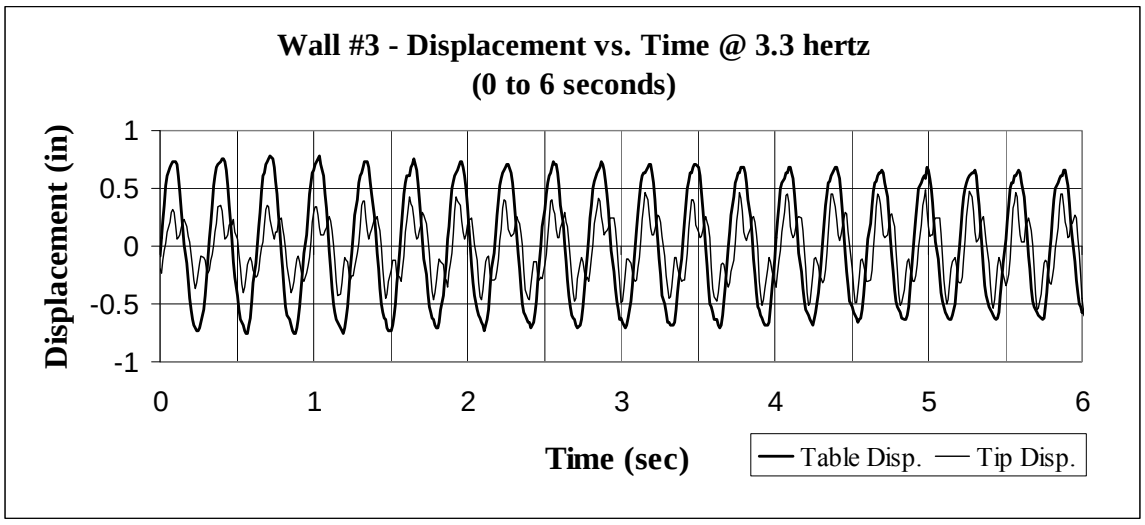

Figure BBB: Wall#3 - Displacement vs. Time Plot A

Source: Author

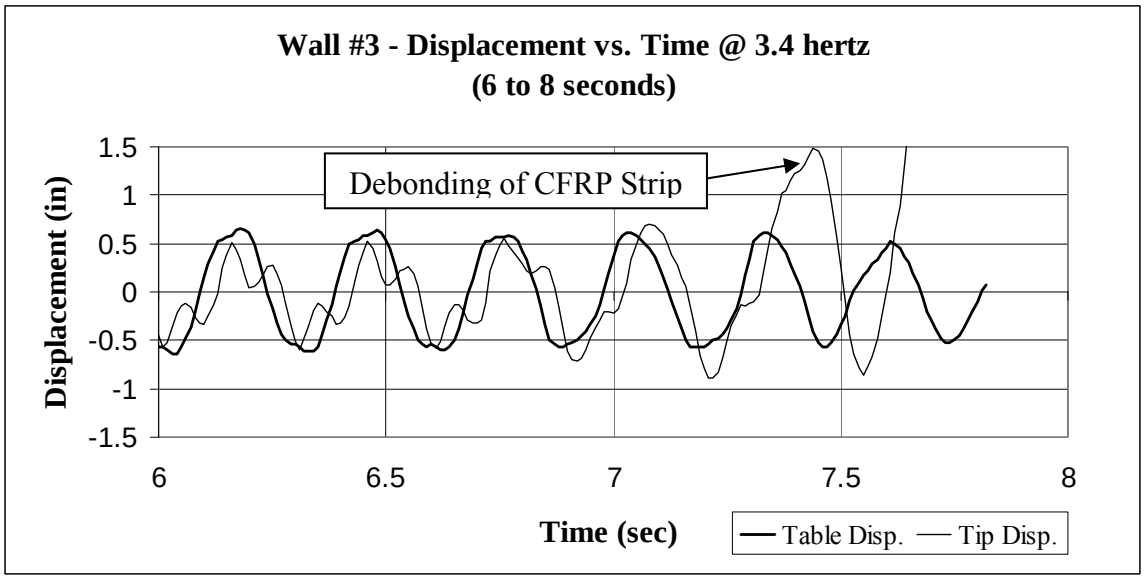

Figure CCC: Wall#3 - Displacement vs. Time Plot B

Source: Author

Although this wall only lasted three cycles before failure, this test still yields valuable information. The plot in Figure BBB shows a different tip displacement response than that of the previous two tests. The tip displacement response for wall #3 has the influence of another mode shape. Although the tip displacement response from this test differs from the previous two tests, the 3.4 hertz frequency was still the same frequency at which wall #2 failed. This shows that despite having another mode shape showing up in the response, the frequency and amplitude of the shake table was still sufficient to create the cracking moment in the wall.

In Figure CCC, the point at which the complete debonding of the CFRP strips is shown to occur after only three complete cycles is shown. Using the displacement

versus time data from Figure CCC, a hysteresis plot was created comparing the wall force, F_p, with the tip deflection of the wall (see Figure DDD).

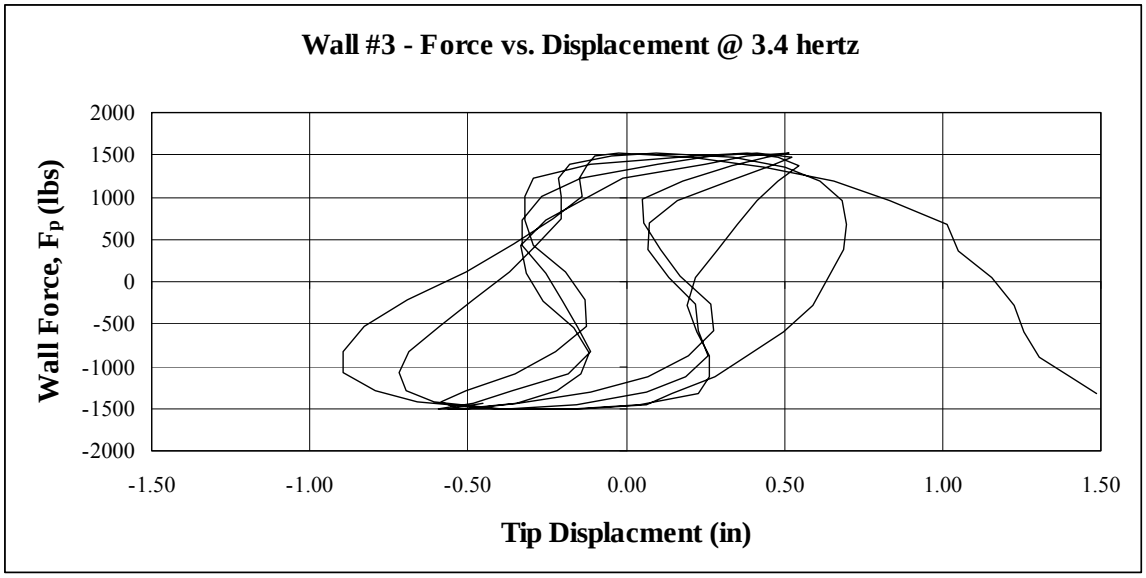

Figure DDD: Wall #3 – Force vs. Displacement Hysteresis Plot

Source: Author

In Figure DDD, it is shown that the wall looses tremendous stiffness after only a few cycles of loading. This can be seen in the hysteresis plot as the shape of the curve opens up and then ultimately fails when the debonding of the CFRP occurred. Also it is noted, the shape of the hysteresis from wall #3 differs from that of walls #1 and #2. The difference in shape is due the influence of the higher order mode shape in the wall response.

5.10.4 Wall #4 – Reinforced with CFRP Strips

The last wall tested was wall #4. To increase the development length of the CFRP strips on the bottom course, in order to avoid a debonding failure similar to wall #3, horizontal strips of CFRP were added below the first mortar joint. This wall cycled at an input frequency of 3.4 hertz for 5000 cycles without any failure. The time history for the 5000 cycles is displayed in Appendix B.

The output frequency and output amplitude for the shake table were equal to 3.38 hertz and 0.74 inches, respectively. The maximum acceleration the wall underwent was 27.81 ft/sec^2 which was only 0.75% less than that which failed the baseline unreinforced wall. Having almost the exact same acceleration as the baseline wall, shows that wall #4 had sufficient force to create the cracking moment in the wall.

The tip deflection response in wall #4 shows a very similar response to that of wall #3, having another higher mode showing up in the response. Even though there are multiple mode shapes in the tip deflection response, it is safe to say that the wall still experienced forces sufficient to produce the cracking moment in the wall based on the testing results seen from wall #3.

Using the displacement versus time data for the wall #4, two hysteresis plots were created comparing the wall force, F_p, with the tip deflection of the wall (see Figure EEE and FFF).

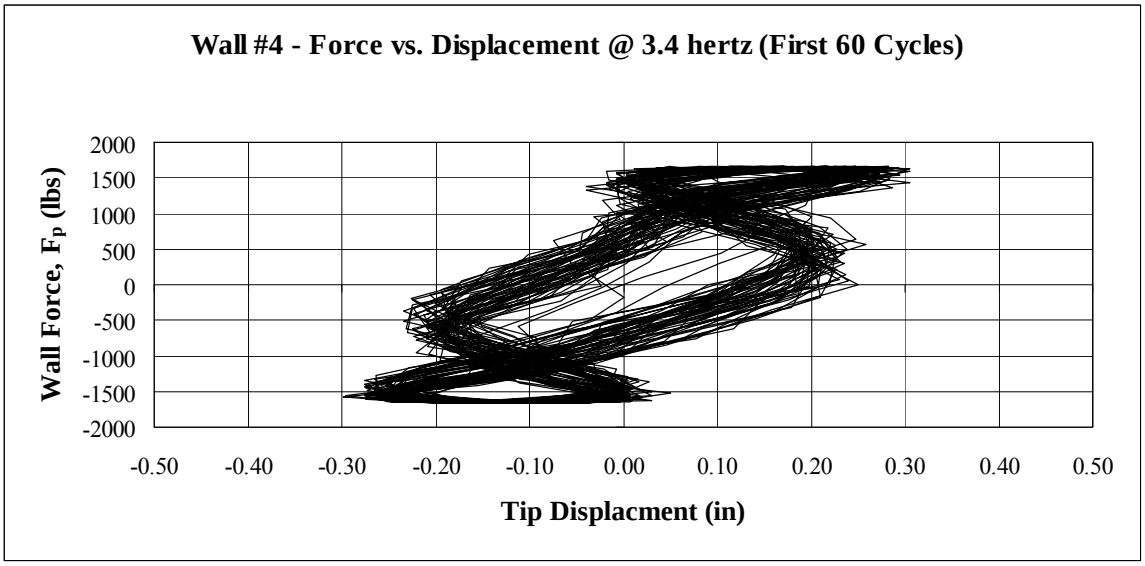

Figure EEE: Wall #4 – Force vs. Displacement Hysteresis Plot A

Source: Author

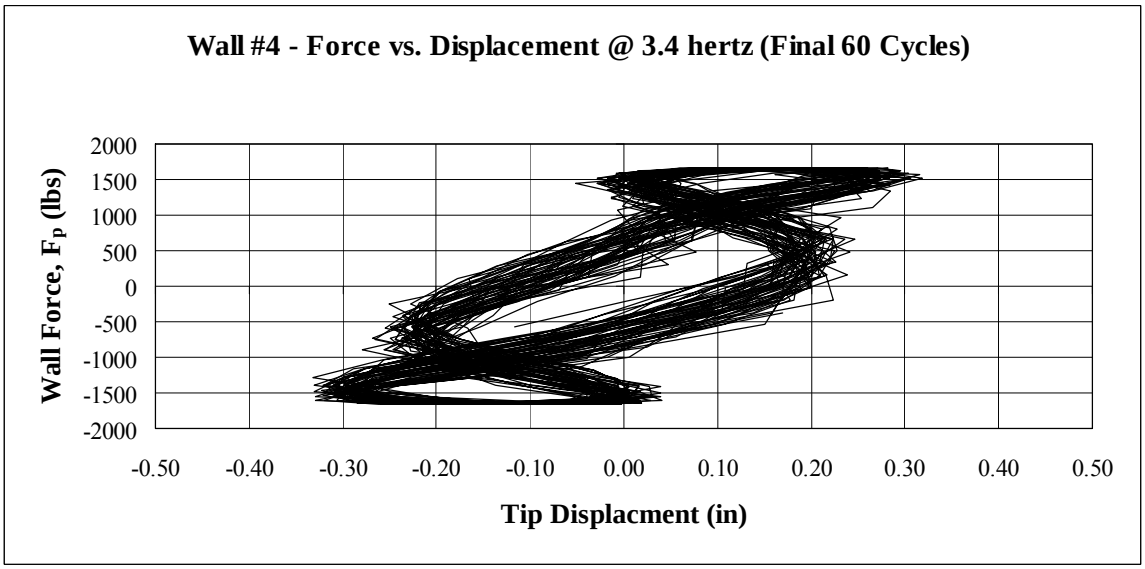

Figure FFF: Wall #3 – Force vs. Displacement Hysteresis Plot B

Source: Author

The first plot, shown in Figure EEE, displays a hysteresis for the wall cycling at 3.4 hertz for the first 60 cycles. The second plot, shown in Figure FFF, displays a hysteresis for the wall cycling at 3.4 hertz for the final 60 cycles of the test. Comparing the two plots shows that there are only slight differences in shape and magnitude. Since the hysteresis in Figure FFF from the final cycles of the test show little difference to the hysteresis in Figure EEE from the beginning of the test, wall #4 shows no signs of fatigue of loss in stiffness due to fatigue.

The tip deflections for wall #4 were also analyzed to see if there was any increase over time due to fatigue. Figure GGG displays the maximum positive and maximum negative tip deflections at time intervals for the duration of the 5000 cycles undergone by wall #4.

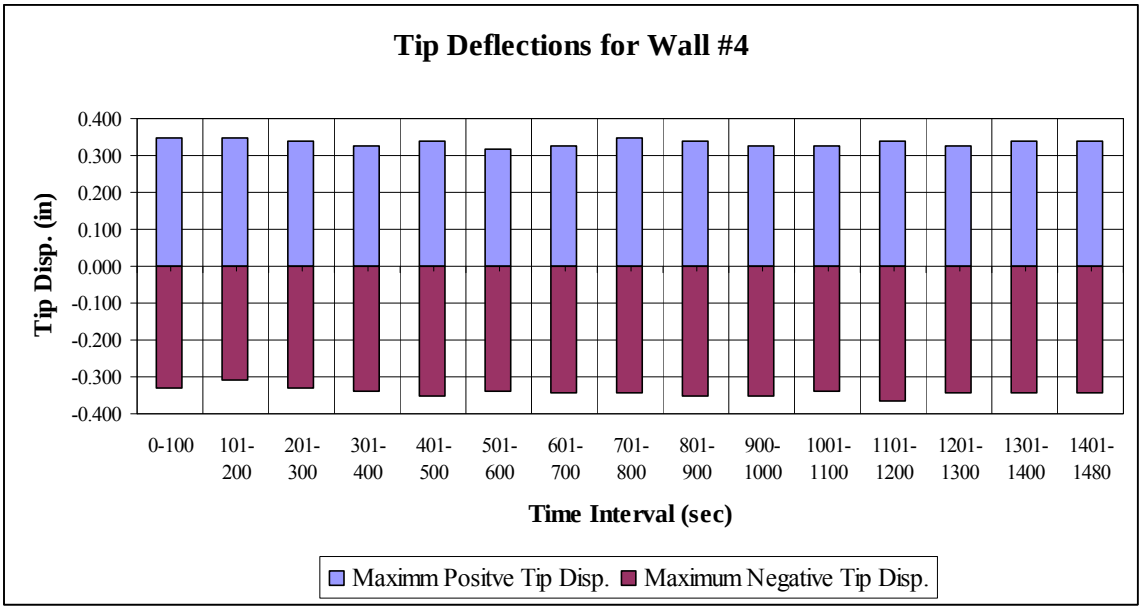

Figure GGG: Maximum Tip Deflections at Time Intervals for Wall #4

Source: Author Figure

Figure GGG shows no correlation between an increase in tip deflection and duration for which the wall was cycled. Therefore, with sufficient development length of the CFRP, wall #4 showed no signs of failure due to fatigue after 5000 cycles.

6.0 CONCLUSION

The purpose of this Master's thesis was to investigate the effects of fatigue on fiber-reinforced polymers (FRP) when applied to masonry walls for out-of-plane loading, as well as to provide further research and add to the general testing database of FRP enhanced masonry. After the completion of the experimental testing performed in this thesis, the following conclusions were made.

The ability for CMU walls, reinforced with carbon fiber reinforced polymer (CFRP) strips, to perform well against out of plane fatigue loading is based on two issues. These two issues are that the CFRP reinforcement must have sufficient strength to provide adequate reinforcement to the out-of-plane loads that are going to be applied to the wall, and sufficient development length allowing the CFRP to develop its design strength. Although both these issues are not new findings and seem very obvious when designing CFRP reinforcement for out-of-plane loading, two of the specimens tested in this thesis failed due to one of these issues.

The failure of wall #2 was due to lack of strength in the CFRP reinforcement. When the CFRP strip was scored by repeated rubbing with the metal shim, the wall then failed due to lack of strength in the CFRP strip. The failure of wall #3 was due to lack of sufficient development length. Even though the wall went through three complete cycles before failure, there was not sufficient development length for the CFRP strips to develop their full capacity. This insufficient development length caused the CFRP strips to completely debond from the first course of CMU causing failure of the wall. From the

testing of the final CFRP reinforced wall, wall #4, it can be seen that a wall with sufficient strength and development length performed exceptionally well in the test lasting all 5000 cycles, far outlasting the duration of any earthquake, without any signs of fatigue. Therefore, the issue of fatigue on masonry walls reinforced with CFRP for out-of-plane loads can be managed by designing walls using typical code design with adequate strength, adequate development length and proper detailing.

Another conclusion, not directly related to the purpose of the thesis, was also made as a result of the experimental testing. This conclusion is that the development length of a vertical CFRP strip can be increased effectively by adding a horizontal strip of CFRP that crosses over the vertical strip. This idea was implemented for the testing of wall #4 to try to increase the development length of the vertical strips due to the debonding failure that occurred in the testing of wall #3. After wall #4 successfully completed the 5000 cycles without fatigue failure, the frequency of the shake table was increased until the wall failed. The failure mechanism occurred when increasing the table's frequency was a tension failure of the CFRP strips. This tension failure of the CFRP strips shows that the CFRP had sufficient development length to develop the CFRP to its full strength. The sufficient development length in this wall was provided through the addition of the horizontal CFRP strips. This method of developing the FRP can be very effective when designing FRP reinforcement in areas where there is not enough space to continue the vertical strips, for example, at a base of a wall or at the intersection of a wall and floor diaphragm.

Lastly, it is noted that surface damage to CFRP may have severe consequences. Looking at the test results form wall #2, the scoring of the CFRP strip from the rubbing of the metal shim drastically reduced the capacity of the strip causing failure of the wall. Therefore, there should be special precautions taken when designing CFRP in places were surface damage may occur. Such precautions may include adding surface protectant over the exposed CFRP to minimize the surface damage of the CFRP.

Overall, the external application of FRP is a very effective solution to strengthening walls for out-of-plane loading.

BIBLIOGRAPHY

(ASCE 2006) American Society of Civil Engineers. *ASCE 7-05: Minimum Design Loads for Buildings and Other Structures*. Reston, VA: ASCE, (2006).

(Buchan and Chen 2007) Buchan, P.A., Chen, J.F. "Blast Resistance of FRP Composites and Polymer Strengthened Concrete and Masonry Structures – A State of the Art Review." *Elsevier.com, Composites Part B: Engineering*. (February 2007) 509-522.

(Carney and Myers 2003) Carney, Preston and Myers, John J. "Shear and Flexural Strengthening of Masonry Infill Walls with FRP for Extreme Out-of-Plane Loading." *Architectural Engineering 2003 Building Integration Solutions*. Austin, Texas. (2003): 246-250.

(Chopra 2001) Chopra, Anil K. Dynamics of Structures: Theory and Applications to Earthquake Engineering. Upper Saddle River, NJ: Prentice-Hall, (2001).

(Edge Structural Composites 2003 A) Edge Structural Composites. "Velacarb 335U: Unidirectional Carbon Fiber Fabric for Structural Strengthening." *Technical Data Sheet*, Sonoma, CA. (November 2003).

(Edge Structural Composites 2003 B) Edge Structural Composites. "Velacarb 600U: Unidirectional Carbon Fiber Fabric for Structural Strengthening." *Technical Data Sheet*, Sonoma, CA. (November 2003).

(Edge Structural Composites 2003 C) Edge Structural Composites. "Velaglass 375B: Bidirectional E-glass Fiber Fabric for Structural Strengthening." *Technical Data Sheet*, Sonoma, CA. (November 2003)

(Edge Structural Composites 2003 D) Edge Structural Composites. "Velaglass 875U: Unidirectional E-glass Fiber Fabric for Structural Strengthening." *Technical Data Sheet*, Sonoma, CA. (November 2003).

(Edge Structural Composites 2003 E) Edge Structural Composites. "Veloxx AP: General Purpose Two-phase Epoxy Adhesive For the Fiber-Bond Strengthening Systems." *Technical Data Sheet*, Sonoma, CA. (November 2003).

(Edge Structural Composites 2003 F) Edge Structural Composites. "Veloxx LR: General Purpose Two-phase Epoxy Adhesive For the Fiber-Bond Strengthening Systems." *Technical Data Sheet*, Sonoma, CA. (November 2003).

(Gussenhoven and Breña 2005) Gussenhoven, R., Breña, S.F. "Fatigue Behavior of Reinforced Concrete Beams Strengthened with Different FRP Laminate Configurations." *7th International Symposium on Fiber Reinforced Polymer Reinforcement for Reinforced Concrete Structures (FRPRCS-7),* Kansas City, MO. (November 11, 2005): 613-630.

(Hamed and Rabinovitch 2006) Hamed, H., Rabinovitch, O. "Out-of-Plane Behavior of Unreinforced Masonry Walls Strengthened With FRP strips." *Composites Science and Technology*. (2006): 489-500.

(Hamilton and Dolan 2001) Hamilton, H. R. and Dolan, C. W. "Flexural Capacity of Glass FRP Strengthened Concrete Masonry Walls." *Journal of Composites for Construction.* (August 2001): 170-178.

(Hamoush, McGinley, Mlakar, Scott, and Murray 2001) Hamoush, S. A., McGinley, M. W., Mlakar, P., Scott, D., and Murray, K. "Out-of-Plane Strengthening of Masonry Walls with Reinforced Composites." *Journal of Composites for Construction*. (August 2001): 139-145.

(Hamoush, McGinley, Mlakar, and Terro 2002) Hamoush, S. A., McGinley, M. W., Malakar, P., Terro, M. J. "Out-of-Plane Behavior of Surface-Reinforced Masonry Walls." *Elsevier.com, Construction and Building Materiasl*. (2002): 341-351.

(HJ3 Composite Technologies 2001 A) HJ3 Composite Technologies. "HJ3 Carbon Fiber Composite (CF-512)." *Technical Data Sheet*, Tucson, AZ. (2001).

(HJ3 Composite Technologies 2001 B) HJ3 Composite Technologies. "HJ3 Carbon Fiber Composite (CF-516)." *Technical Data Sheet*, Tucson, AZ. (2001).

(HJ3 Composite Technologies 2001 C) HJ3 Composite Technologies. "HJ3 Saturating Epoxy Winter (SRW-400)." *Technical Data Sheet*, Tucson, AZ. (2001).

(Milani, Rotunno, Sacco, and Tralli 2006) Milani, G., Rotunno, T., Sacco, E., and Tralli, A. "Failure Load of FRP Strengthened Masonry Walls: Experimental Results and Numerical Models." *Structural Durability& Health Modeling; SDMH.* (2006): 29-58.

(MSJC 2008) Masonry Standards Joint Committee. *Building Code Requirements and Specification for Masonry Structures.* Reston, VA: ASCE, (2008).

(QuakeWrap 2008 A) QuakeWrap Inc. "QuakeBond J100WP Waterproofing Primer." *Product Data Sheet*, Tucson, AZ. (2008).

(QuakeWrap 2008 B) QuakeWrap Inc. "QuakeBond J200TC Tack Coat." *Product Data Sheet*, Tucson, AZ. (2008).

(QuakeWrap 2008 C) QuakeWrap Inc. "QuakeBond J300SR Saturating Resin." *Product Data Sheet*, Tucson, AZ. (2008).

(QuakeWrap 2008 D) QuakeWrap Inc. "QuakeWrap Carbon Fabrics." *Product Data Sheet*, Tucson, AZ. (2008).

(QuakeWrap 2008 E) QuakeWrap Inc. "QuakeWrap Glass Fabrics." *Product Data Sheet*, Tucson, AZ. (2008).

(U.S. Department of Air Force 2000) U.S. Department of Air Force. *Engineering Technical Letter (ETL) 00-09: Airblast Protection Retrofit for Unreinforced Concrete Masonry Walls*. Headquarters Air Force Civil Engineering Support Agency. Tynadall AFB, FL. (August 8, 2000).

APPENDIX A – INSTRUMENTATION SPECIFICATIONS

In this appendix the product specifications for the instrumentation devices used during testing are given. The shake table displacement was measured using a Series Linear Displacement Transducer (Transducers Direct series # TD590-175). The displacement at the top of the wall was measured using a LED Based Linear Displacement Sensor (Banner L-Gage model # Q50BVU).

A.1 Series Linear Displacement Transducer

TRANSDUCERS direct™

"APPLYING TODAY'S TOOLS WITH YESTERDAY'S EXPERIENCE PROVIDING OUR CUSTOMERS THE SOLUTIONS OF TOMORROW."

Introducing the TD590 Series Linear Displacement Transducer.

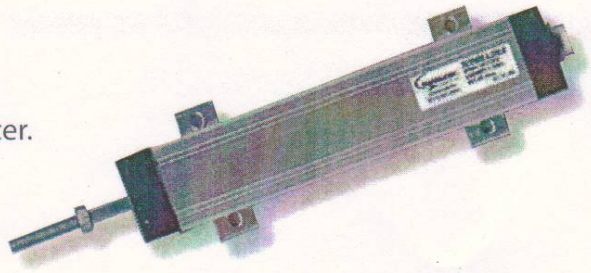

SERIES: TD590

FEATURES

- 50 to 1000 mm stroke.
- Mechanical linkage using M6 thread
- Independent linearity ± 0.3%
- Repeatability 0.01 mm.
- Infinite resolution
- No variation of electrical signal outside theoretical electrical stroke
- Displacement speed 10 m/s
- Working temperature: -55 to +125°C
- Electrical connections:
  4 pin connector DIN 43650 Large (18mm),
  5 pin connector DIN 43322
  4 pin connector mini DIN 43650 (9.4)
- Life duration: > $25x10^6$ meters or > $100x10^6$ operations whichever is the smaller
- Grade of protection for shaft: IP65

DIMENSIONS

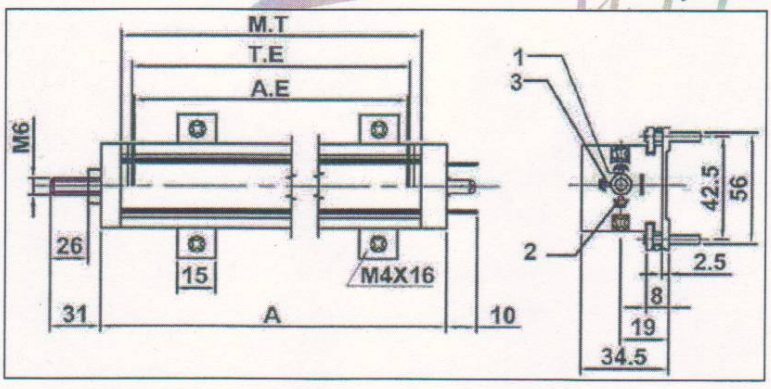

Dimensions In Inches And Are Reference Only.

PHONE 513-583-9491 WWW.TRANSDUCERSDIRECT.COM FAX 513-583-9476

TRANSDUCERS direct™

"APPLYING TODAY'S TOOLS WITH YESTERDAY'S EXPERIENCE PROVIDING OUR CUSTOMERS THE SOLUTIONS OF TOMORROW."

SPECIFICATIONS

Useful electrical stroke (in mm)	50/75/100/130/150/175/200/225/250/275/300/350/375 400/425/450/500/550/600/650/700/750/800/900/1000
Independent linearity	± 0.3%
Displacement speed Standard	10m/s
Displacement force	10N for shaft IP65
Vibrations	5 to 2000Hz, Amax =0.75 mm amax. = 20 g
Shock	50 g, 11ms.
Operative acceleration	200 m/s2 max (20g)
Tolerance on resistance	± 20%
Recommended cursor current	< 0.1 mA
Maximum cursor current	10mA
Maximum applicable voltage	60V
Electrical isolation	>100M at 500V=, 1bar, 2s
Dielectric strength	< 100 mA at 500V~, 50Hz, 2s, 1bar
Dissipation at 40°C (0W at 120°C)	3W
Temp. Coeff. of the resistance	-200 ± 200ppm/°C
Actual Temperature Coefficient of the output voltage	< 1.5ppm/°C
Working temperature	-55 to +125°C
Storage temperature	-50 to +120°C
Case material 40	Anodized aluminum Nylon 66 GF
Control rod material	Stainless steel AISI 303
Fixing	Brackets with variable longitudinal axis

MECHANICAL / ELECTRICAL DATA

TD590 SERIES		50	75	100	130	150	175	200	225	250	275	300	350	375	400	425	450	500	550	600	650	700	750	800	900	1000
Total Electrical Travel(T.E)	mm	51	76	102	132	152	177	202	229	254	279	305	355	381	405	430	457	507	557	610	660	710	762	812	914	1014
Active Electrical Travel(A.E)	mm	51	75	100	130	150	175	200	226	253	276	302	352	378	403	428	455	505	555	607	657	707	759	809	912	1012
Resistance+-20%	K ohm	5.0	5.0	5.0	5.0	5.0	5.0	5.0	5.0	5.0	5.0	5.0	5.0	5.0	5.0	5.0	5.0	5.0	5.0	5.0	10	10	10	10	10	10
Linearity		0.3%													0.3%											
Mechanical Travel(M.T)	mm	58	79	104	135	155	179	204	231	256	281	307	357	384	404	429	460	506	508	612	662	712	765	815	917	1017
Resolution		Infinite																								
Current	mA	<10																								
Temperature	°C	-55 -- +125																								
Dimension A	mm	114	139	164	195	215	241	266	291	316	341	367	417	444	467	494	520	570	622	672	722	772	825	875	977	1077

PHONE 513-583-9491 WWW.TRANSDUCERSDIRECT.COM FAX 513-583-9476

TRANSDUCERS direct™

"APPLYING TODAY'S TOOLS WITH YESTERDAY'S EXPERIENCE
PROVIDING OUR CUSTOMERS THE SOLUTIONS OF TOMORROW"

ELECTRICAL CONNECTIONS

(5 pin and large din)

Connector output	Connector Cable
3 (+)	Red
2	White
1 (–)	Black

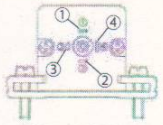

43850 mini din 9.4mm
(standard)

(mini din)

Connector output	Connector Cable
1 (+)	Red
3	White
2 (–)	Black

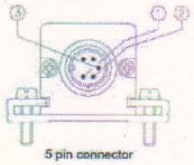

5 pin connector

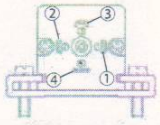

43650 large din 18mm

ACCESSORIES

Includes 2 mounting feet w/M4x26 screws

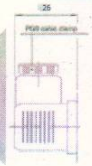

4 pin IP65
TD4P9-00
mini din

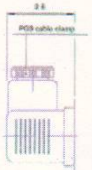

4 pin IP65
TD4PL-00
large din

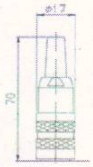

TD5P-CS-00
5 pin straight

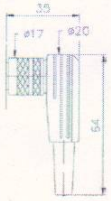

TD5P-CR-00
5 pin Right Angle

ORDERING

Series	Connector	StrokeLength (in mm)
TD590M	D	150

D= 4 pin mini Din
4= 4 Pin Large Din
5= 5 Pin

50	350
75	375
100	400
130	425
150	450
175	500
200	550
225	600
250	650
275	700
300	750
	800
	900
	1000

**= Consult factory for further options.

REV: 12.05

PHONE 513-583-9491 WWW.TRANSDUCERSDIRECT.COM FAX 513-583-9476

A.2 LED Based Linear Displacement Sensor

BANNER
more sensors, more solutions

L-GAGE™ Q50 Series with Analog Output

LED-Based Linear Displacement Sensor with Analog Output and TEACH-Mode Programming

L-GAGE Q50 Analog Output Sensor Features

- Fast, easy-to-use TEACH-Mode programming; no potentiometer adjustments
- Selectable output response speeds: 4 milliseconds or 64 milliseconds (see hookup)
- Teach a sensing window size and position, or a set-point threshold centered within a 100 mm window
- Two sensing ranges, depending on model: 100 to 300 mm (visible red beam models), and 100 to 400 mm (infrared beam models)
- Sensor linearity is better than 3 mm
- Banner's patented scalable analog output (U.S. patent #6,122,039) automatically distributes the output signal over the width of the programmed sensing window
- Analog output slope can be either positive or negative, depending upon which window limit is programmed first
- Two bicolor Status LEDs
- Choose 2 meter or 9 meter unterminated cable, or swivel 5-pin Euro-style QD connector
- Rugged construction withstands demanding sensing environments; rated IEC IP67, NEMA 6
- Select models with either visible red or infrared beam
- Select models with either a 0-10V or 4-20 mA output

WARNING . . .
Not To Be Used for Personnel Protection

Never use these products as sensing devices for personnel protection. Doing so could lead to serious injury or death.

These sensors do NOT include the self-checking redundant circuitry necessary to allow their use in personnel safety applications. A sensor failure or malfunction can cause either an energized or de-energized sensor output condition. Consult your current Banner Safety Products catalog for safety products which meet OSHA, ANSI and IEC standards for personnel protection.

L-GAGE Q50 Analog Output Sensor Models

Model Number	Sensing Range	Cable*	Supply Voltage	Beam	Output
Q50BVI	100 to 300 mm (3.9" to 11.8")	5-wire, 2 m (6.5') cable	15 to 30V dc	Visible Red LED	4 to 20 mA
Q50BVIQ		5-pin Euro-style QD			
Q50BVU		5-wire, 2 m (6.5') cable			0 to 10V
Q50BVUQ		5-pin Euro-style QD			
Q50BI	100 to 400 mm (3.9" to 15.7")	5-wire, 2 m (6.5') cable		Infrared LED	4 to 20 mA
Q50BIQ		5-pin Euro-style QD			
Q50BU		5-wire, 2 m (6.5') cable			0 to 10V
Q50BUQ		5-pin Euro-style QD			

* 9 meter cables are available by adding suffix "**W/30**" to the model number of any cabled sensor (e.g., **Q50BRI W/30**). A model with a QD connector requires a mating cable; see page 8.

Printed in USA 03/01 P/N 64323 Rev. A

L-GAGE Q50 – Analog Output Sensor

L-GAGE Q50 Analog Output Sensor Overview

The Q50 is an easy-to-use triangulation sensor which provides a sophisticated, yet cost-effective solution for demanding measurement applications. Q50 Series sensors feature compact, all-in-one design and require no separate controller.

Near and far sensing window limits are set quickly using simple push-button or remote signal TEACH-mode programming. The analog output has the option of being set with a sensing distance centered within a 100 mm window. The sensor features Banner's patented digital signal processing algorithm (U.S. patent #6,122,039), which automatically distributes the 0 to 10V dc (or 4 to 20 mA) output signal over the width of the programmed window.

Optical Triangulation
The function of the Q50 Sensor is based on optical triangulation (see Figure 1). The emitter circuitry and optics create a light source which is directed toward a target. The light source bounces off the target, scattering some of its light through the sensor's receiver lens to its position-sensitive-device (PSD) receiver element. The target's distance from the receiver determines the light's angle to the receiver element; this angle determines where the returned light will touch the PSD receiver element.

The position of the light on the PSD receiver element is processed through analog and digital electronics and analyzed by the microprocessor, which calculates the appropriate output value. The analog output provides either a current or voltage output proportional to the target's position within the user-programmed analog window limits (see page 4).

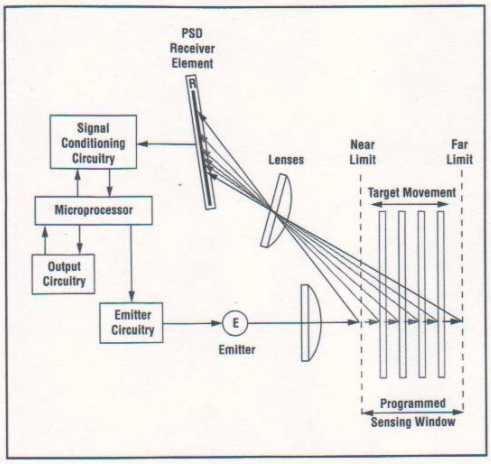

Figure 1. Using optical triangulation to determine sensing distance

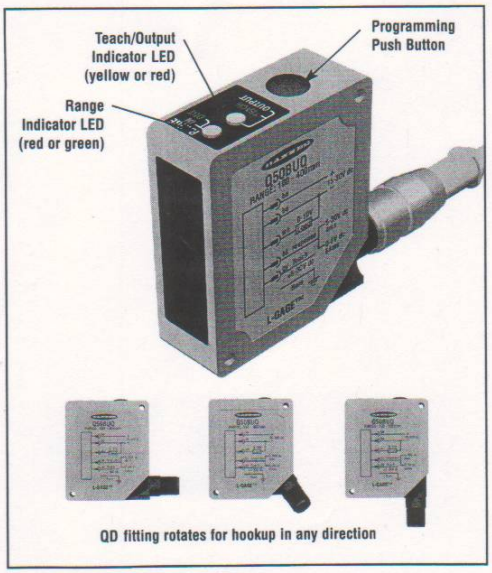

Figure 2. L-GAGE Q50 sensor features

Banner Engineering Corp. • Minneapolis, U.S.A.
www.bannerengineering.com • Tel: 763.544.3164

L-GAGE Q50 – Analog Output Sensor

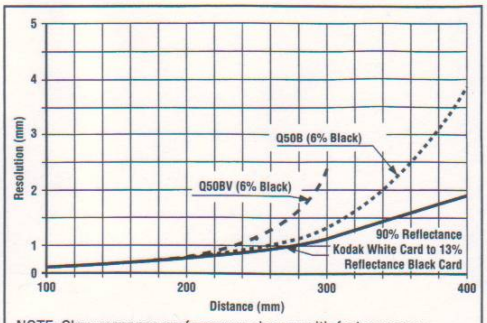

NOTE: Slow response performance shown; with fast response, resolution is 4 times larger.

Figure 3. L-GAGE Q50 resolution

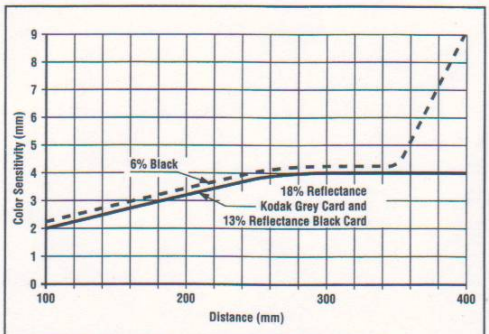

NOTES: Color sensitivity is independent of response time
Q50B (infrared models) span is 100-400 mm
Q50BV (visible red models) span is 100-300 mm

Figure 4. L-GAGE Q50 color sensitivity (This represents the expected change in output when the target color is changed from a 90% reflectance Kodak White Card to a 6%, 13% or 18% reflectance surface.)

Using the L-GAGE Q50 Analog Output Sensor

Response Speed

To control the response speed, connect the black wire as follows:

Fast Speed (4 ms): Connect black wire to +5 to 30V dc
Slow Speed (64 ms): Connect black wire to 0 to +2V dc (or open connection)

Window Limits

Window limits may be taught to the sensor either remotely (using the gray wire) or by using the sensor's Teach push button.

The Q50 sensor operates in two modes: TEACH (or programming) mode and RUN mode.

NOTE: All LED indicators momentarily go OFF when the sensor changes state between RUN and TEACH modes.

Indicator Status Conditions

Indicator	Status
Range LED (green/red)	Green — Target is within sensing range
	Red — Target is outside sensing range
	OFF — Sensor Power OFF
Teach/Output LED (yellow/red)	Yellow — Target is within taught window limits
	OFF — Target is outside taught window limits
	Red — Sensor is in TEACH mode

TEACH-Mode Programming

Push-Button Procedure

1. Press the Teach push button until the Teach LED turns red (hold button in for about 2 seconds). This indicates the sensor is waiting for the first window limit.
2. Position the target for the first limit. The Range LED should be green, indicating a valid target. Briefly "click" the Teach push button. This will teach the sensor the first limit. The Teach LED will flash red at 2 Hz to acknowledge receiving the first window limit; it is now waiting for the second limit.
3. Position the target for the second limit and "click" the Teach push button again to teach the sensor the second limit. The Teach LED will return to either yellow or OFF as the sensor returns to RUN mode.

Banner Engineering Corp. • Minneapolis, U.S.A.
www.bannerengineering.com • Tel: 763.544.3164

L-GAGE Q50 – Analog Output Sensor

Teaching Analog Limits Using a Fixed 100 mm Window
For some analog applications, a sensing distance set point centered within a sensing window is required. The TEACH procedure is simple: teaching the same limit twice causes the sensor to program a window centered on the position taught. This window is 100 mm wide (taught position ±50 mm).

Remote Programming
A function is provided to program the sensor remotely or to disable/enable the push button; this is accomplished via the gray wire. Disabling the push button prevents anyone on the production floor from adjusting any of the programming settings. Connect the gray wire of the Q50 Gauging Sensor to +5 to 30V dc, with a remote programming switch connected between them. NOTE: The impedance of the remote teach input is 15 kΩ

To program, pulse the wire as illustrated in Figure 5. NOTE: The duration of each pulse (corresponding to a push button "click") is 0.04 to 0.8 seconds.

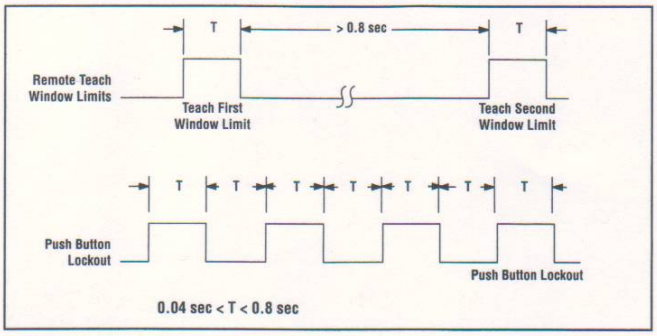

Figure 5. Timing for remote TEACH programming

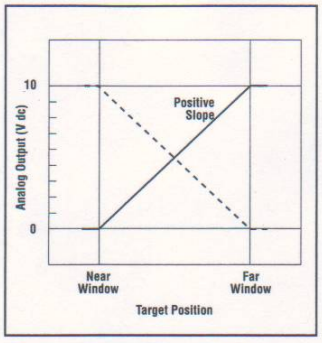

Figure 6. Analog voltage output as a function of target position (loss of signal – 0 Volts)

Run Mode
NOTE: All LED indicators momentarily go OFF when the sensor changes state between RUN and TEACH modes.

Range LED
When the sensor detects a target within its sensing range (either 100 to 300 mm for visible-beam models, or 100 to 400 mm for infrared beam models) the LED will be solid green. In the absence of a target, the Range LED is solid red. Refer to the Indicator Status table on page 3.

Teach/Output LED
In RUN mode, the Output LED is yellow when a target is sensed within the programmed window limits; otherwise the Output LED is red. Refer to the Indicator Status table on page 3.

Analog Output
The Q50 gauging sensor may be programmed for either a positive or a negative output slope (see Figure 6). If the near limit is taught first, the slope will be positive; if the far limit is taught first, the slope will be negative. Banner's patented scalable analog output automatically distributes the output signal over the width of the programmed sensing window. (Output is either 0 to 10V or 4 to 20 mA, depending on model.)

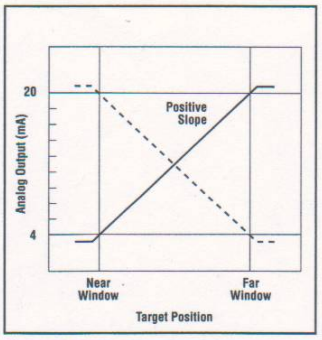

Figure 7. Analog current output as a function of target position (loss of signal – 3.6 mA)

Banner Engineering Corp. • Minneapolis, U.S.A.
www.bannerengineering.com • Tel: 763.544.3164

L-GAGE Q50 – Analog Output Sensor

Installation Notes

Some targets (those with a stepped plane facing the sensor, a boundary line, or rounded targets) pose specific problems for sensing distances. For such applications, see Figure 8 for suggested mounting orientations.

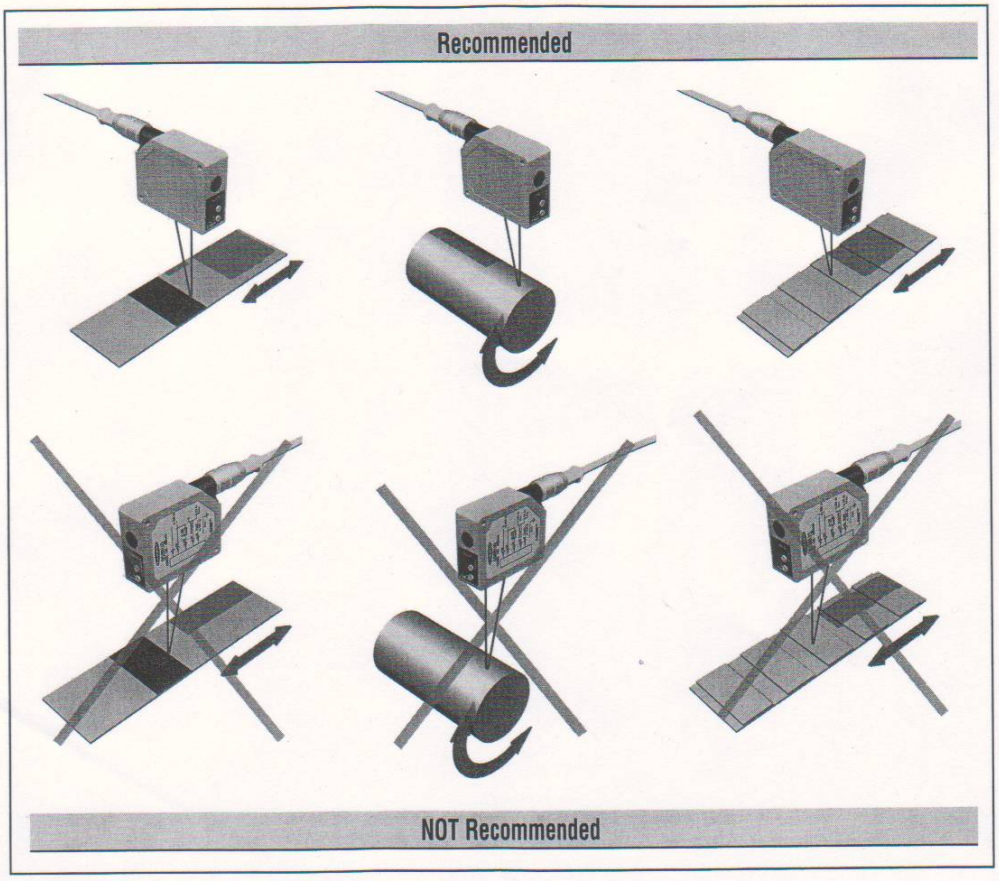

Figure 8. Sensor orientations for typical targets

L-GAGE Q50 – Analog Output Sensor

L-GAGE Q50 Analog Output Sensor Specifications

Sensing Range	**Q50BV:** 100 to 300 mm (3.9" to 11.8")	**Q50B:** 100 to 400 mm (3.9" to 15.7")
Supply Voltage	15 to 30V dc (10% maximum ripple); 70 mA max. (exclusive of load)	
Supply Protection Circuitry	Protected against reverse polarity and transient overvoltages	
Delay at Power-up	2 seconds	
Sensing Beam	**Wave length** **Q50BV:** 685 nm (typical) **Q50B:** 880 nm (typical) **Beam Size** **Q50BV:** 20 mm dia. (max.) **Q50B:** 20 mm dia. (max.)	
Output Configuration	**Depending on model** **4-20 mA current sourcing models:** 1 kΩ max. load @ 24V dc. Max. load = [(V_{CC} -4.5)/0.02]Ω Loss of signal or target outside of sensor range: 3.6 mA **0-10V voltage sourcing models:** 15 mA max. Loss of signal or target outside of sensor range: 0V	
Output Protection	Protected against short circuit conditions	
Output Response Time	**Analog Output** / **Average Interval** / **Update Rate** / **-3 dB Frequency Response** **Fast:** 4 ms 1 ms 112 Hz **Slow:** 64 ms 4 ms 7 Hz	
Resolution	See Figure 3 for typical values **Target Distance:** 200 mm **Slow Response:** 1 mm max. **Fast Response:** 4 mm max.	
Linearity	±3 mm	
Color Sensitivity (typical)	See Figure 4	
Temperature Drift	**From 0° to 50°C:** -0.25 mm/°C **From -10° to 55°C:** -0.35 mm/°C	
Remote and Speed Input Impedance	15 kΩ	
Remote Teach Input	**To Teach:** Connect gray wire to +5 to 30V dc **To Disable:** Connect gray wire to 0 to +2V dc (or open connection)	
Adjustments	**Response Speed:** **Fast Speed:** Connect black wire to +5 to 30V dc **Slow Speed:** Connect black wire to 0 to +2V dc (or open connection)	
Indicators	**Range LED Indicator (green/red)** Green — Target is within sensing range Red — Target is outside sensing range OFF — Sensor Power OFF **Teach/Output LED Indicator (yellow/red)** Yellow — Target is within taught window limits OFF — Target is outside taught window limits Red — Sensor is in TEACH mode	
Minimum Taught Window	**Target distance at 300 mm:** 50 mm window **Target distance at 125 mm:** 10 mm window	
Ambient Light Immunity	<10,000 Lux	

Banner Engineering Corp. • Minneapolis, U.S.A.
www.bannerengineering.com • Tel: 763.544.3164

L-GAGE Q50 – Analog Output Sensor

L-GAGE Q50 Analog Output Sensor Specifications (continued)

Construction	**Housing:** Molded ABS/Polycarbonate **Window Lens:** Acrylic
Environmental Rating	IEC IP67, NEMA 6
Connections	2 m or 9 m 5-conductor PVC-covered attached cable or 5-pin Euro-style quick disconnect
Operating Conditions	**Temperature:** -10° to +55°C (+14° to +131°F) **Max. Rel. Humidity:** 90% at +50°C (non-condensing)
Vibration and Mechanical Shock	All models meet Mil. Std. 202F requirements. Method 201A (Vibration: 10 to 60Hz max. double amplitude 0.06", maximum acceleration 10G). Also meets IEC 947-5-2 requirements: 30G, 11 ms duration, half sine wave.
Application Notes	Allow 15-minute warm-up for maximum linearity.
Hardware	M3 hardware is included.

L-GAGE Q50 Dimensions

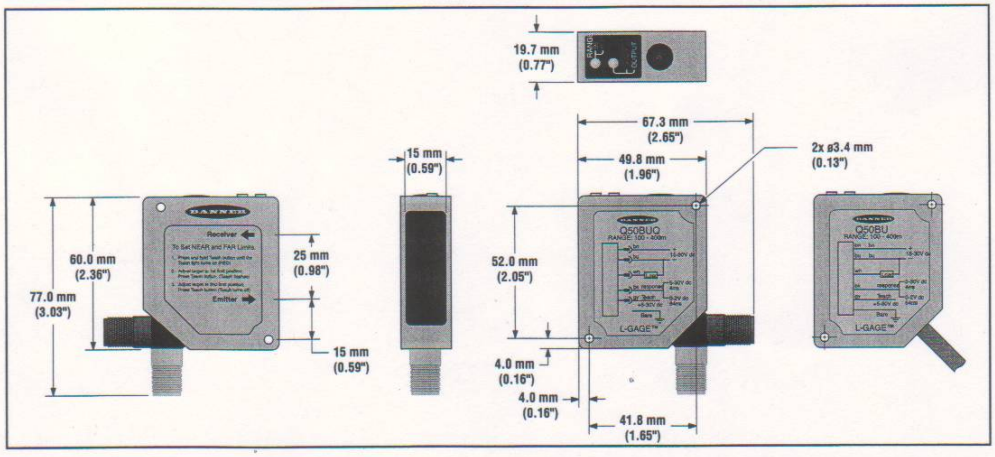

L-GAGE Q50 Hookups

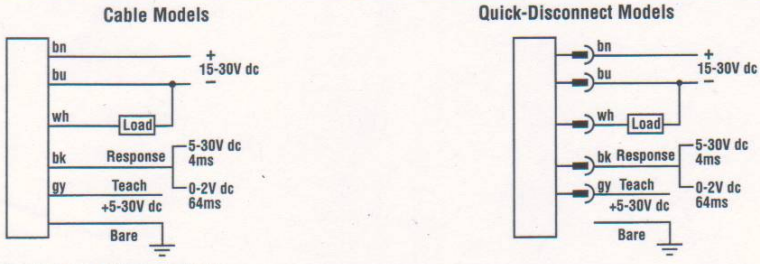

L-GAGE Q50 – Analog Output Sensor

Accessories

Euro-Style Quick-Disconnect Cables

Style	Model	Length	Connector	Pin-out
5-Pin Euro Straight	MQDEC2-506 MQDEC2-515 MQDEC2-530	2 m (6.5') 5 m (15') 9 m (30')	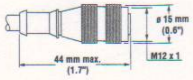	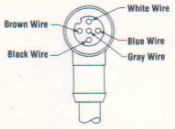
5-Pin Euro Right-angle	MQDEC2-506RA MQDEC2-515RA MQDEC2-530RA	2 m (6.5') 5 m (15') 9 m (30')	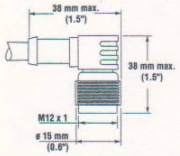	

Mounting Brackets

SMBQ50	• Right-angle bracket • 14-ga., 304 Stainless Steel

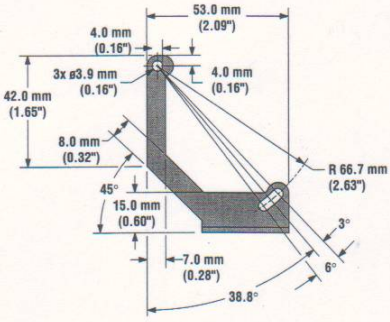

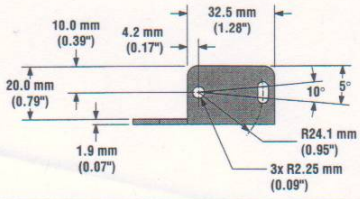

BANNER®
more sensors, more solutions

WARRANTY: Banner Engineering Corp. warrants its products to be free from defects for one year. Banner Engineering Corp. will repair or replace, free of charge, any product of its manufacture found to be defective at the time it is returned to the factory during the warranty period. This warranty does not cover damage or liability for the improper application of Banner products. This warranty is in lieu of any other warranty either expressed or implied.

Banner Engineering Corp., 9714 Tenth Ave. No., Minneapolis, MN 55441 • Phone: 763.544.3164 • www.bannerengineering.com • Email: sensors@baneng.com

APPENDIX B – WALL #4 DATA OUTPUT

The following plots display the time versus table displacement and time versus tip displacement for the 5000 cycles of testing for Wall #4.

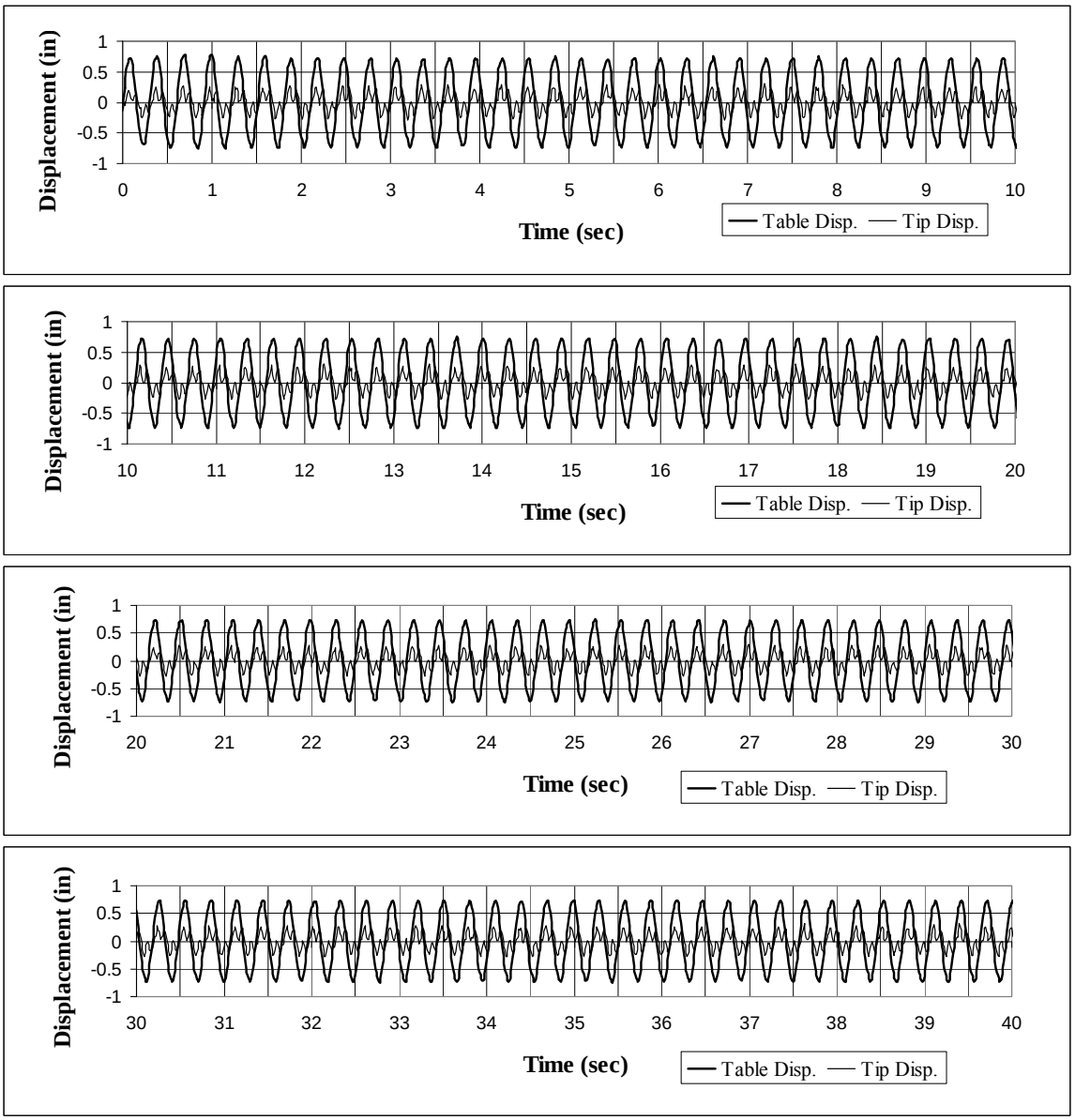

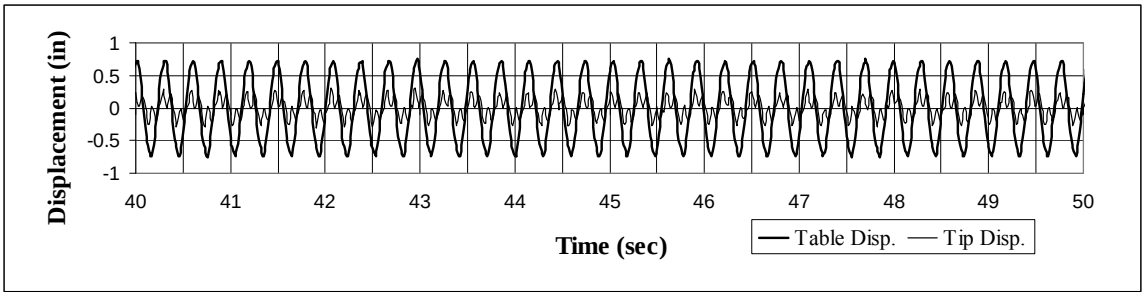
Displacement (in)
1
0.5
0
-0.5
-1
40 41 42 43 44 45 46 47 48 49 50
Time (sec)
Table Disp. Tip Disp.

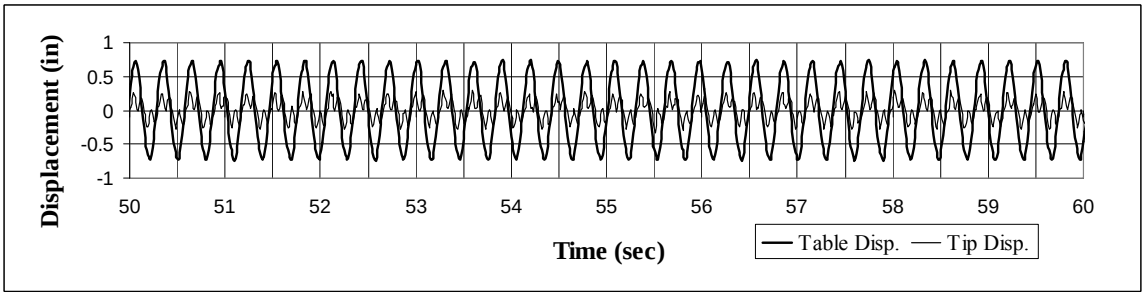
Displacement (in)
1
0.5
0
-0.5
-1
50 51 52 53 54 55 56 57 58 59 60
Time (sec)
Table Disp. Tip Disp.

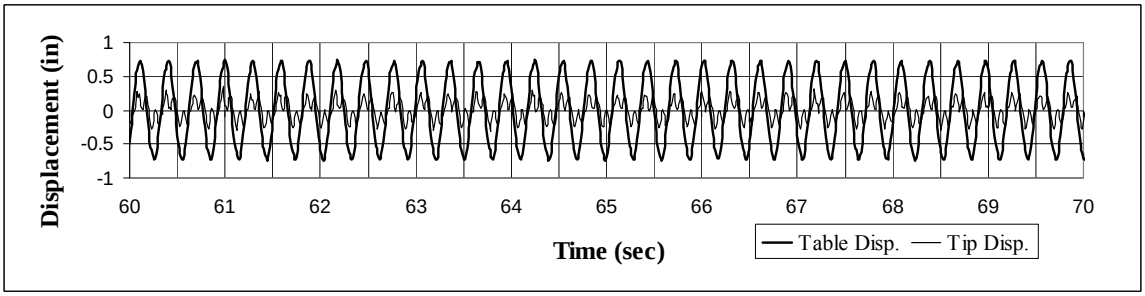
Displacement (in)
1
0.5
0
-0.5
-1
60 61 62 63 64 65 66 67 68 69 70
Time (sec)
Table Disp. Tip Disp.

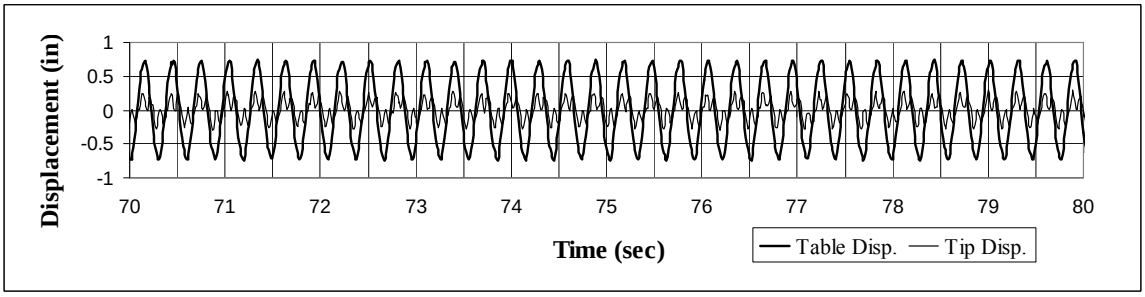
Displacement (in)
1
0.5
0
-0.5
-1
70 71 72 73 74 75 76 77 78 79 80
Time (sec)
Table Disp. Tip Disp.

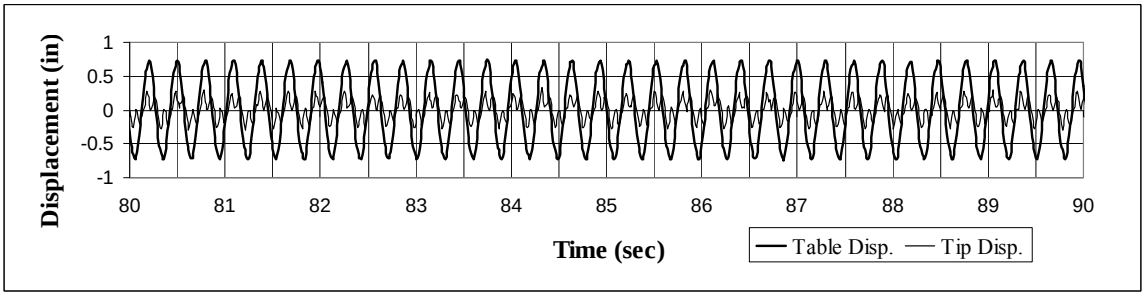
Displacement (in)
1
0.5
0
-0.5
-1
80 81 82 83 84 85 86 87 88 89 90
Time (sec)
Table Disp. Tip Disp.

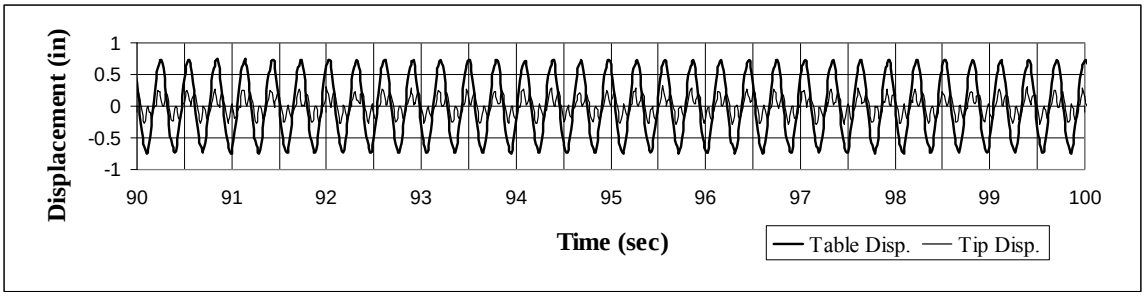
Displacement (in)
1
0.5
0
-0.5
-1
90 91 92 93 94 95 96 97 98 99 100
Time (sec)
Table Disp. Tip Disp.

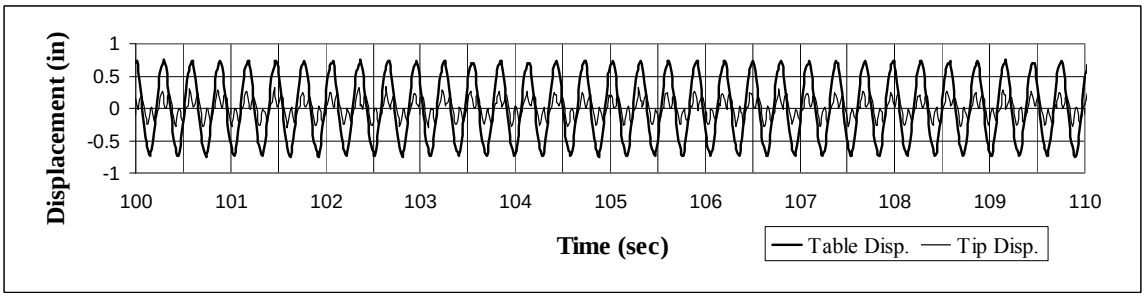
Displacement (in)
1
0.5
0
-0.5
-1
100 101 102 103 104 105 106 107 108 109 110
Time (sec)
Table Disp. Tip Disp.

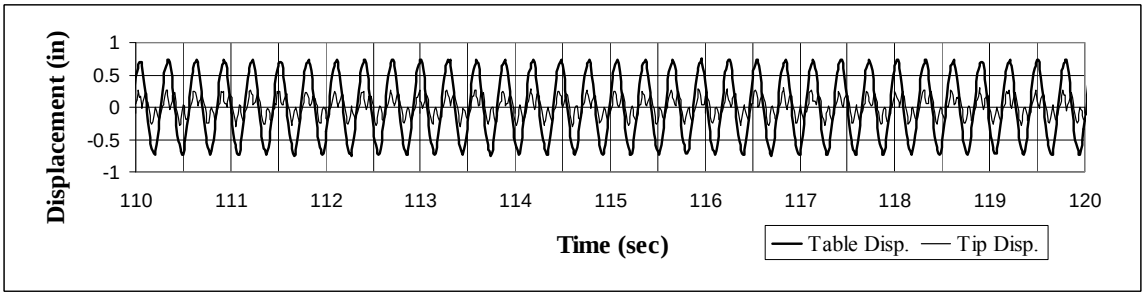
Displacement (in)
1
0.5
0
-0.5
-1
110 111 112 113 114 115 116 117 118 119 120
Time (sec)
Table Disp. Tip Disp.

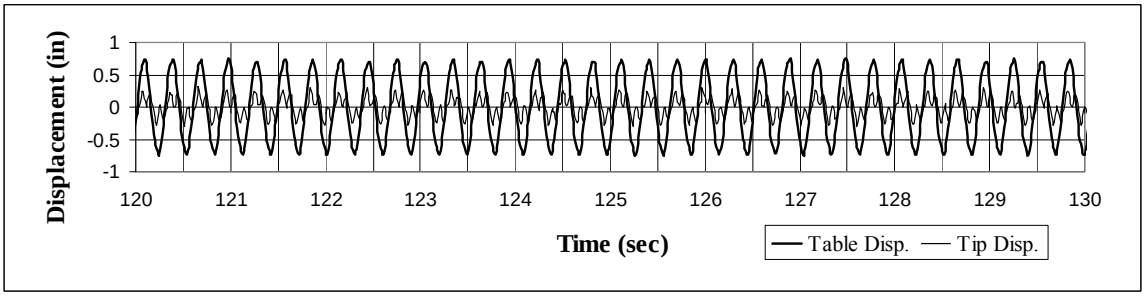
Displacement (in)
1
0.5
0
-0.5
-1
120 121 122 123 124 125 126 127 128 129 130
Time (sec)
Table Disp. Tip Disp.

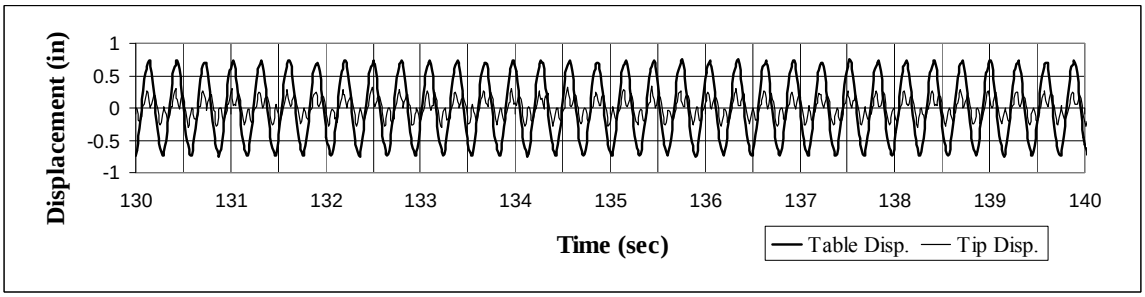
Displacement (in)
1
0.5
0
-0.5
-1
130 131 132 133 134 135 136 137 138 139 140
Time (sec)
Table Disp. Tip Disp.

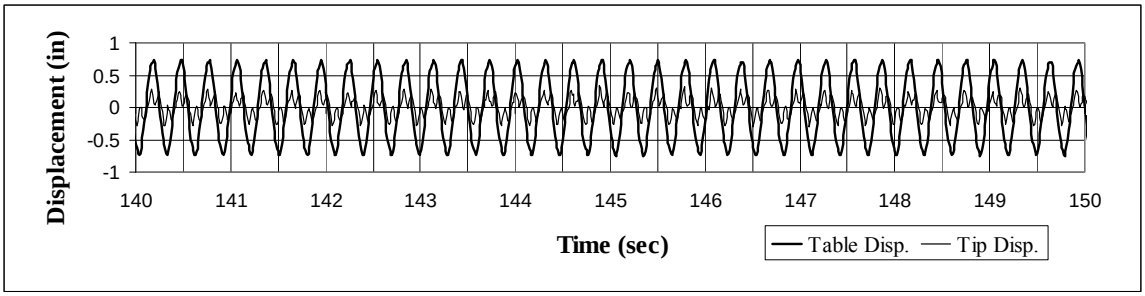
Displacement (in)
1
0.5
0
-0.5
-1
140 141 142 143 144 145 146 147 148 149 150
Time (sec)
Table Disp.
Tip Disp.

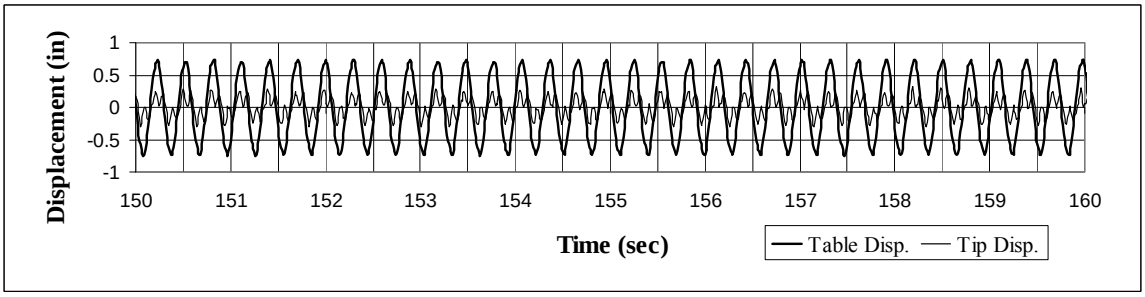
Displacement (in)
1
0.5
0
-0.5
-1
150 151 152 153 154 155 156 157 158 159 160
Time (sec)
Table Disp.
Tip Disp.

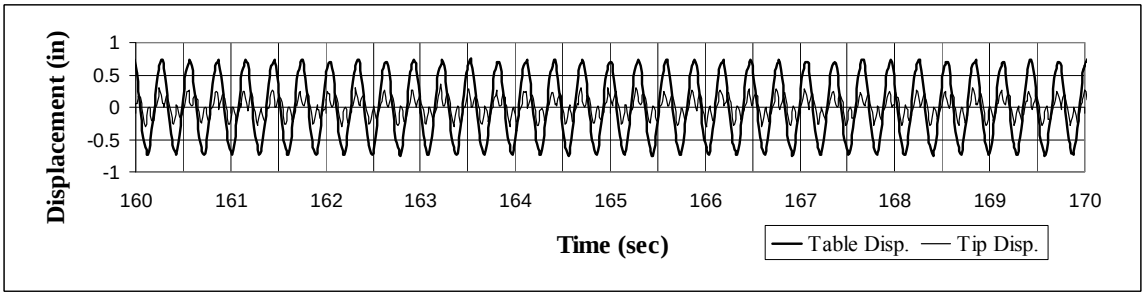
Displacement (in)
1
0.5
0
-0.5
-1
160 161 162 163 164 165 166 167 168 169 170
Time (sec)
Table Disp.
Tip Disp.

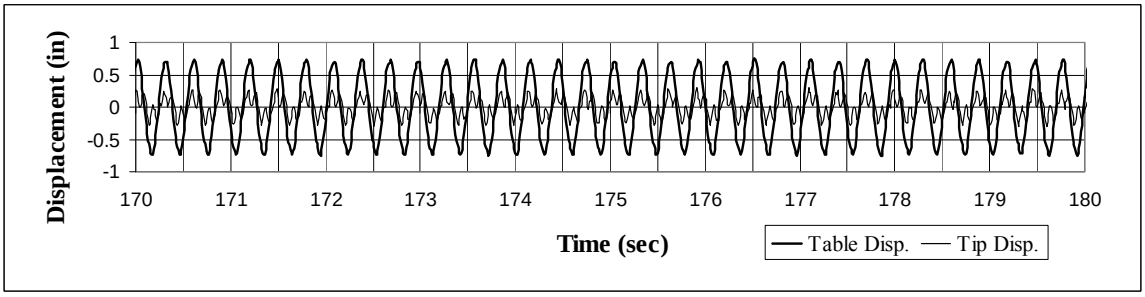
Displacement (in)
1
0.5
0
-0.5
-1
170 171 172 173 174 175 176 177 178 179 180
Time (sec)
Table Disp.
Tip Disp.

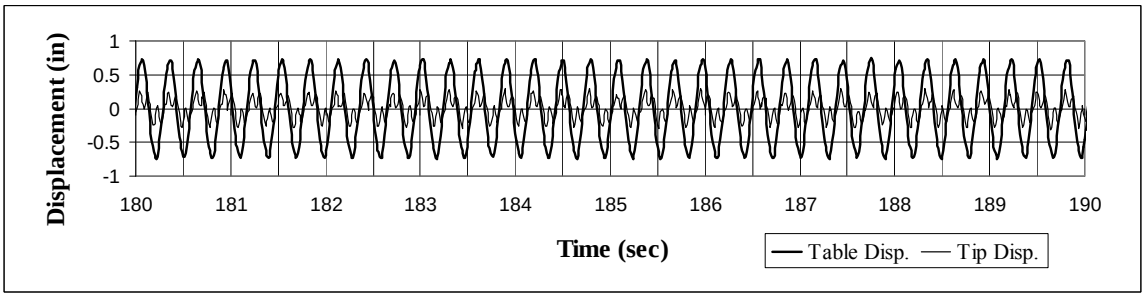
Displacement (in)
1
0.5
0
-0.5
-1
180 181 182 183 184 185 186 187 188 189 190
Time (sec)
Table Disp.
Tip Disp.

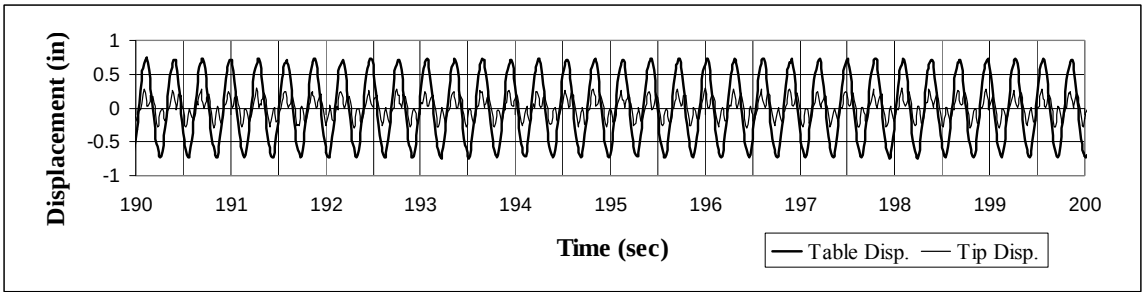
Displacement (in)
1
0.5
0
-0.5
-1
190 191 192 193 194 195 196 197 198 199 200
Time (sec)
Table Disp. Tip Disp.

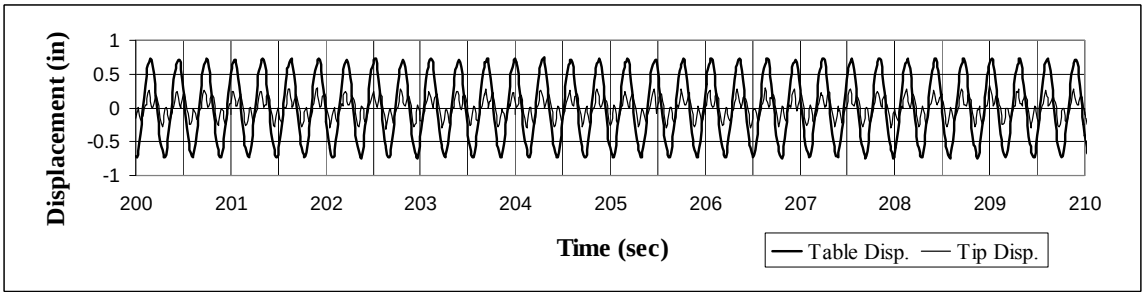
Displacement (in)
1
0.5
0
-0.5
-1
200 201 202 203 204 205 206 207 208 209 210
Time (sec)
Table Disp. Tip Disp.

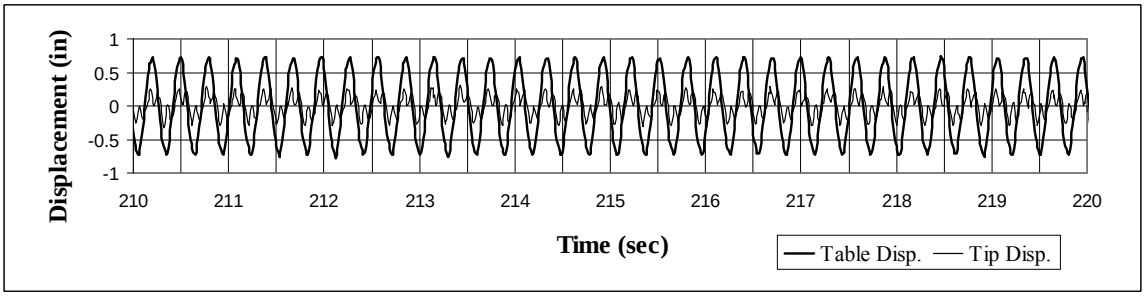
Displacement (in)
1
0.5
0
-0.5
-1
210 211 212 213 214 215 216 217 218 219 220
Time (sec)
Table Disp. Tip Disp.

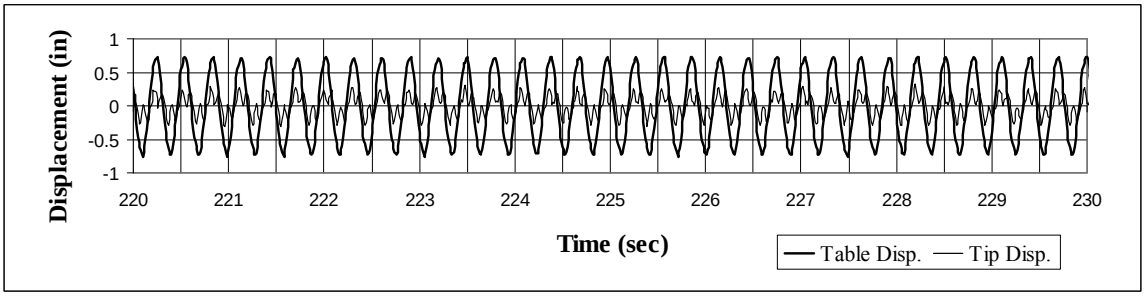
Displacement (in)
1
0.5
0
-0.5
-1
220 221 222 223 224 225 226 227 228 229 230
Time (sec)
Table Disp. Tip Disp.

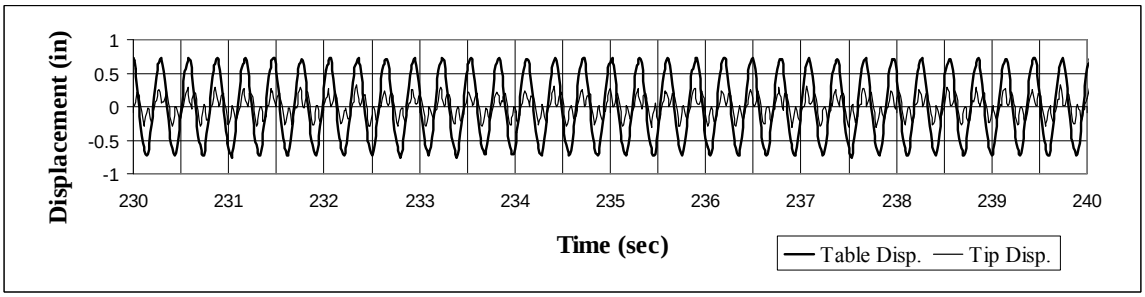
Displacement (in)
1
0.5
0
-0.5
-1
230 231 232 233 234 235 236 237 238 239 240
Time (sec)
Table Disp. Tip Disp.

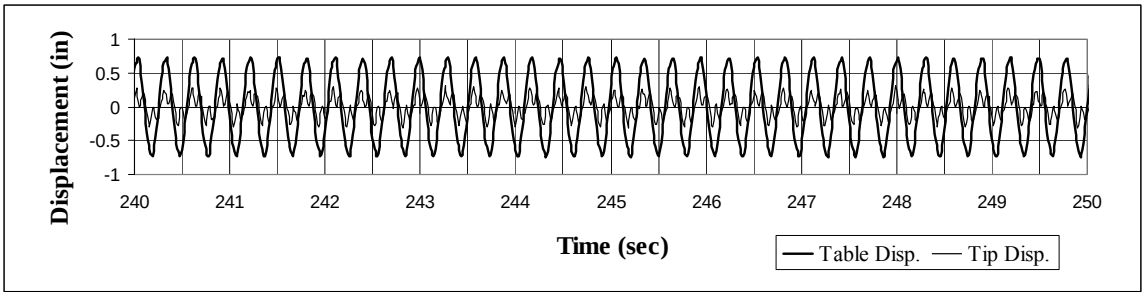
Displacement (in)
1
0.5
0
-0.5
-1
240 241 242 243 244 245 246 247 248 249 250
Time (sec)
Table Disp. Tip Disp.

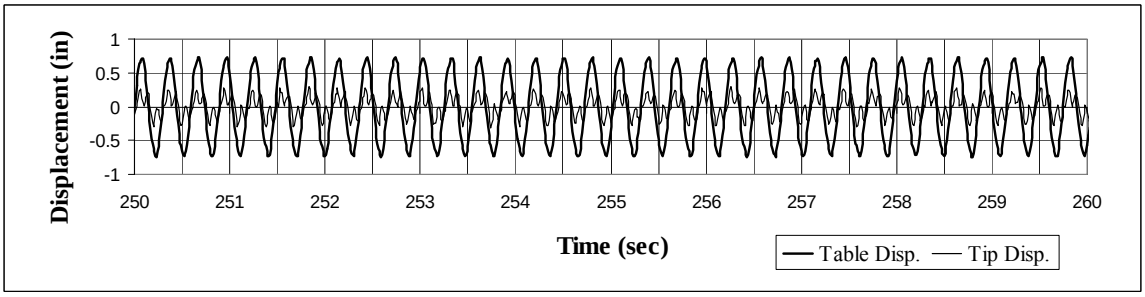
Displacement (in)
1
0.5
0
-0.5
-1
250 251 252 253 254 255 256 257 258 259 260
Time (sec)
Table Disp. Tip Disp.

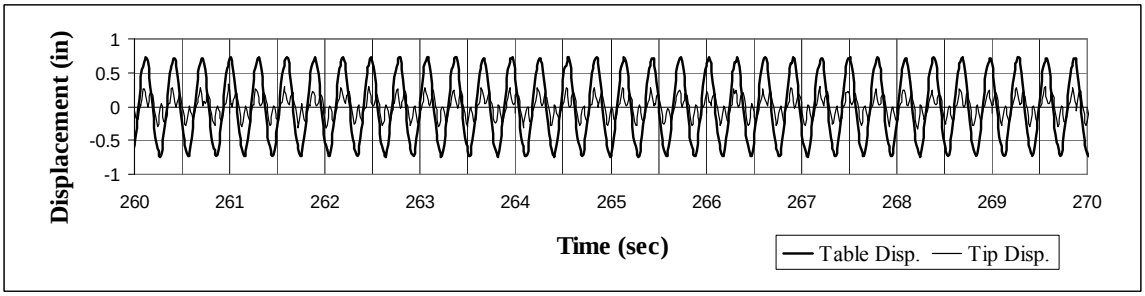
Displacement (in)
1
0.5
0
-0.5
-1
260 261 262 263 264 265 266 267 268 269 270
Time (sec)
Table Disp. Tip Disp.

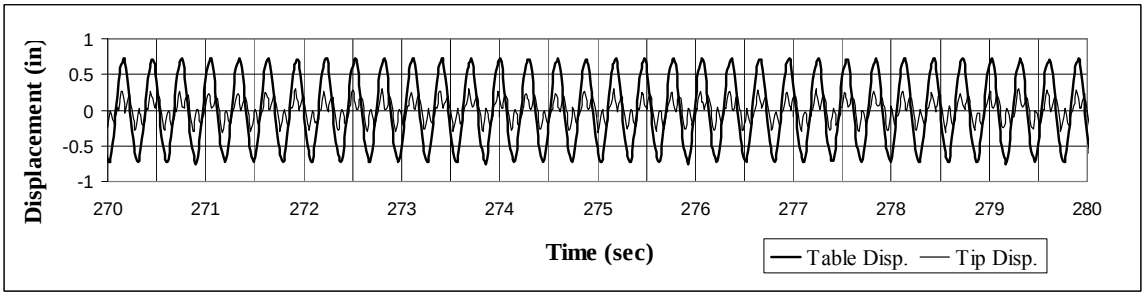
Displacement (in)
1
0.5
0
-0.5
-1
270 271 272 273 274 275 276 277 278 279 280
Time (sec)
Table Disp. Tip Disp.

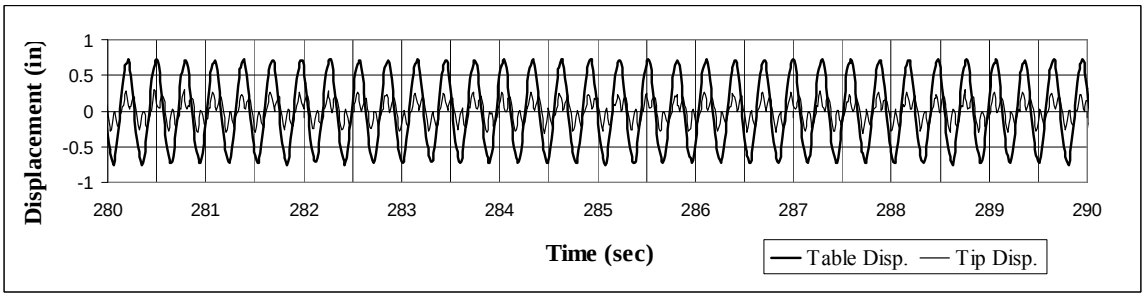
Displacement (in)
1
0.5
0
-0.5
-1
280 281 282 283 284 285 286 287 288 289 290
Time (sec)
Table Disp. Tip Disp.

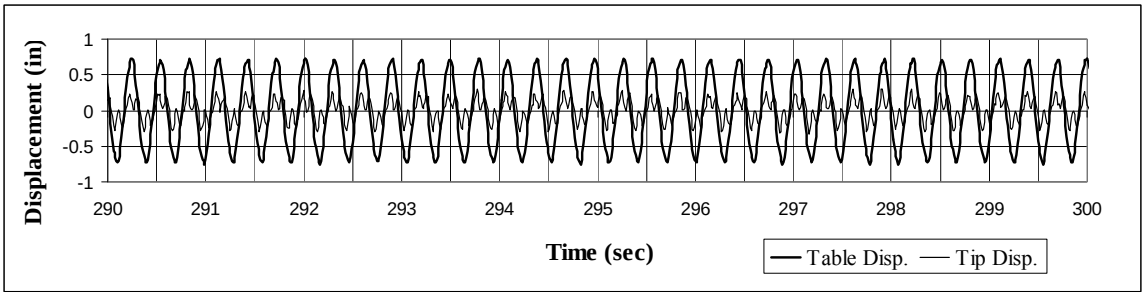
Displacement (in)
1
0.5
0
-0.5
-1
290 291 292 293 294 295 296 297 298 299 300
Time (sec)
Table Disp. Tip Disp.

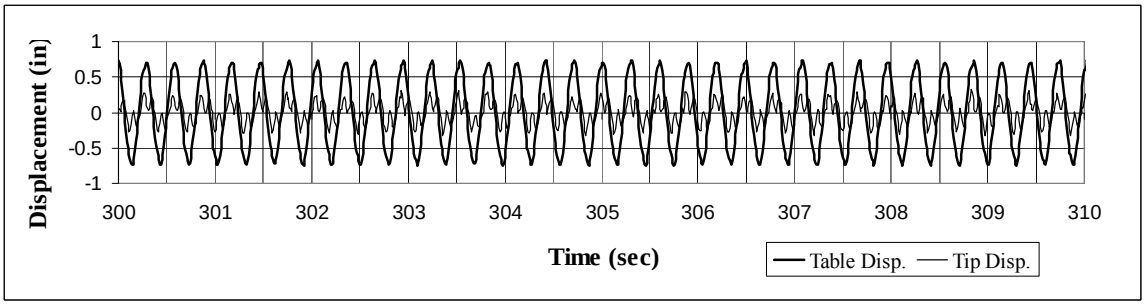
Displacement (in)
1
0.5
0
-0.5
-1
300 301 302 303 304 305 306 307 308 309 310
Time (sec)
Table Disp. Tip Disp.

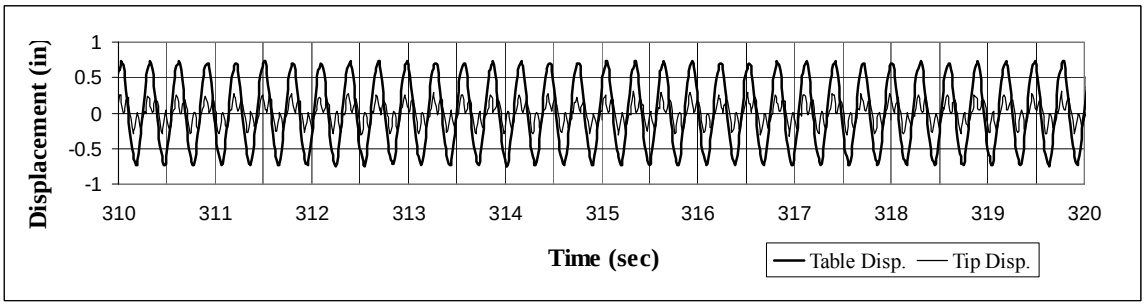
Displacement (in)
1
0.5
0
-0.5
-1
310 311 312 313 314 315 316 317 318 319 320
Time (sec)
Table Disp. Tip Disp.

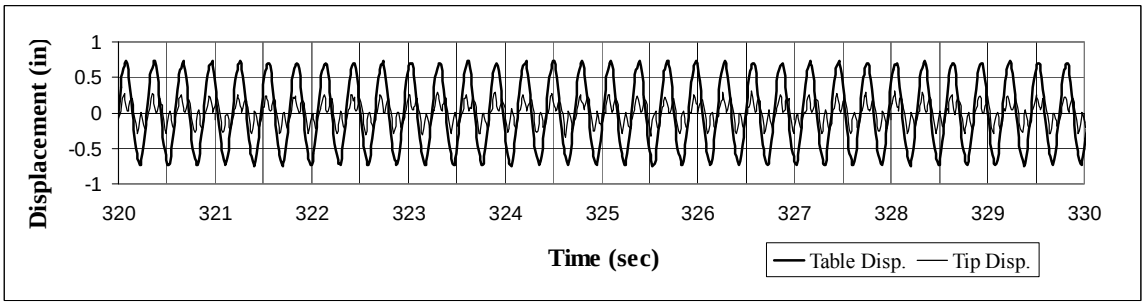
Displacement (in)
1
0.5
0
-0.5
-1
320 321 322 323 324 325 326 327 328 329 330
Time (sec)
Table Disp. Tip Disp.

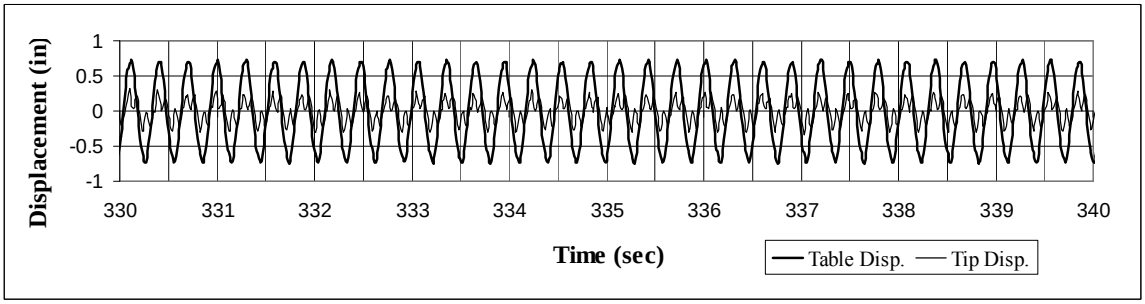
Displacement (in)
1
0.5
0
-0.5
-1
330 331 332 333 334 335 336 337 338 339 340
Time (sec)
Table Disp. Tip Disp.

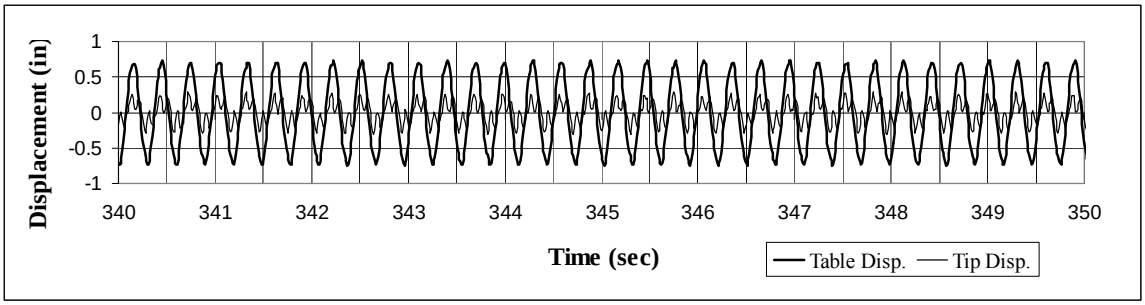
Displacement (in)
1
0.5
0
-0.5
-1
340 341 342 343 344 345 346 347 348 349 350
Time (sec)
Table Disp.
Tip Disp.

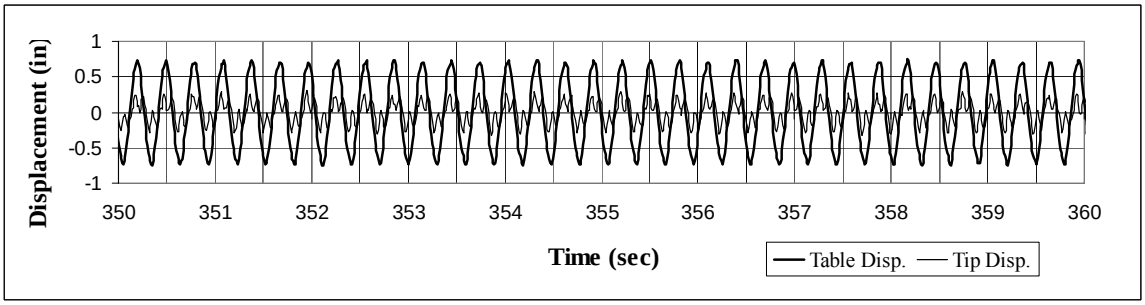
Displacement (in)
1
0.5
0
-0.5
-1
350 351 352 353 354 355 356 357 358 359 360
Time (sec)
Table Disp.
Tip Disp.

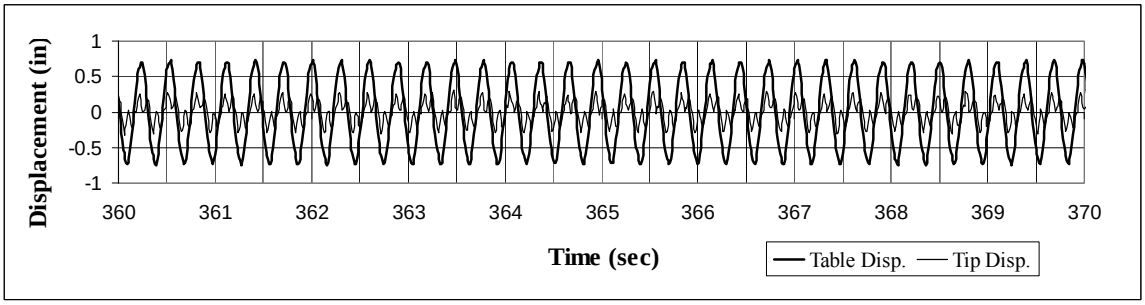
Displacement (in)
1
0.5
0
-0.5
-1
360 361 362 363 364 365 366 367 368 369 370
Time (sec)
Table Disp.
Tip Disp.

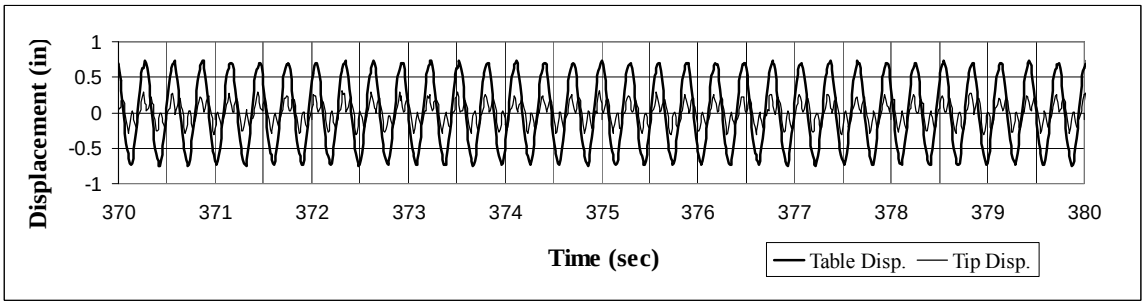
Displacement (in)
1
0.5
0
-0.5
-1
370 371 372 373 374 375 376 377 378 379 380
Time (sec)
Table Disp.
Tip Disp.

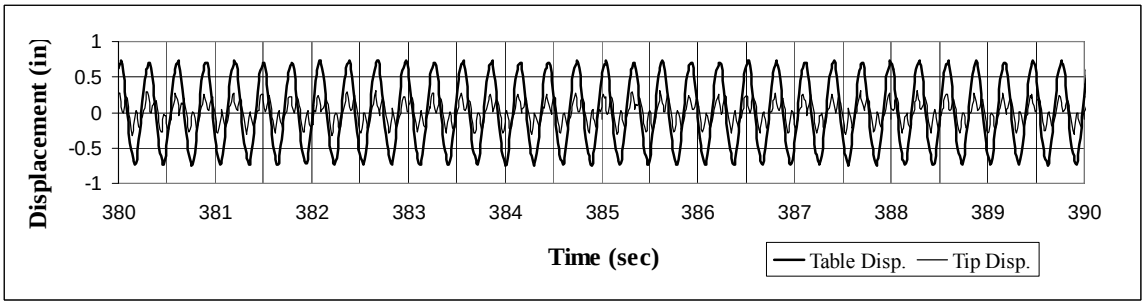
Displacement (in)
1
0.5
0
-0.5
-1
380 381 382 383 384 385 386 387 388 389 390
Time (sec)
Table Disp.
Tip Disp.

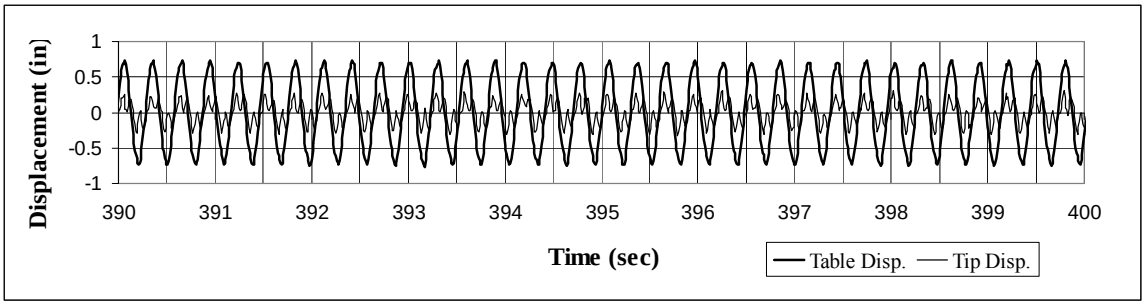
Displacement (in)
1
0.5
0
-0.5
-1
390 391 392 393 394 395 396 397 398 399 400
Time (sec)
Table Disp. Tip Disp.

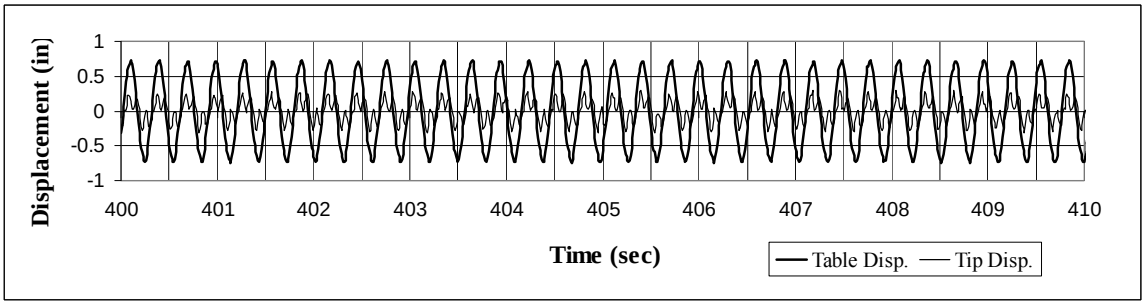
Displacement (in)
1
0.5
0
-0.5
-1
400 401 402 403 404 405 406 407 408 409 410
Time (sec)
Table Disp. Tip Disp.

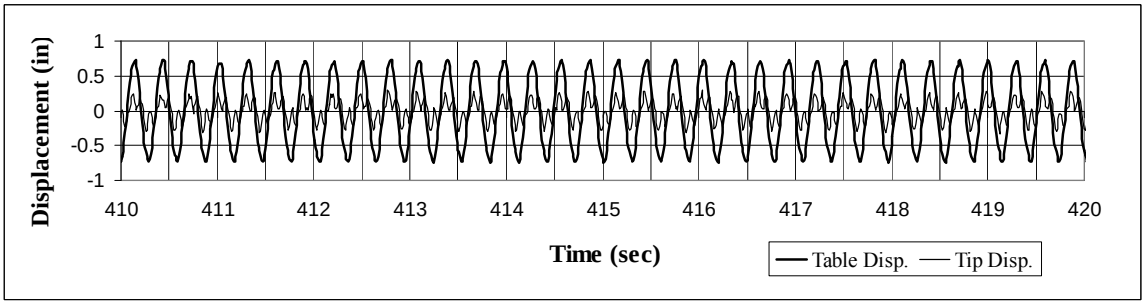
Displacement (in)
1
0.5
0
-0.5
-1
410 411 412 413 414 415 416 417 418 419 420
Time (sec)
Table Disp. Tip Disp.

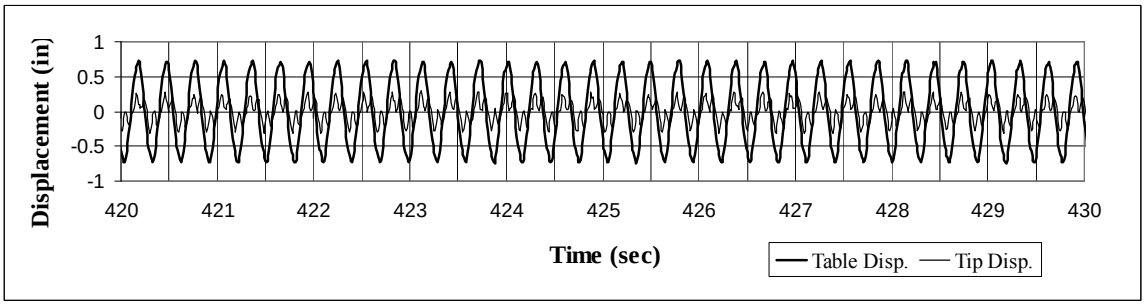
Displacement (in)
1
0.5
0
-0.5
-1
420 421 422 423 424 425 426 427 428 429 430
Time (sec)
Table Disp. Tip Disp.

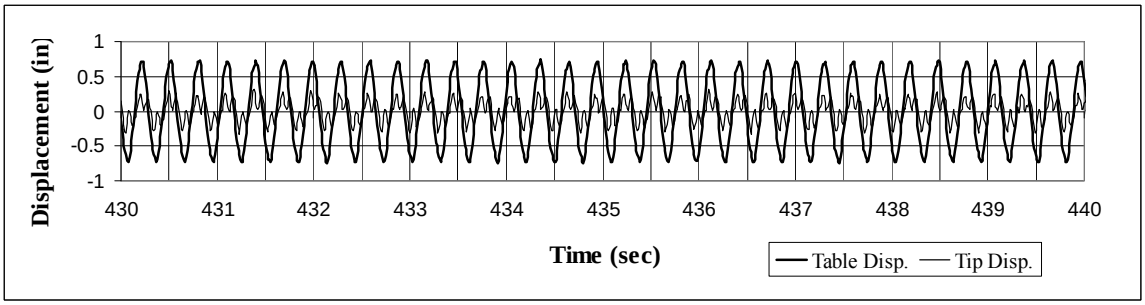
Displacement (in)
1
0.5
0
-0.5
-1
430 431 432 433 434 435 436 437 438 439 440
Time (sec)
Table Disp. Tip Disp.

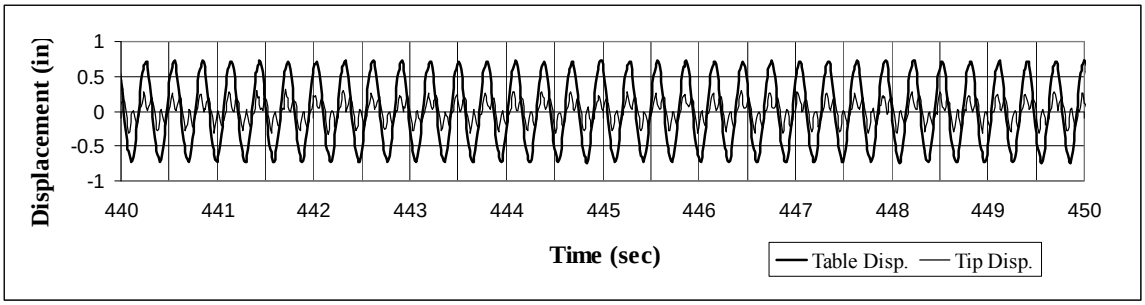
Displacement (in)
1
0.5
0
-0.5
-1
440 441 442 443 444 445 446 447 448 449 450
Time (sec)
Table Disp. Tip Disp.

f

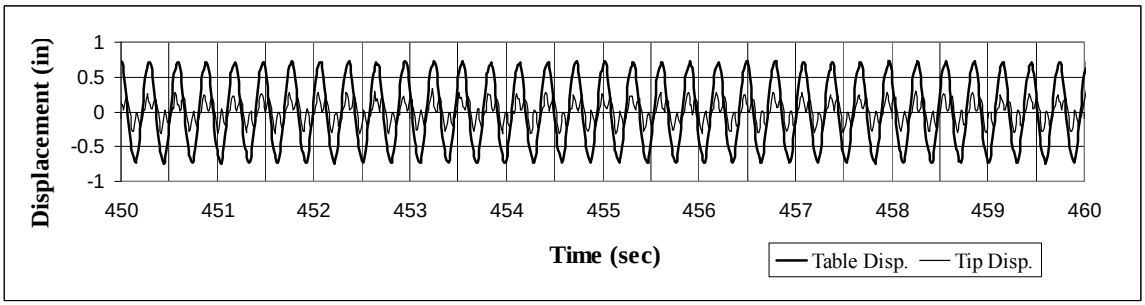
Displacement (in)
1
0.5
0
-0.5
-1
450 451 452 453 454 455 456 457 458 459 460
Time (sec)
Table Disp. Tip Disp.

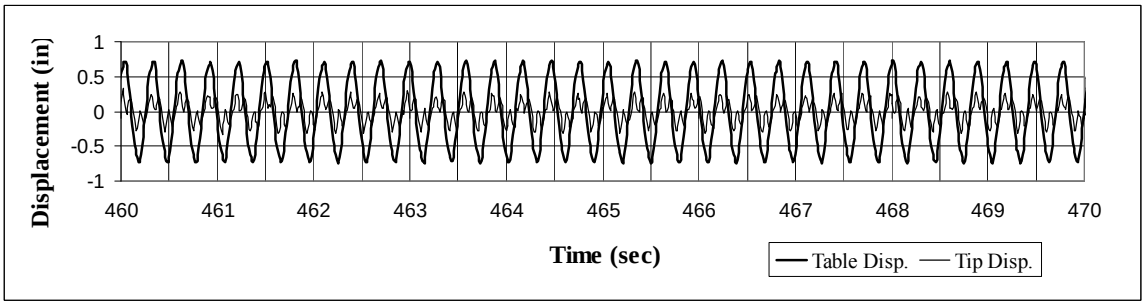
Displacement (in)
1
0.5
0
-0.5
-1
460 461 462 463 464 465 466 467 468 469 470
Time (sec)
Table Disp. Tip Disp.

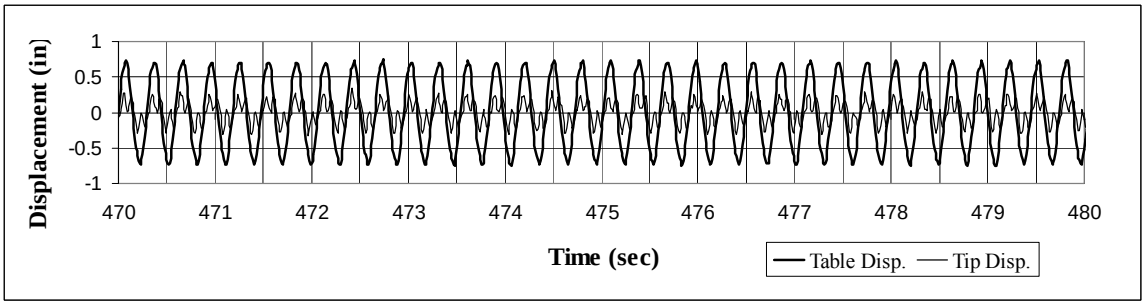
Displacement (in)
1
0.5
0
-0.5
-1
470 471 472 473 474 475 476 477 478 479 480
Time (sec)
Table Disp. Tip Disp.

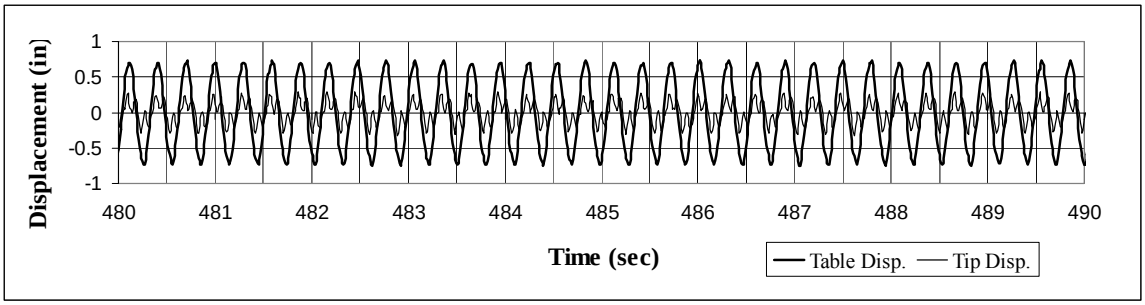
Displacement (in)
1
0.5
0
-0.5
-1
480 481 482 483 484 485 486 487 488 489 490
Time (sec)
Table Disp.
Tip Disp.

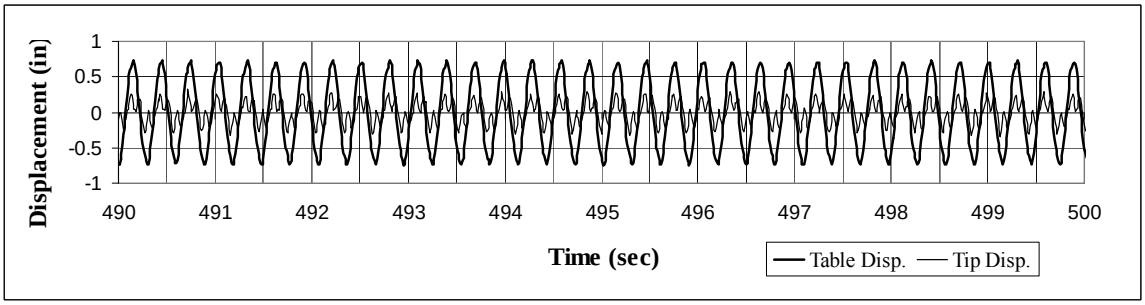
Displacement (in)
1
0.5
0
-0.5
-1
490 491 492 493 494 495 496 497 498 499 500
Time (sec)
Table Disp.
Tip Disp.

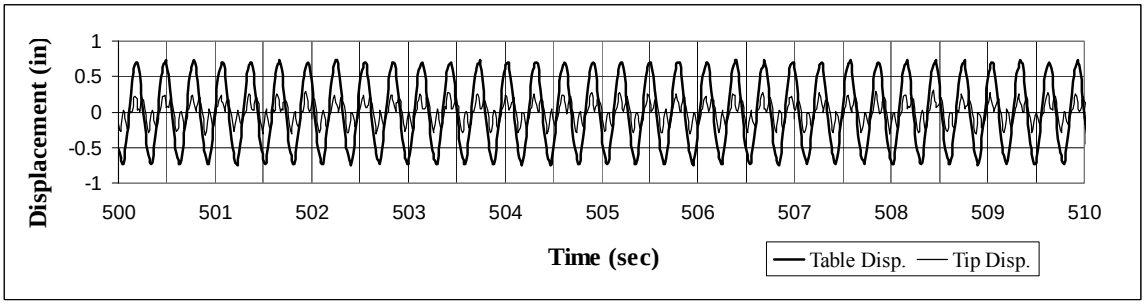
Displacement (in)
1
0.5
0
-0.5
-1
500 501 502 503 504 505 506 507 508 509 510
Time (sec)
Table Disp.
Tip Disp.

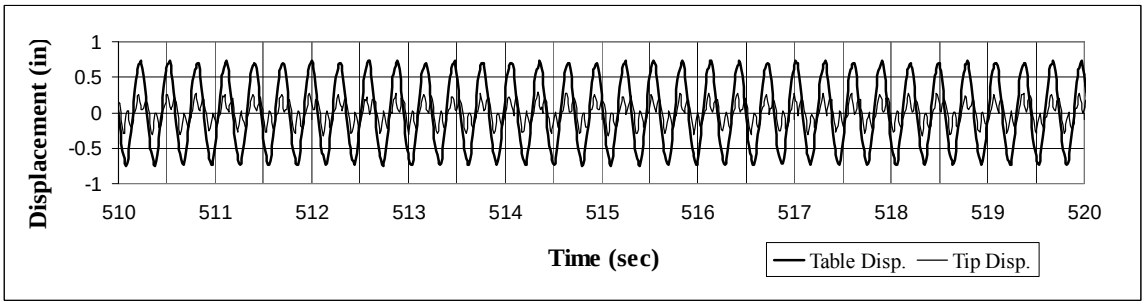
Displacement (in)
1
0.5
0
-0.5
-1
510 511 512 513 514 515 516 517 518 519 520
Time (sec)
Table Disp.
Tip Disp.

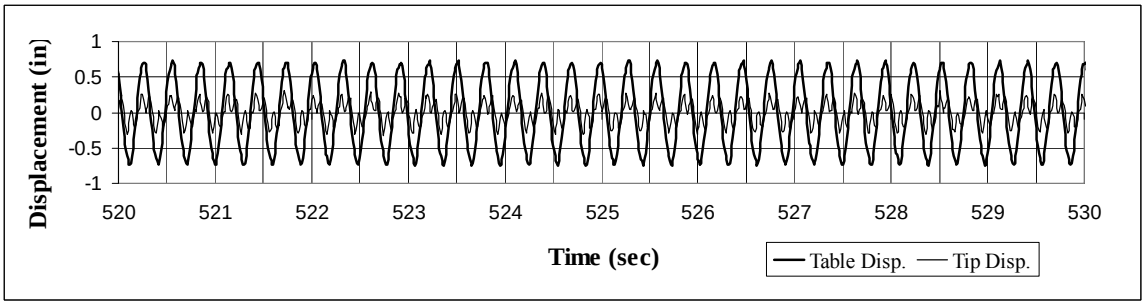
Displacement (in)
1
0.5
0
-0.5
-1
520 521 522 523 524 525 526 527 528 529 530
Time (sec)
Table Disp.
Tip Disp.

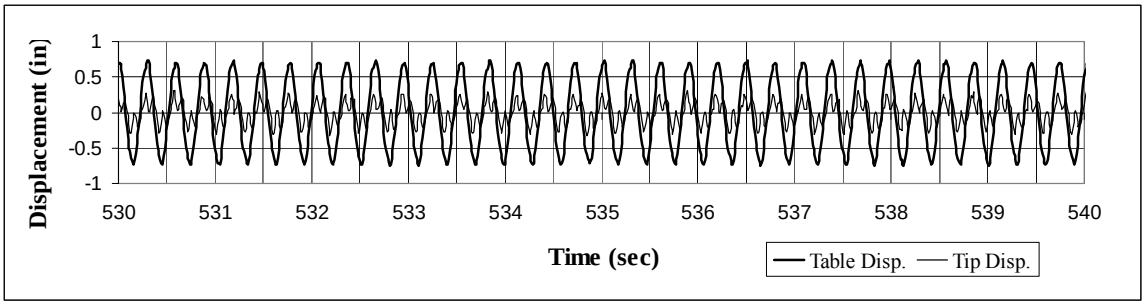
Displacement (in)
1
0.5
0
-0.5
-1
530 531 532 533 534 535 536 537 538 539 540
Time (sec)
Table Disp.
Tip Disp.

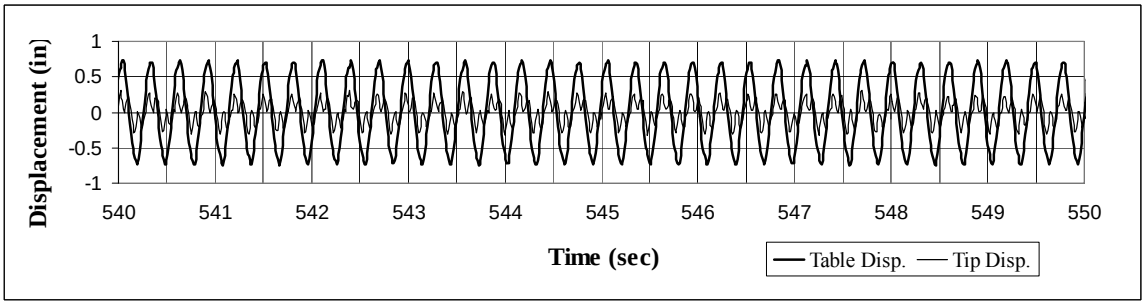
Displacement (in)
1
0.5
0
-0.5
-1
540 541 542 543 544 545 546 547 548 549 550
Time (sec)
Table Disp.
Tip Disp.

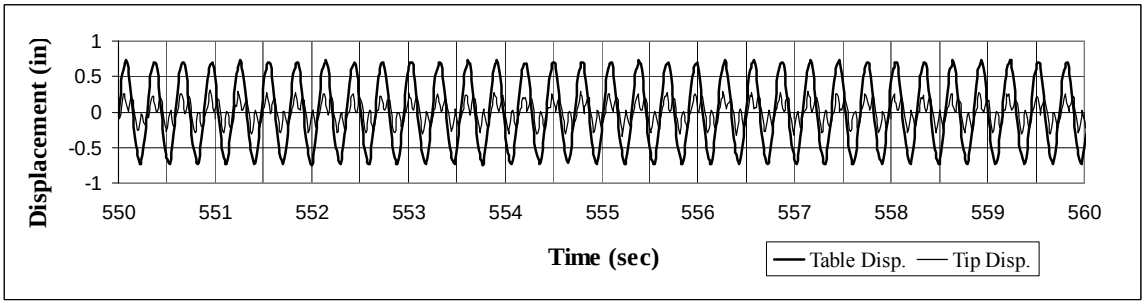
Displacement (in)
1
0.5
0
-0.5
-1
550 551 552 553 554 555 556 557 558 559 560
Time (sec)
Table Disp.
Tip Disp.

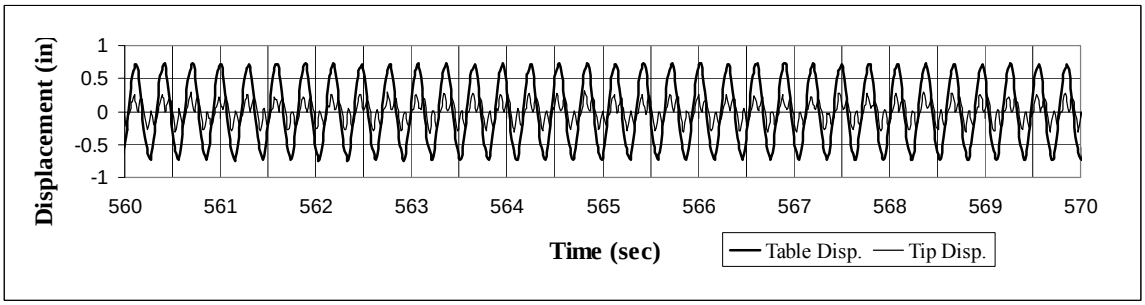
Displacement (in)
1
0.5
0
-0.5
-1
560 561 562 563 564 565 566 567 568 569 570
Time (sec)
Table Disp.
Tip Disp.

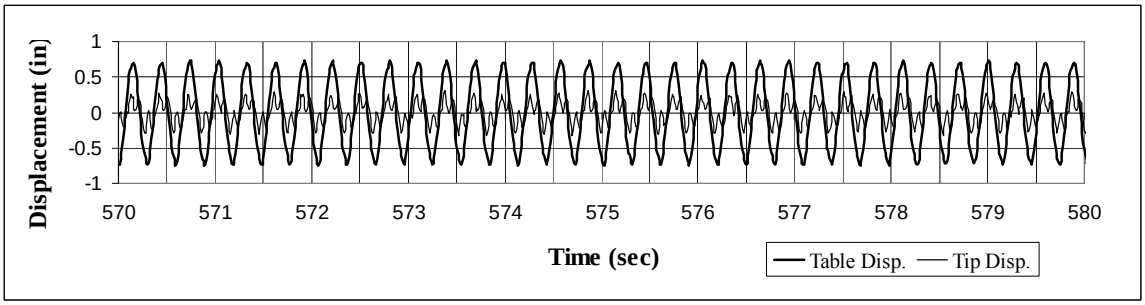
Displacement (in)
1
0.5
0
-0.5
-1
570 571 572 573 574 575 576 577 578 579 580
Time (sec)
Table Disp.
Tip Disp.

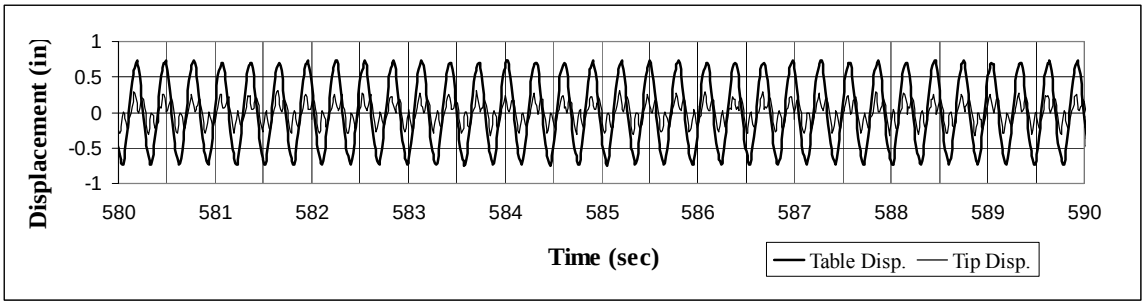
Displacement (in)
1
0.5
0
-0.5
-1
580 581 582 583 584 585 586 587 588 589 590
Time (sec)
Table Disp. Tip Disp.

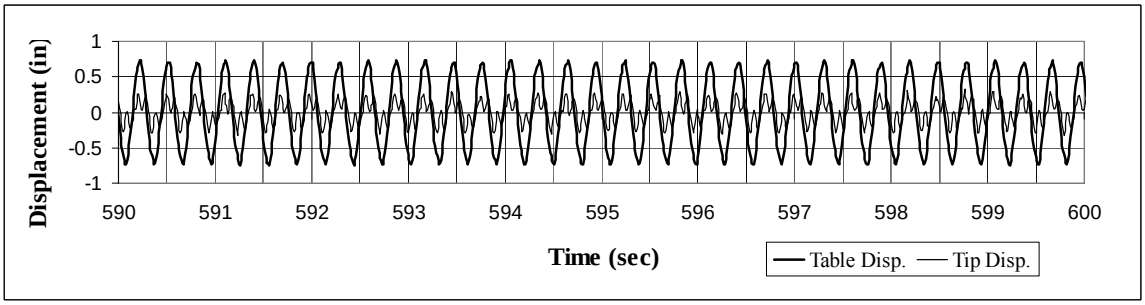
Displacement (in)
1
0.5
0
-0.5
-1
590 591 592 593 594 595 596 597 598 599 600
Time (sec)
Table Disp. Tip Disp.

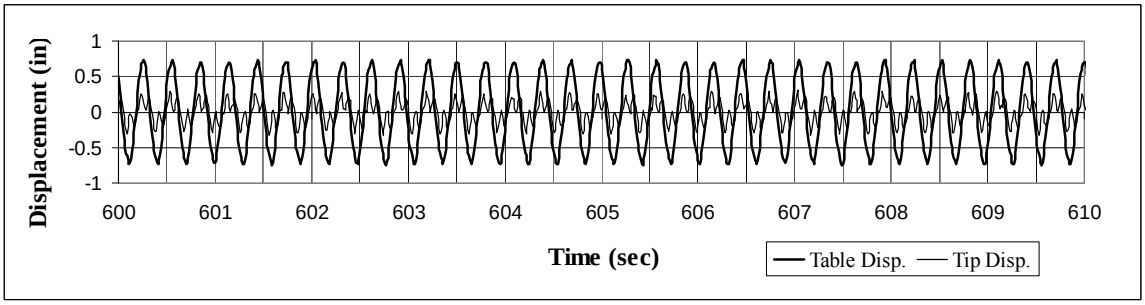
Displacement (in)
1
0.5
0
-0.5
-1
600 601 602 603 604 605 606 607 608 609 610
Time (sec)
Table Disp. Tip Disp.

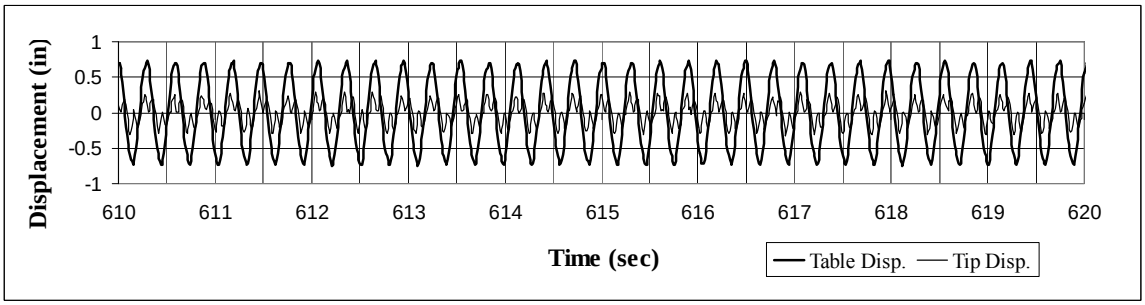
Displacement (in)
1
0.5
0
-0.5
-1
610 611 612 613 614 615 616 617 618 619 620
Time (sec)
Table Disp. Tip Disp.

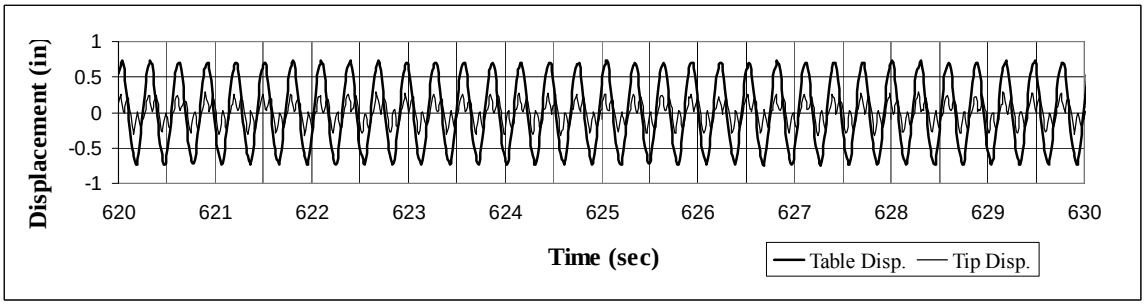
Displacement (in)
1
0.5
0
-0.5
-1
620 621 622 623 624 625 626 627 628 629 630
Time (sec)
Table Disp. Tip Disp.

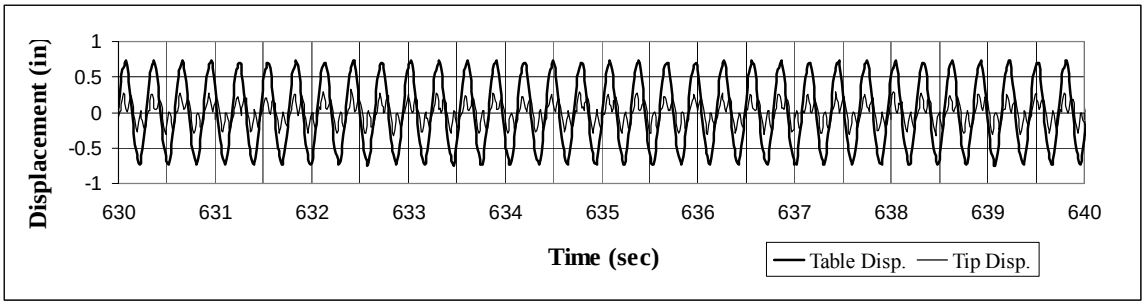
Displacement (in)
1
0.5
0
-0.5
-1
630 631 632 633 634 635 636 637 638 639 640
Time (sec)
Table Disp.
Tip Disp.

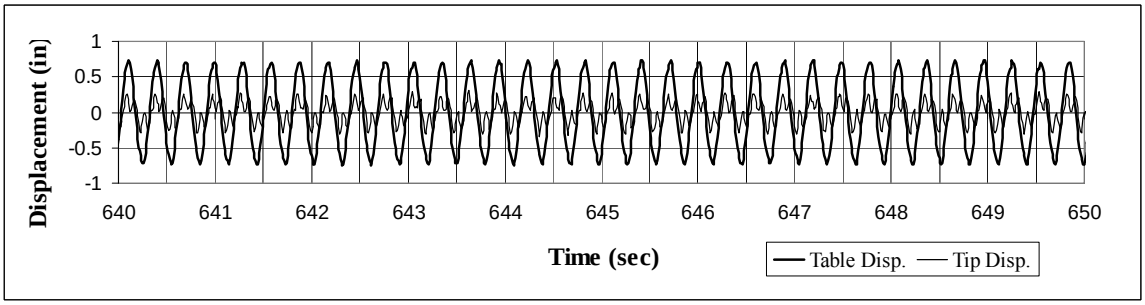
Displacement (in)
1
0.5
0
-0.5
-1
640 641 642 643 644 645 646 647 648 649 650
Time (sec)
Table Disp.
Tip Disp.

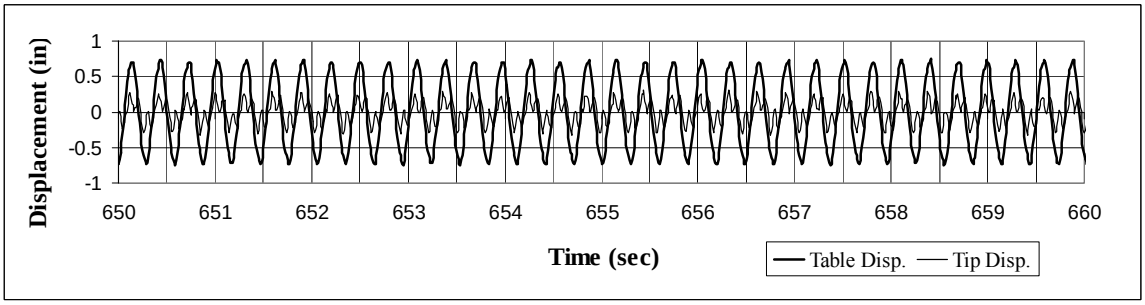
Displacement (in)
1
0.5
0
-0.5
-1
650 651 652 653 654 655 656 657 658 659 660
Time (sec)
Table Disp.
Tip Disp.

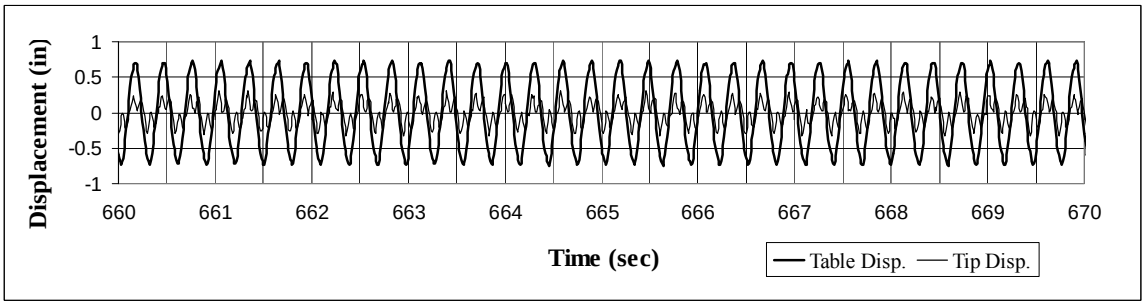
Displacement (in)
1
0.5
0
-0.5
-1
660 661 662 663 664 665 666 667 668 669 670
Time (sec)
Table Disp.
Tip Disp.

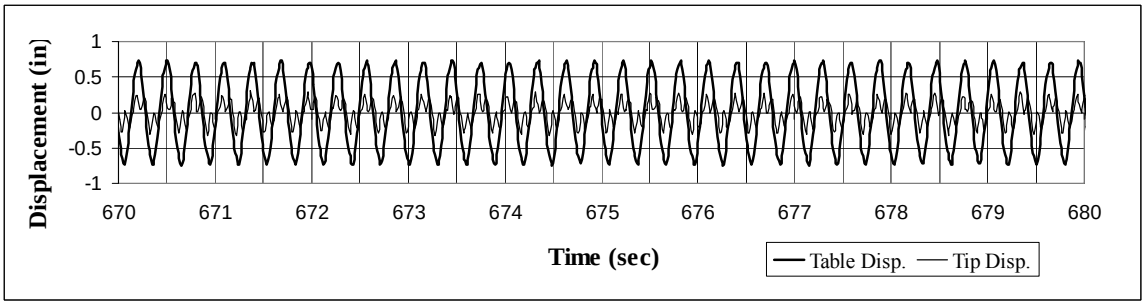
Displacement (in)
1
0.5
0
-0.5
-1
670 671 672 673 674 675 676 677 678 679 680
Time (sec)
Table Disp.
Tip Disp.

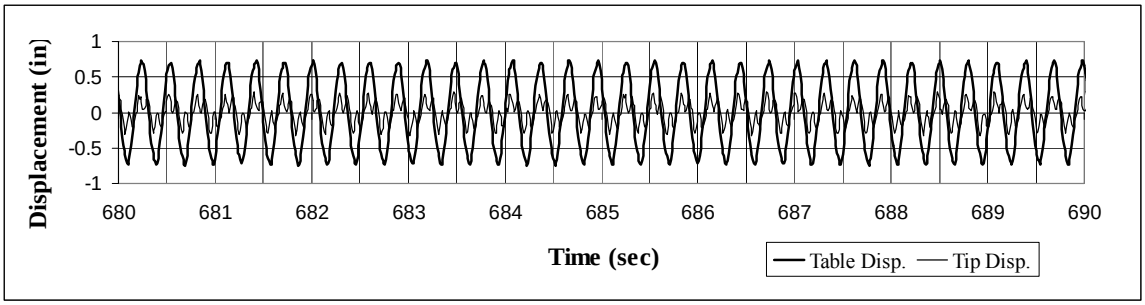
Displacement (in)
1
0.5
0
-0.5
-1
680 681 682 683 684 685 686 687 688 689 690
Time (sec)
Table Disp. Tip Disp.

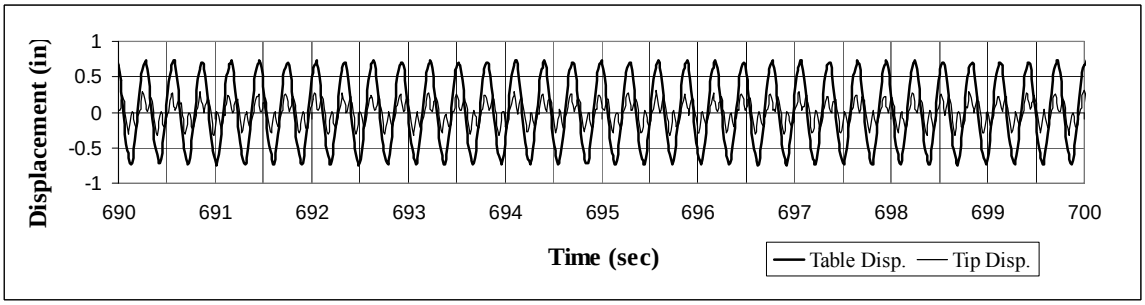
Displacement (in)
1
0.5
0
-0.5
-1
690 691 692 693 694 695 696 697 698 699 700
Time (sec)
Table Disp. Tip Disp.

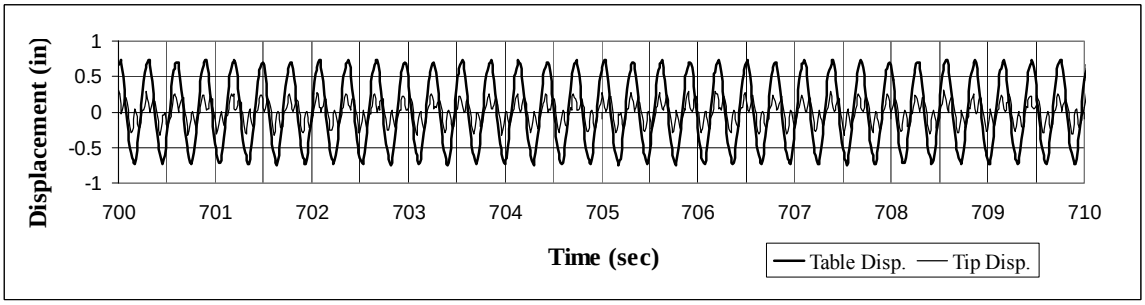
Displacement (in)
1
0.5
0
-0.5
-1
700 701 702 703 704 705 706 707 708 709 710
Time (sec)
Table Disp. Tip Disp.

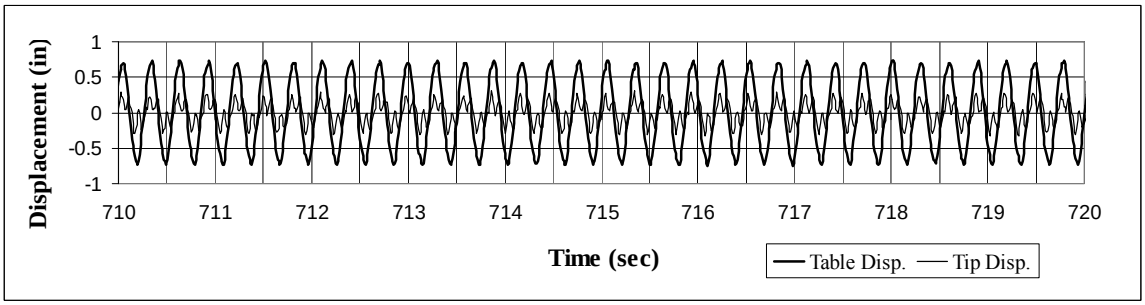
Displacement (in)
1
0.5
0
-0.5
-1
710 711 712 713 714 715 716 717 718 719 720
Time (sec)
Table Disp. Tip Disp.

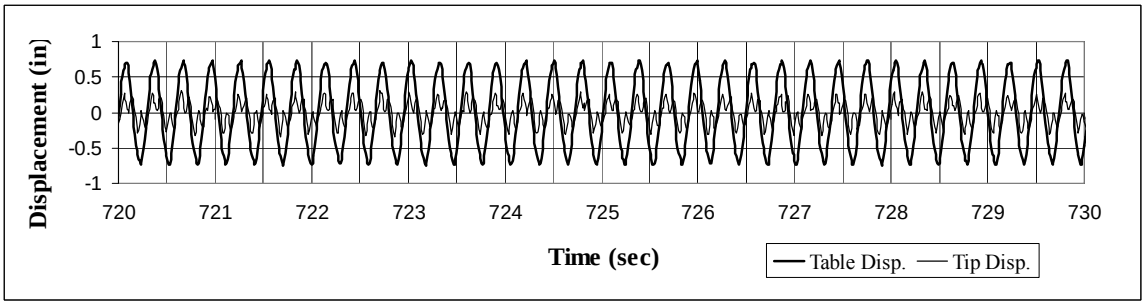
Displacement (in)
1
0.5
0
-0.5
-1
720 721 722 723 724 725 726 727 728 729 730
Time (sec)
Table Disp. Tip Disp.

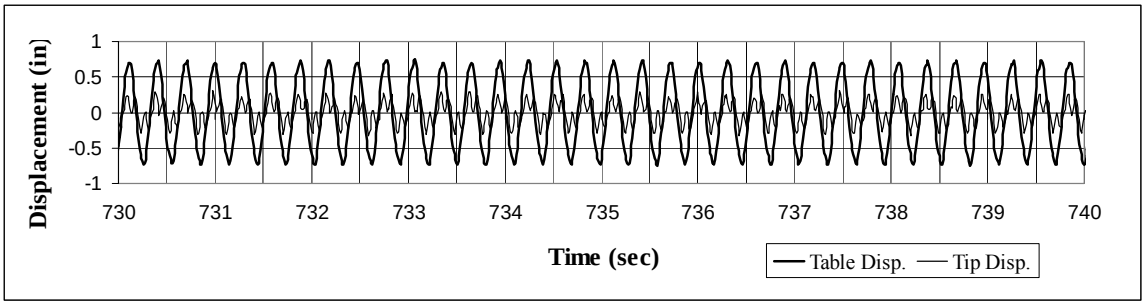
Displacement (in)
1
0.5
0
-0.5
-1
730 731 732 733 734 735 736 737 738 739 740
Time (sec)
Table Disp. Tip Disp.

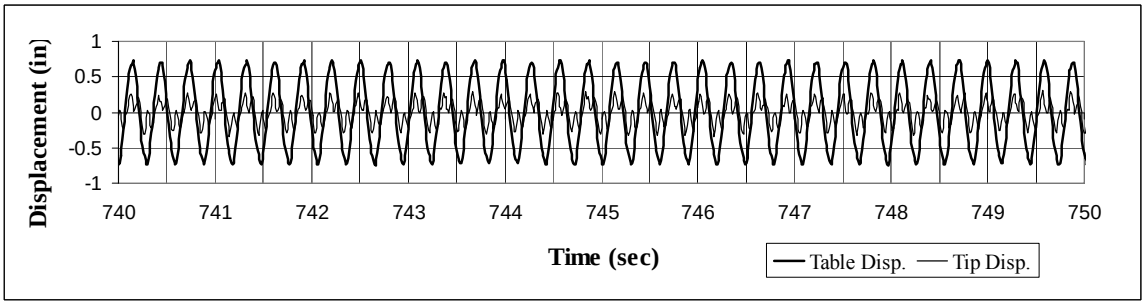
Displacement (in)
1
0.5
0
-0.5
-1
740 741 742 743 744 745 746 747 748 749 750
Time (sec)
Table Disp. Tip Disp.

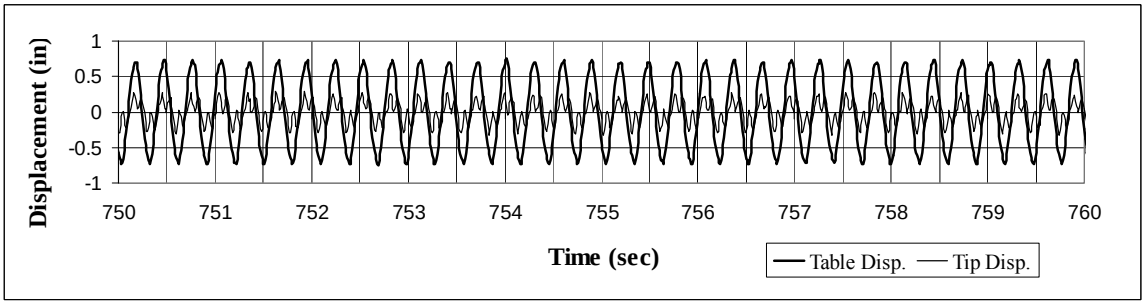
Displacement (in)
1
0.5
0
-0.5
-1
750 751 752 753 754 755 756 757 758 759 760
Time (sec)
Table Disp. Tip Disp.

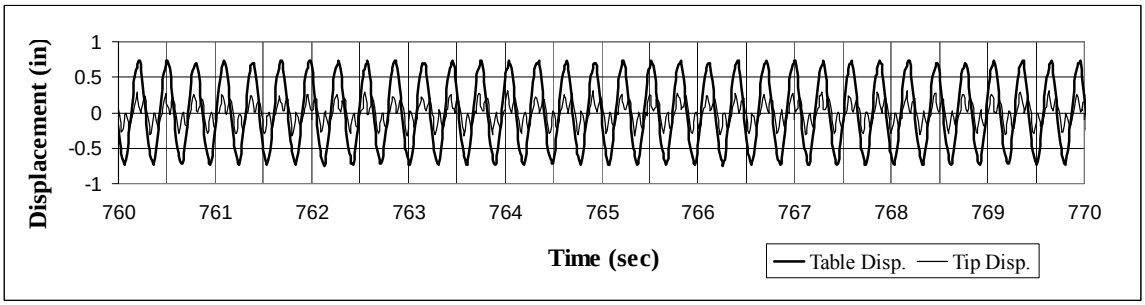
Displacement (in)
1
0.5
0
-0.5
-1
760 761 762 763 764 765 766 767 768 769 770
Time (sec)
Table Disp. Tip Disp.

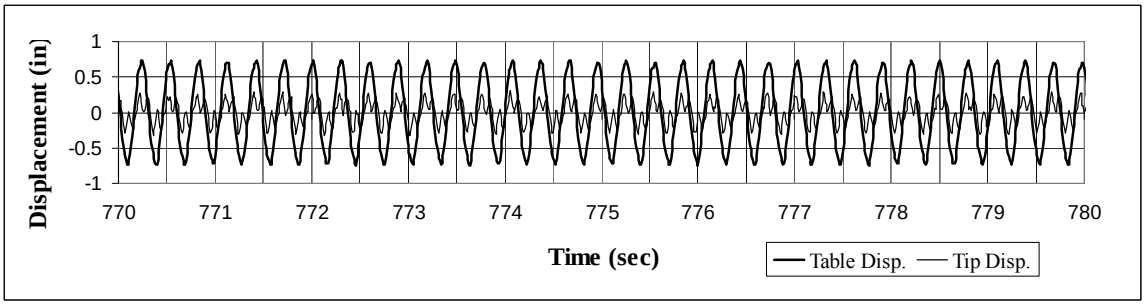
Displacement (in)
1
0.5
0
-0.5
-1
770 771 772 773 774 775 776 777 778 779 780
Time (sec)
Table Disp. Tip Disp.

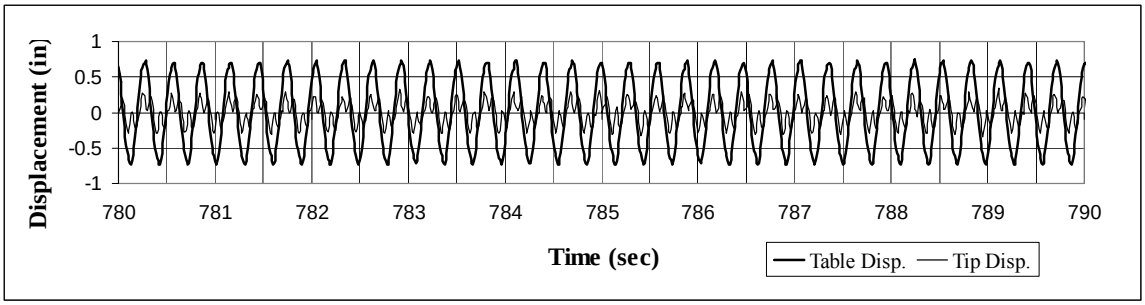
Displacement (in)
1
0.5
0
-0.5
-1
780 781 782 783 784 785 786 787 788 789 790
Time (sec)
Table Disp. Tip Disp.

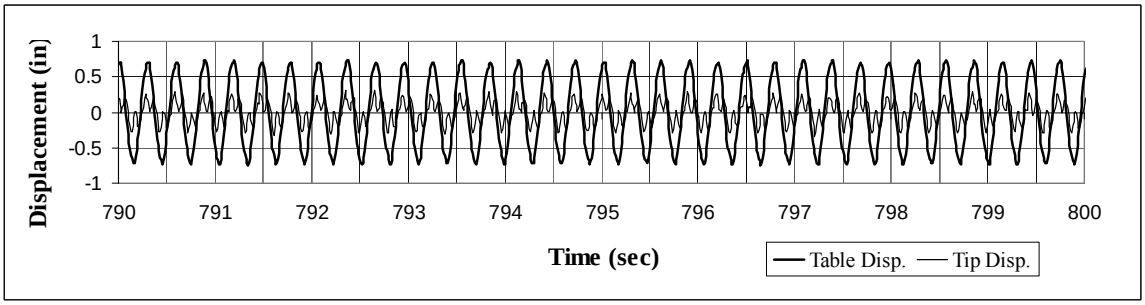
Displacement (in)
1
0.5
0
-0.5
-1
790 791 792 793 794 795 796 797 798 799 800
Time (sec)
Table Disp. Tip Disp.

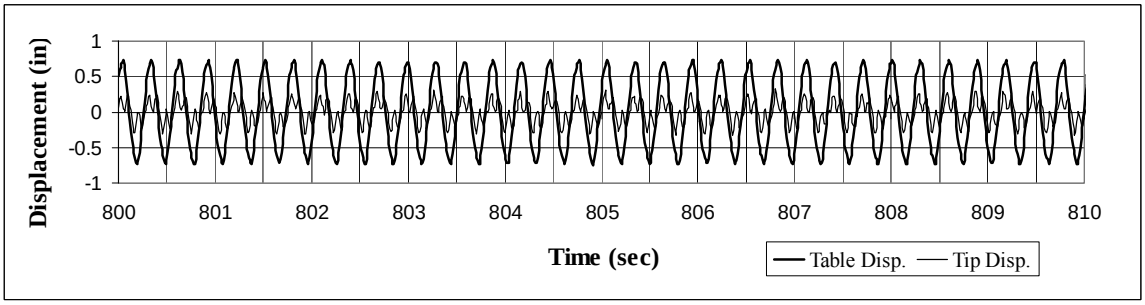
Displacement (in)
1
0.5
0
-0.5
-1
800 801 802 803 804 805 806 807 808 809 810
Time (sec)
Table Disp. Tip Disp.

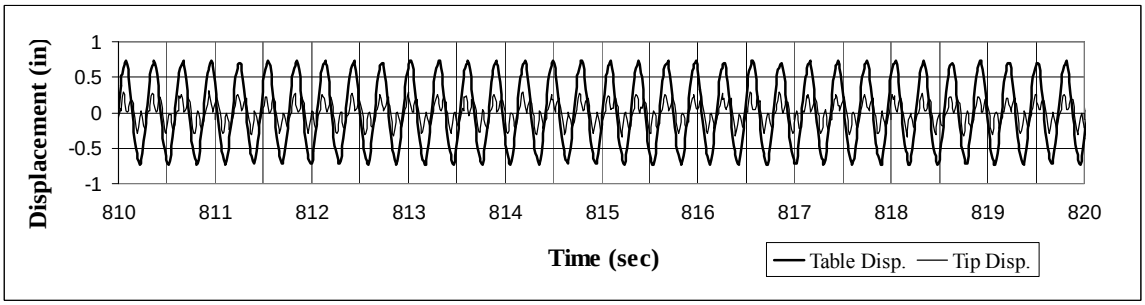
Displacement (in)
1
0.5
0
-0.5
-1
810 811 812 813 814 815 816 817 818 819 820
Time (sec)
Table Disp. Tip Disp.

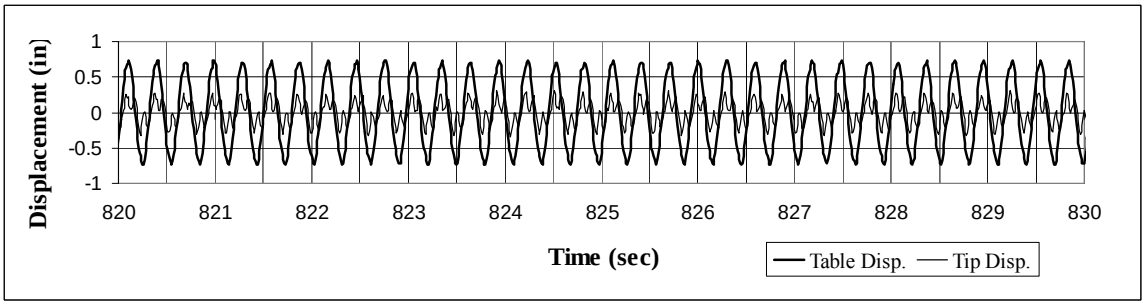
Displacement (in)
1
0.5
0
-0.5
-1
820 821 822 823 824 825 826 827 828 829 830
Time (sec)
Table Disp. Tip Disp.

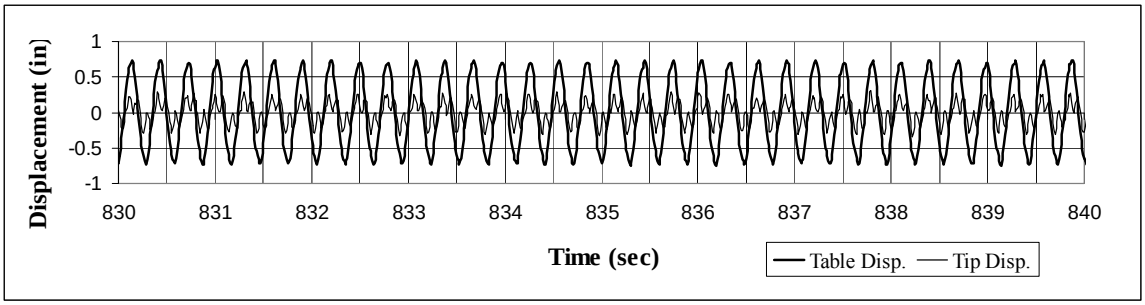
Displacement (in)
1
0.5
0
-0.5
-1
830 831 832 833 834 835 836 837 838 839 840
Time (sec)
Table Disp. Tip Disp.

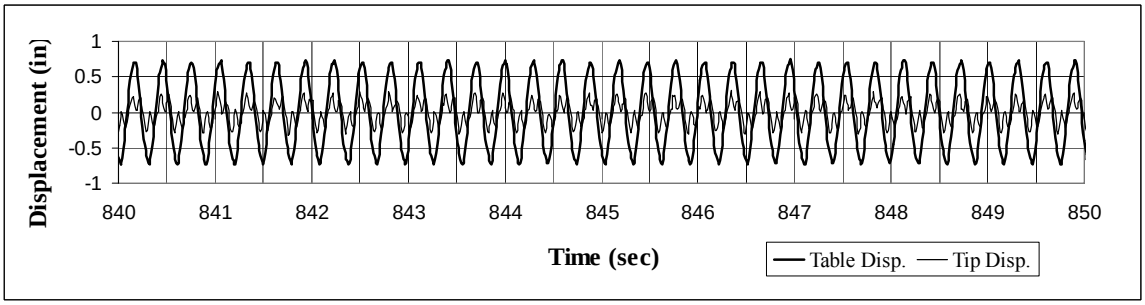
Displacement (in)
1
0.5
0
-0.5
-1
840 841 842 843 844 845 846 847 848 849 850
Time (sec)
Table Disp. Tip Disp.

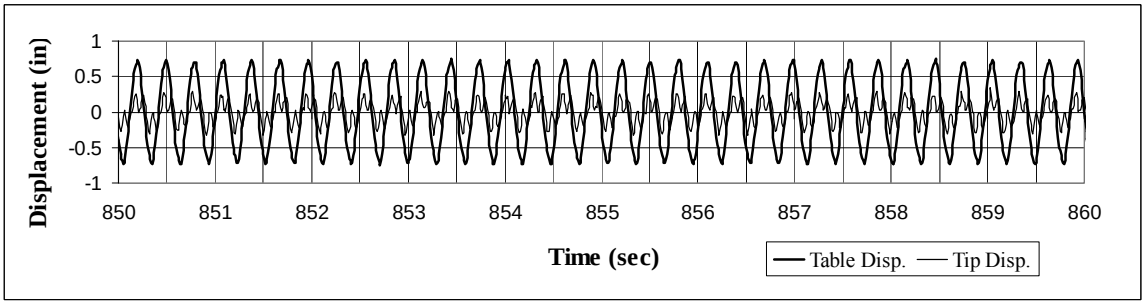
Displacement (in)
1
0.5
0
-0.5
-1
850 851 852 853 854 855 856 857 858 859 860
Time (sec)
Table Disp. Tip Disp.

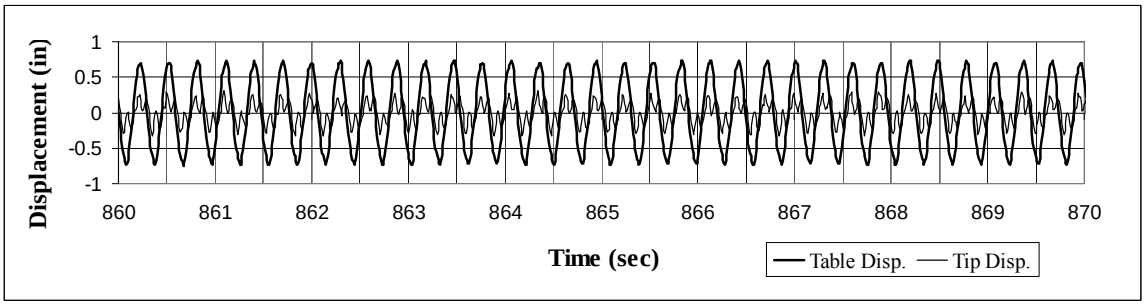
Displacement (in)
1
0.5
0
-0.5
-1
860 861 862 863 864 865 866 867 868 869 870
Time (sec)
Table Disp. Tip Disp.

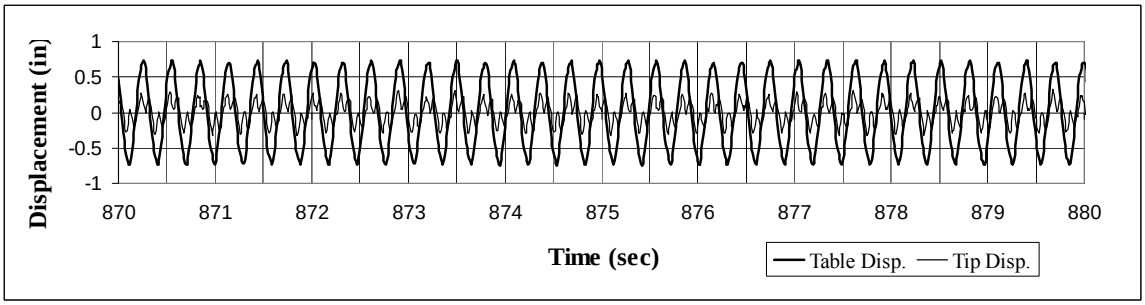
Displacement (in)
1
0.5
0
-0.5
-1
870 871 872 873 874 875 876 877 878 879 880
Time (sec)
Table Disp. Tip Disp.

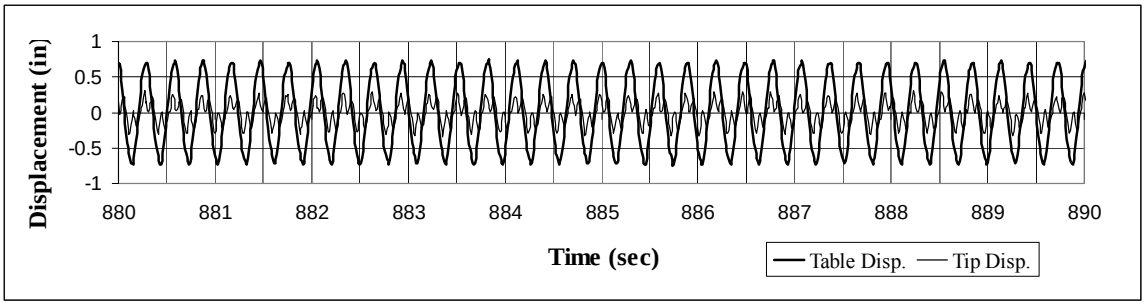
Displacement (in)
1
0.5
0
-0.5
-1
880 881 882 883 884 885 886 887 888 889 890
Time (sec)
Table Disp. Tip Disp.

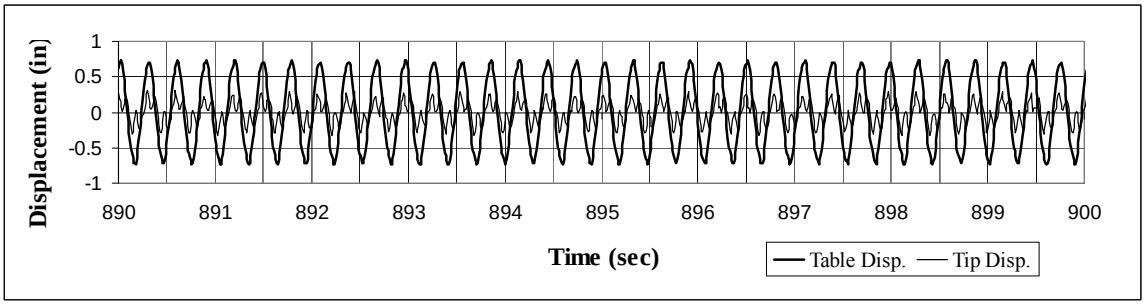
Displacement (in)
1
0.5
0
-0.5
-1
890 891 892 893 894 895 896 897 898 899 900
Time (sec)
Table Disp. Tip Disp.

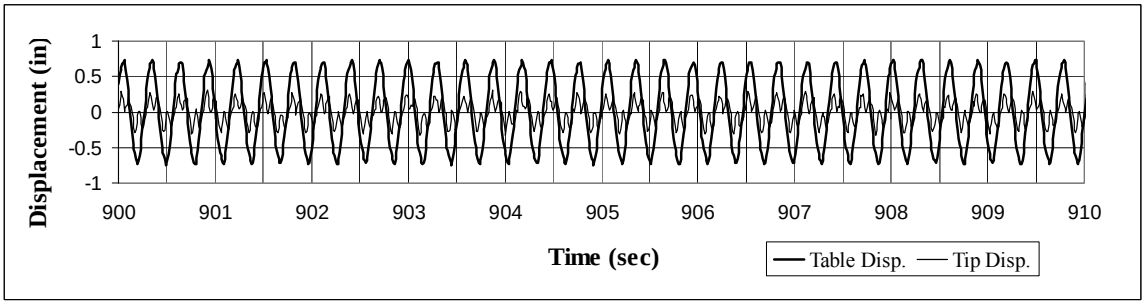
Displacement (in)
1
0.5
0
-0.5
-1
900 901 902 903 904 905 906 907 908 909 910
Time (sec)
Table Disp. Tip Disp.

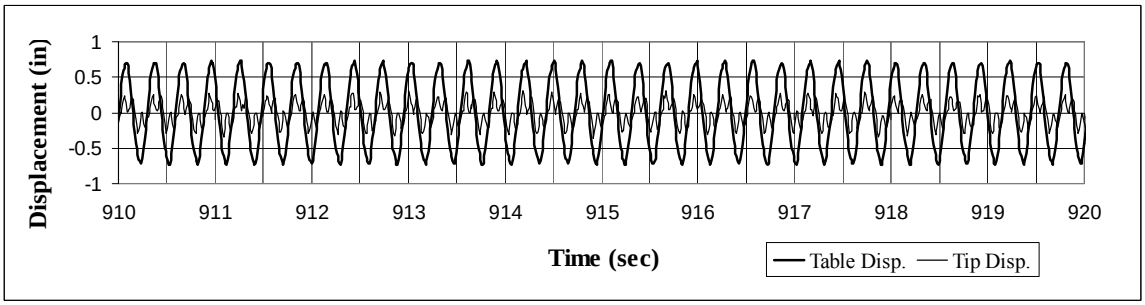
Displacement (in)
1
0.5
0
-0.5
-1
910 911 912 913 914 915 916 917 918 919 920
Time (sec)
Table Disp. Tip Disp.

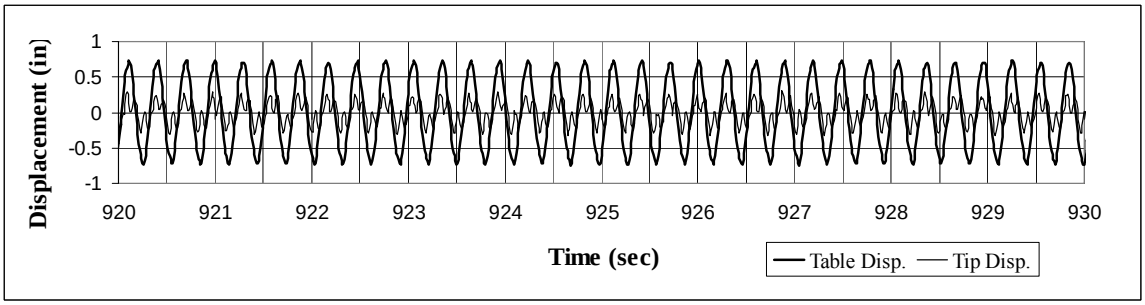
Displacement (in)
1
0.5
0
-0.5
-1
920 921 922 923 924 925 926 927 928 929 930
Time (sec)
Table Disp. Tip Disp.

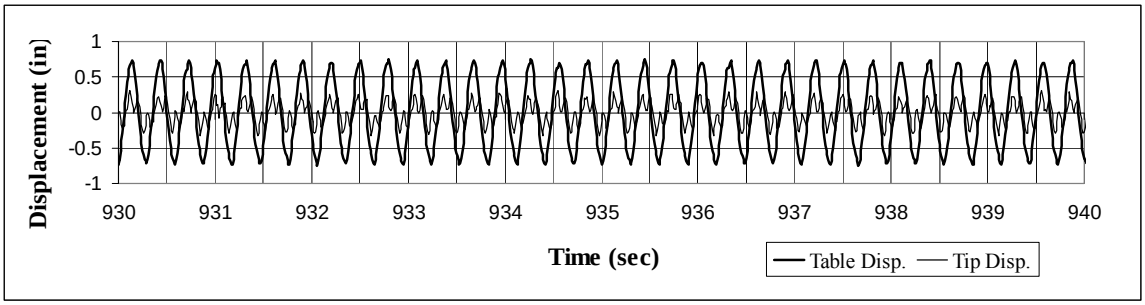
Displacement (in)
1
0.5
0
-0.5
-1
930 931 932 933 934 935 936 937 938 939 940
Time (sec)
Table Disp. Tip Disp.

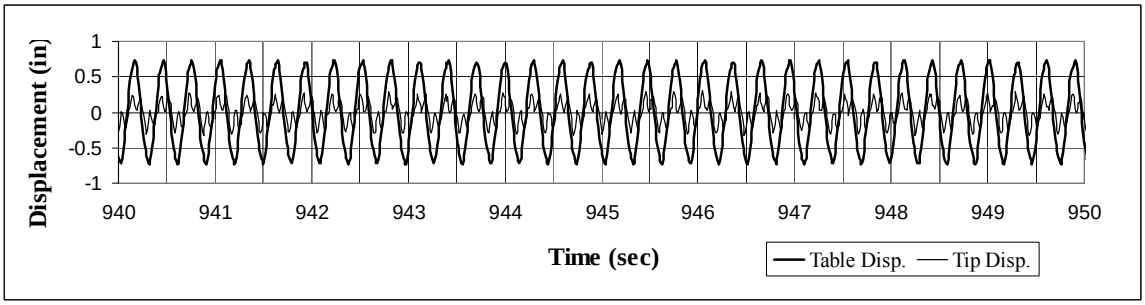
Displacement (in)
1
0.5
0
-0.5
-1
940 941 942 943 944 945 946 947 948 949 950
Time (sec)
Table Disp. Tip Disp.

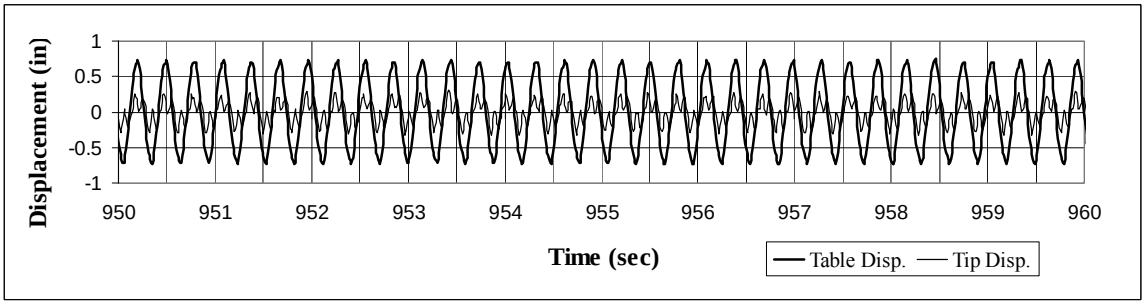
Displacement (in)
1
0.5
0
-0.5
-1
950 951 952 953 954 955 956 957 958 959 960
Time (sec)
Table Disp. Tip Disp.

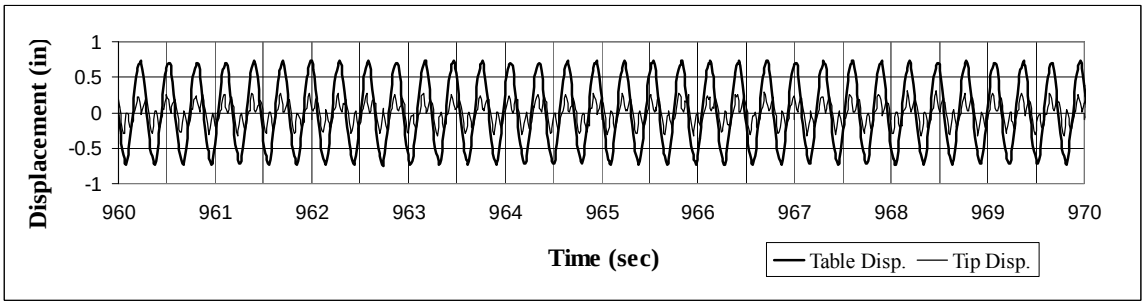
Displacement (in)
1
0.5
0
-0.5
-1
960 961 962 963 964 965 966 967 968 969 970
Time (sec)
Table Disp. Tip Disp.

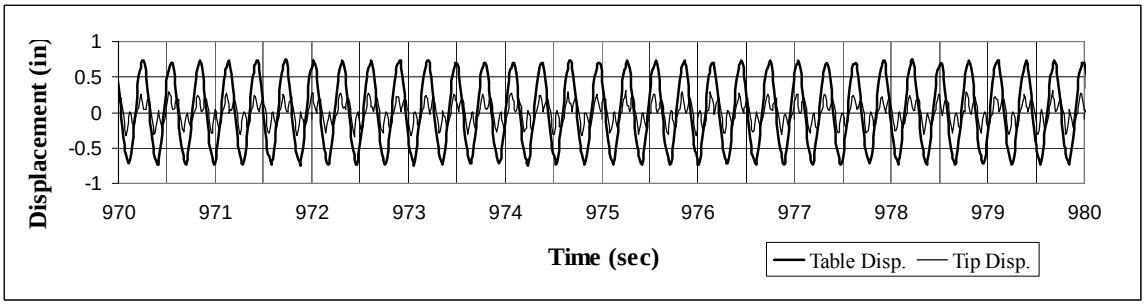
Displacement (in)
1
0.5
0
-0.5
-1
970 971 972 973 974 975 976 977 978 979 980
Time (sec)
Table Disp. Tip Disp.

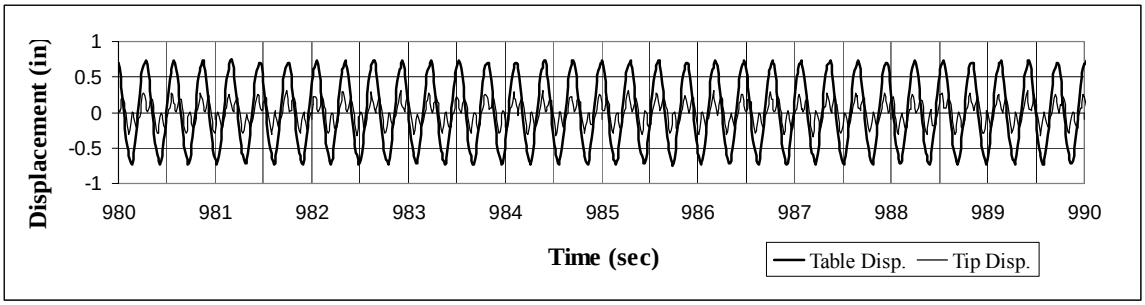
Displacement (in)
1
0.5
0
-0.5
-1
980 981 982 983 984 985 986 987 988 989 990
Time (sec)
Table Disp. Tip Disp.

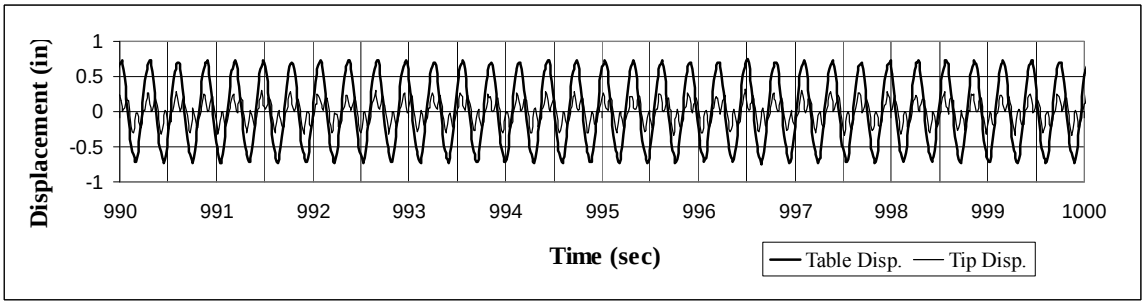
Displacement (in)
1
0.5
0
-0.5
-1
990 991 992 993 994 995 996 997 998 999 1000
Time (sec)
Table Disp. Tip Disp.

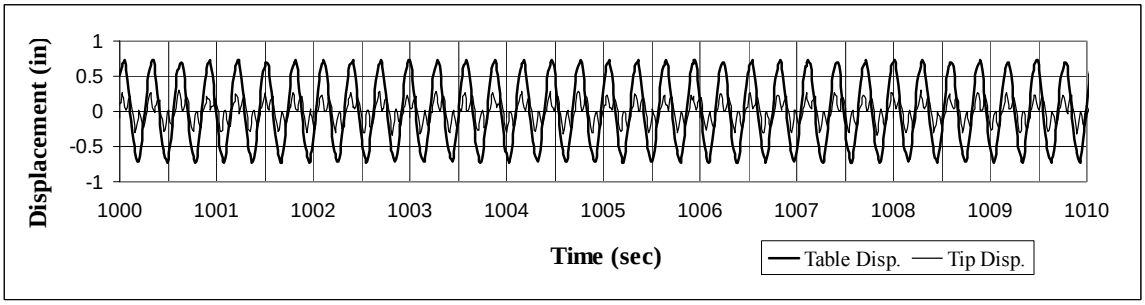
Displacement (in)
1
0.5
0
-0.5
-1
1000 1001 1002 1003 1004 1005 1006 1007 1008 1009 1010
Time (sec)
Table Disp. Tip Disp.

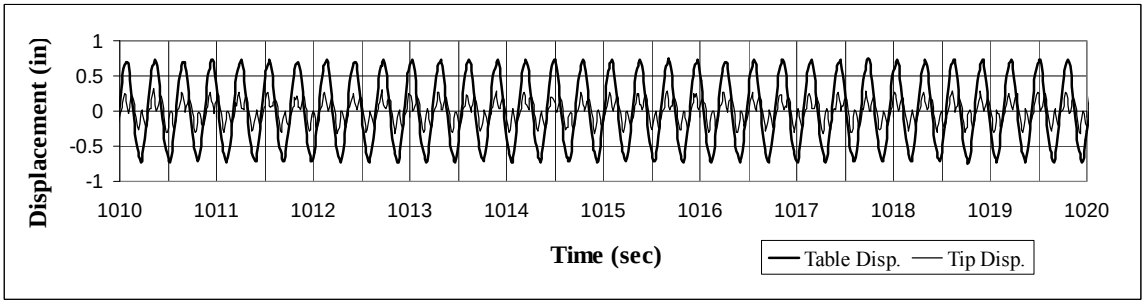
Displacement (in)
1
0.5
0
-0.5
-1
1010 1011 1012 1013 1014 1015 1016 1017 1018 1019 1020
Time (sec)
Table Disp. Tip Disp.

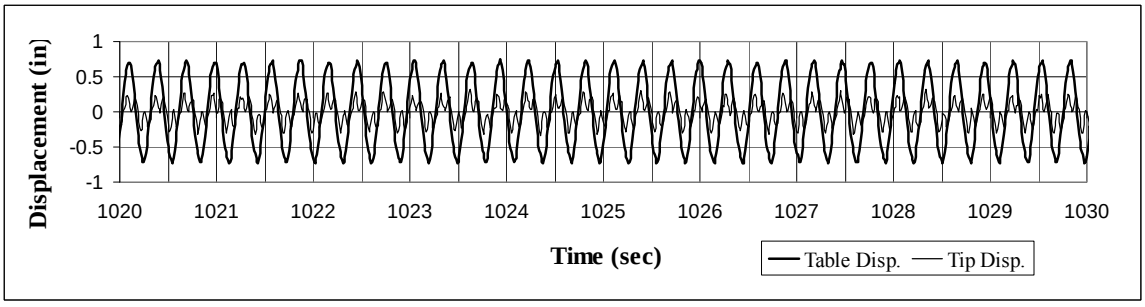
Displacement (in)
1
0.5
0
-0.5
-1
1020 1021 1022 1023 1024 1025 1026 1027 1028 1029 1030
Time (sec)
Table Disp. Tip Disp.

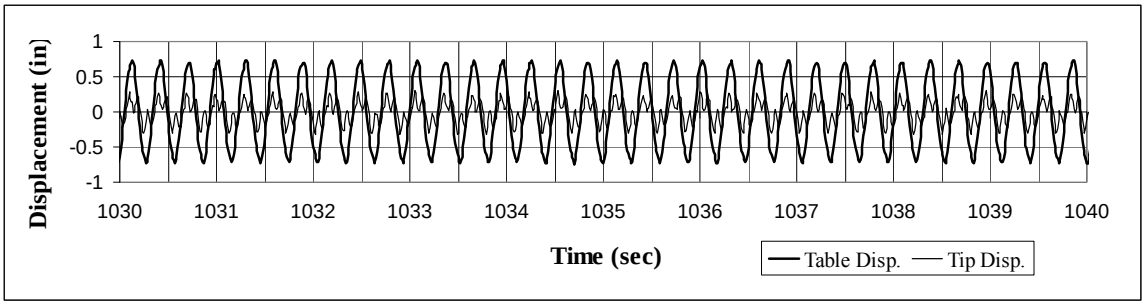
Displacement (in)
1
0.5
0
-0.5
-1
1030 1031 1032 1033 1034 1035 1036 1037 1038 1039 1040
Time (sec)
Table Disp. Tip Disp.

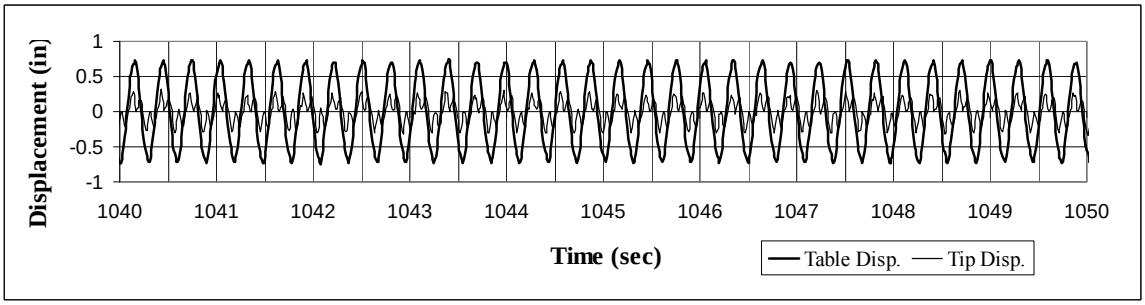
Displacement (in)
1
0.5
0
-0.5
-1
1040 1041 1042 1043 1044 1045 1046 1047 1048 1049 1050
Time (sec)
Table Disp. Tip Disp.

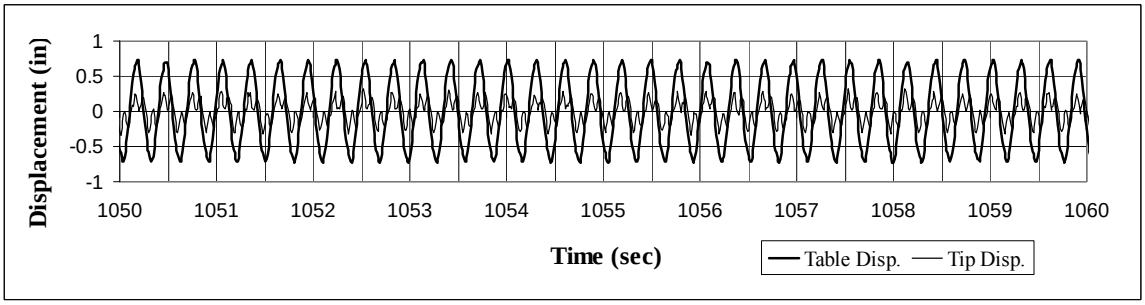
Displacement (in)
1
0.5
0
-0.5
-1
1050 1051 1052 1053 1054 1055 1056 1057 1058 1059 1060
Time (sec)
Table Disp. Tip Disp.

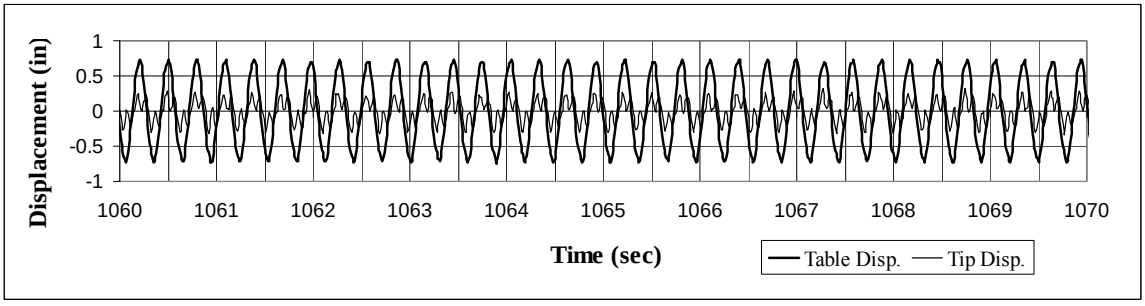
Displacement (in)
1
0.5
0
-0.5
-1
1060 1061 1062 1063 1064 1065 1066 1067 1068 1069 1070
Time (sec)
Table Disp. Tip Disp.

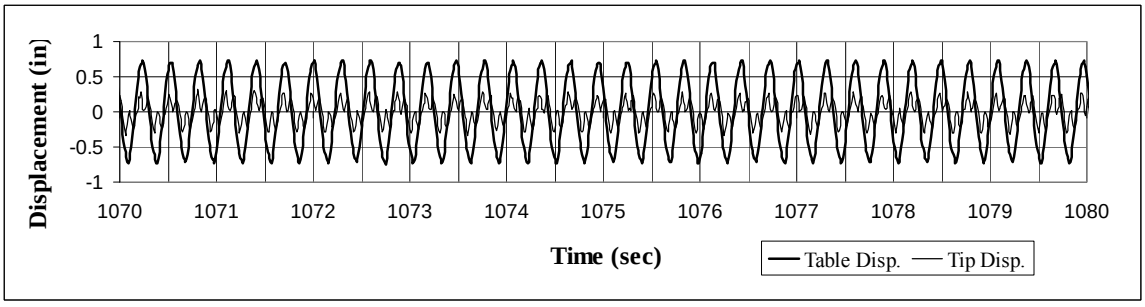
Displacement (in)
1
0.5
0
-0.5
-1
1070 1071 1072 1073 1074 1075 1076 1077 1078 1079 1080
Time (sec)
Table Disp. Tip Disp.

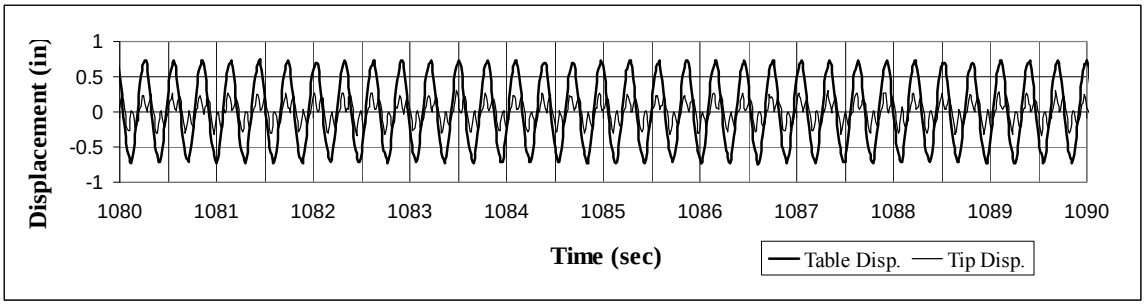
Displacement (in)
1
0.5
0
-0.5
-1
1080 1081 1082 1083 1084 1085 1086 1087 1088 1089 1090
Time (sec)
Table Disp.
Tip Disp.

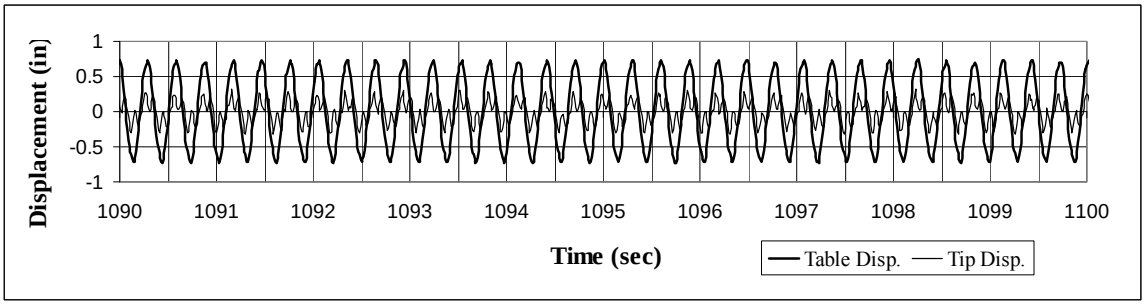
Displacement (in)
1
0.5
0
-0.5
-1
1090 1091 1092 1093 1094 1095 1096 1097 1098 1099 1100
Time (sec)
Table Disp.
Tip Disp.

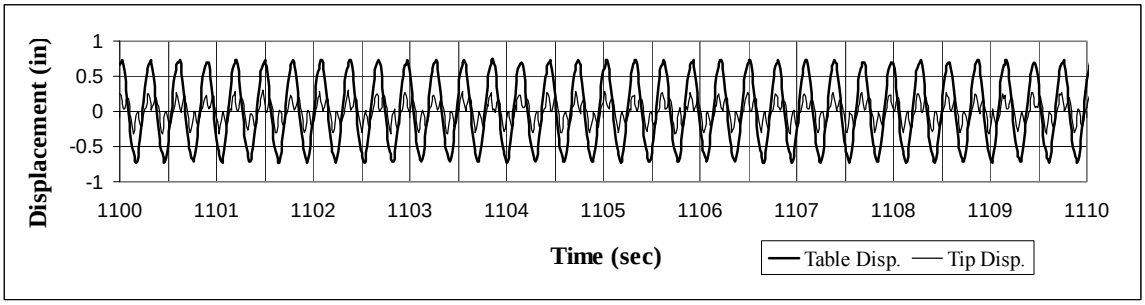
Displacement (in)
1
0.5
0
-0.5
-1
1100 1101 1102 1103 1104 1105 1106 1107 1108 1109 1110
Time (sec)
Table Disp.
Tip Disp.

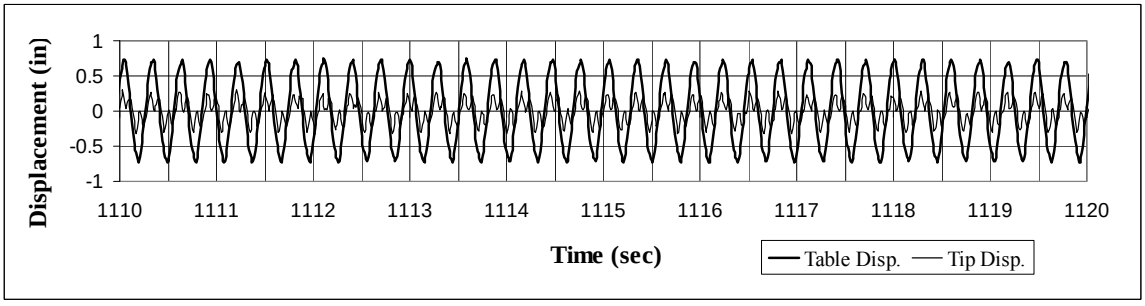
Displacement (in)
1
0.5
0
-0.5
-1
1110 1111 1112 1113 1114 1115 1116 1117 1118 1119 1120
Time (sec)
Table Disp.
Tip Disp.

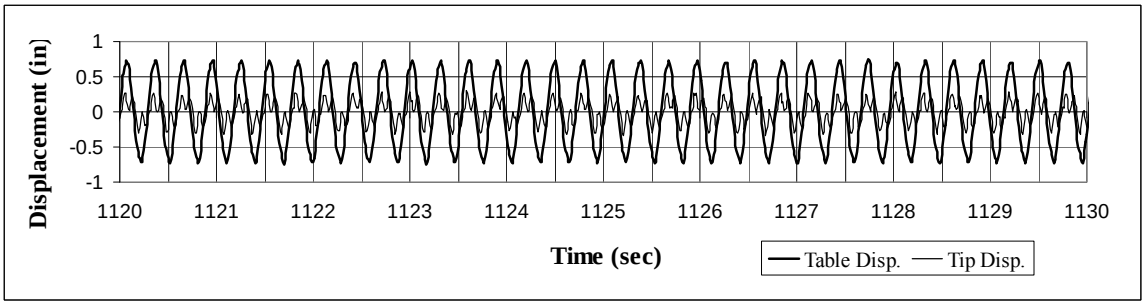
Displacement (in)
1
0.5
0
-0.5
-1
1120 1121 1122 1123 1124 1125 1126 1127 1128 1129 1130
Time (sec)
Table Disp.
Tip Disp.

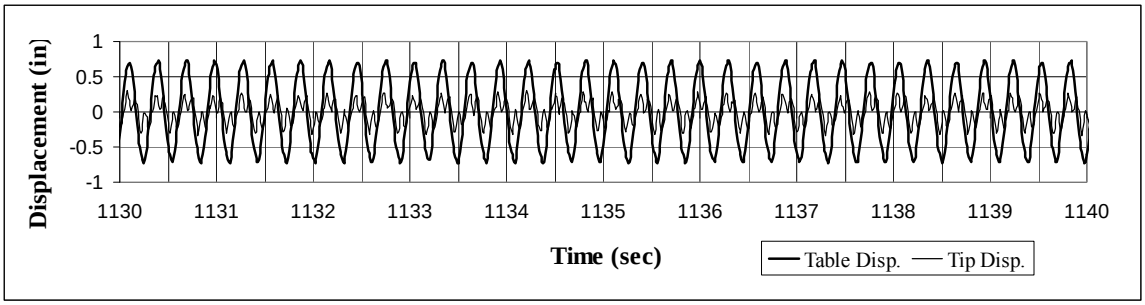
Displacement (in)
1
0.5
0
-0.5
-1
1130 1131 1132 1133 1134 1135 1136 1137 1138 1139 1140
Time (sec)
Table Disp.
Tip Disp.

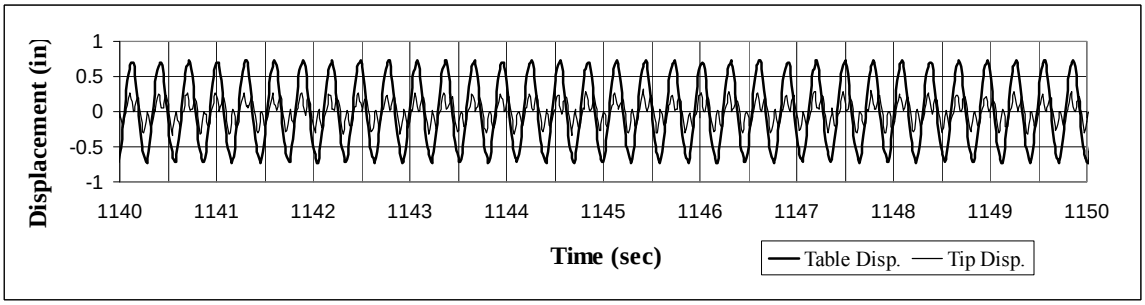
Displacement (in)
1
0.5
0
-0.5
-1
1140 1141 1142 1143 1144 1145 1146 1147 1148 1149 1150
Time (sec)
Table Disp.
Tip Disp.

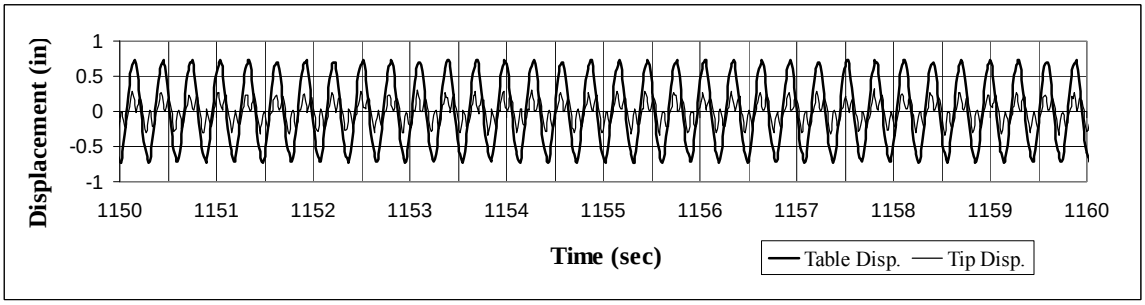
Displacement (in)
1
0.5
0
-0.5
-1
1150 1151 1152 1153 1154 1155 1156 1157 1158 1159 1160
Time (sec)
Table Disp.
Tip Disp.

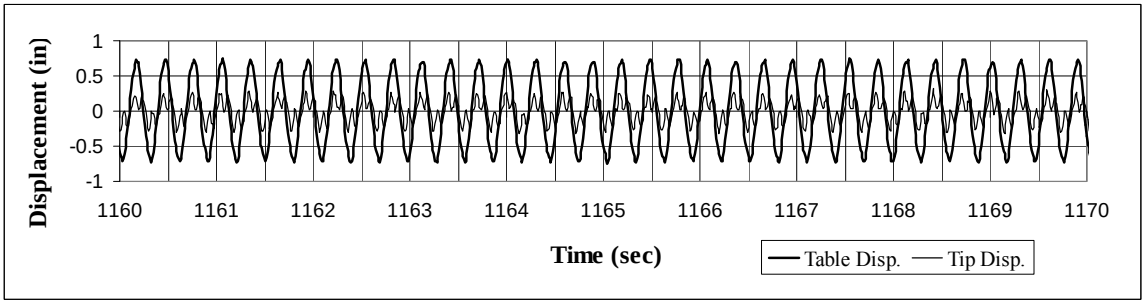
Displacement (in)
1
0.5
0
-0.5
-1
1160 1161 1162 1163 1164 1165 1166 1167 1168 1169 1170
Time (sec)
Table Disp.
Tip Disp.

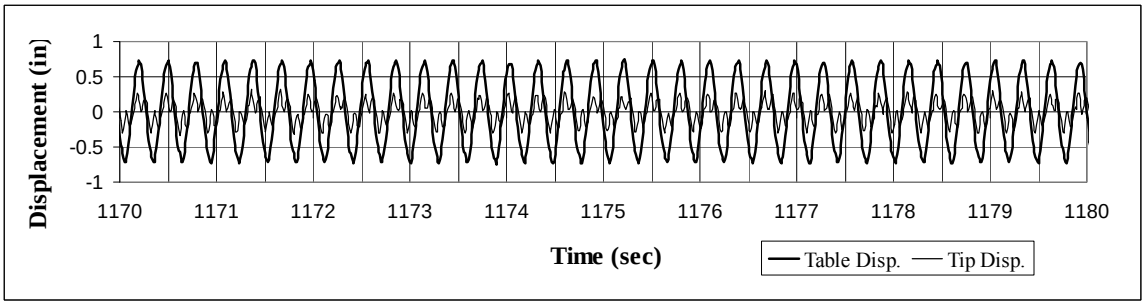
Displacement (in)
1
0.5
0
-0.5
-1
1170 1171 1172 1173 1174 1175 1176 1177 1178 1179 1180
Time (sec)
Table Disp.
Tip Disp.

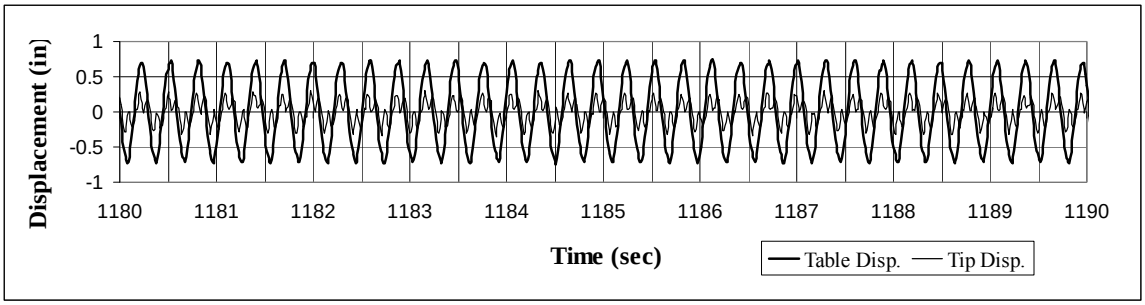
Displacement (in)
1
0.5
0
-0.5
-1
1180 1181 1182 1183 1184 1185 1186 1187 1188 1189 1190
Time (sec)
Table Disp.
Tip Disp.

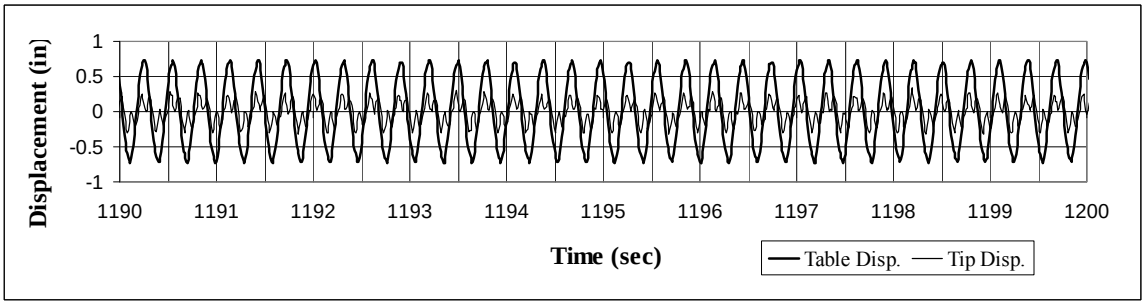
Displacement (in)
1
0.5
0
-0.5
-1
1190 1191 1192 1193 1194 1195 1196 1197 1198 1199 1200
Time (sec)
Table Disp.
Tip Disp.

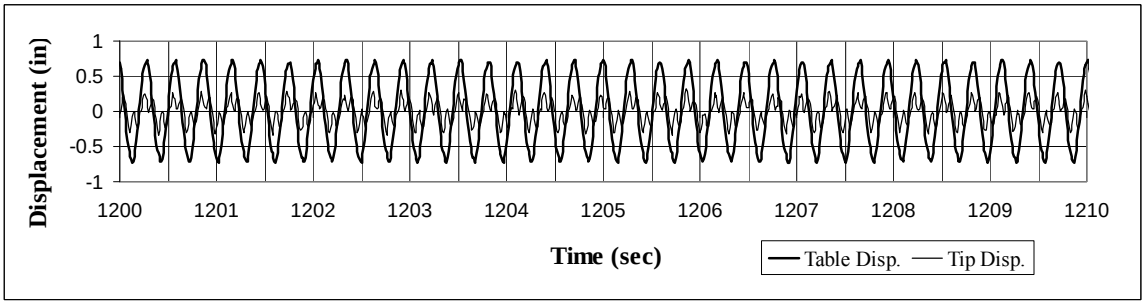
Displacement (in)
1
0.5
0
-0.5
-1
1200 1201 1202 1203 1204 1205 1206 1207 1208 1209 1210
Time (sec)
Table Disp.
Tip Disp.

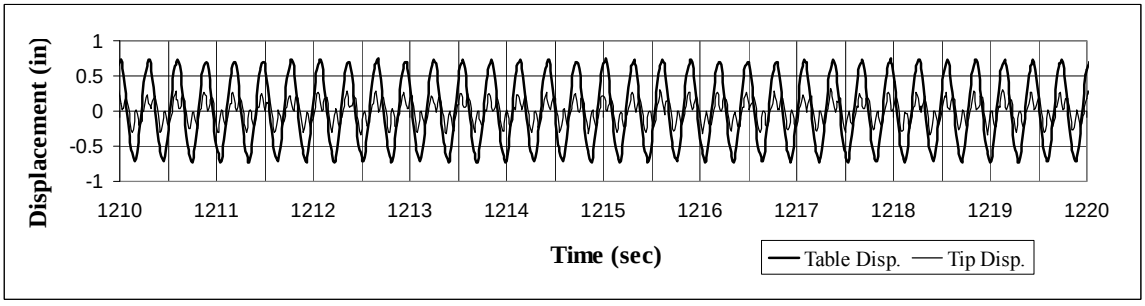
Displacement (in)
1
0.5
0
-0.5
-1
1210 1211 1212 1213 1214 1215 1216 1217 1218 1219 1220
Time (sec)
Table Disp.
Tip Disp.

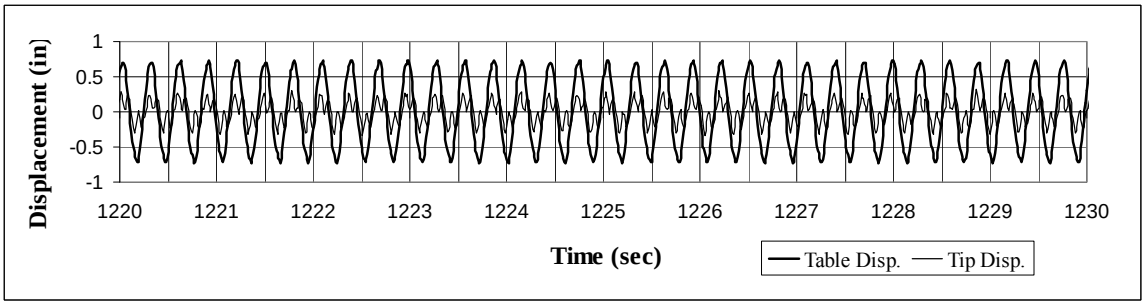
Displacement (in)
1
0.5
0
-0.5
-1
1220 1221 1222 1223 1224 1225 1226 1227 1228 1229 1230
Time (sec)
Table Disp.
Tip Disp.

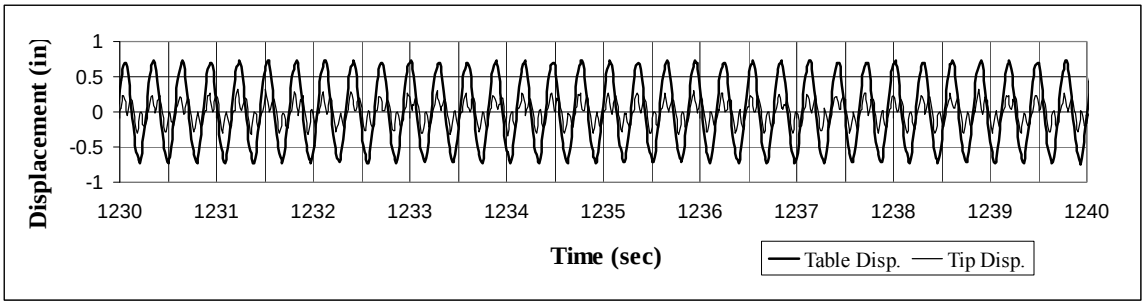
Displacement (in)
1
0.5
0
-0.5
-1
1230 1231 1232 1233 1234 1235 1236 1237 1238 1239 1240
Time (sec)
Table Disp.
Tip Disp.

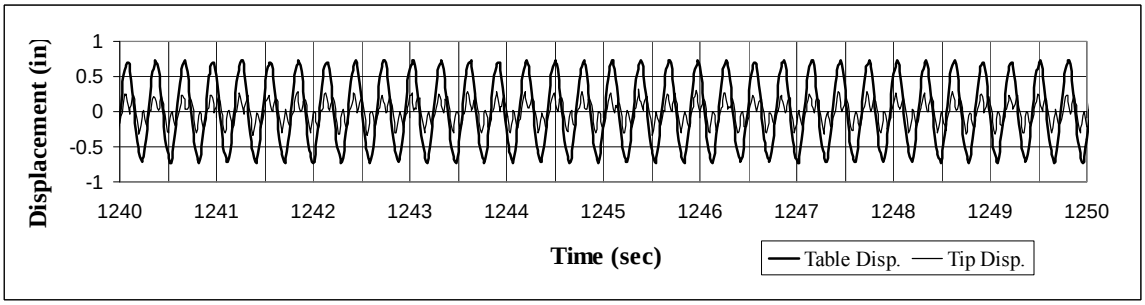
Displacement (in)
1
0.5
0
-0.5
-1
1240 1241 1242 1243 1244 1245 1246 1247 1248 1249 1250
Time (sec)
Table Disp.
Tip Disp.

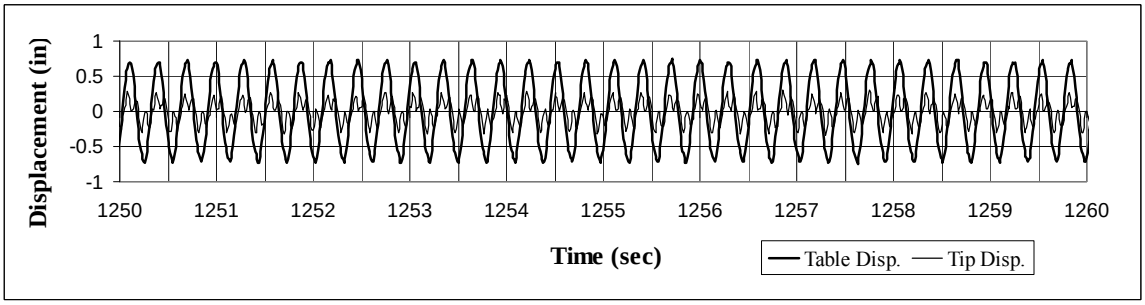
Displacement (in)
1
0.5
0
-0.5
-1
1250 1251 1252 1253 1254 1255 1256 1257 1258 1259 1260
Time (sec)
Table Disp.
Tip Disp.

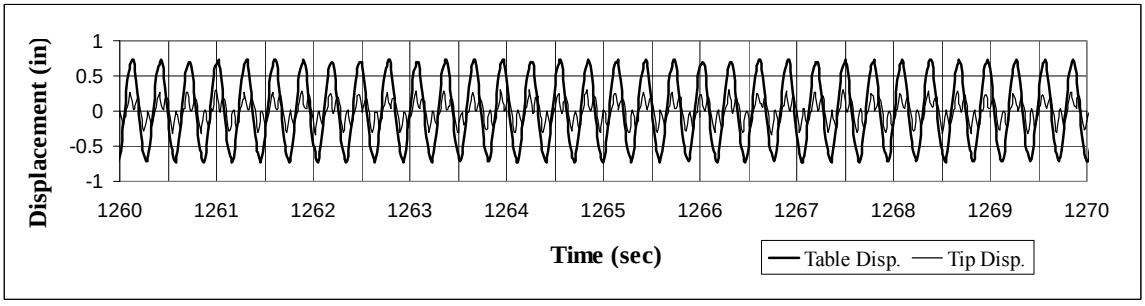
Displacement (in)
1
0.5
0
-0.5
-1
1260 1261 1262 1263 1264 1265 1266 1267 1268 1269 1270
Time (sec)
Table Disp.
Tip Disp.

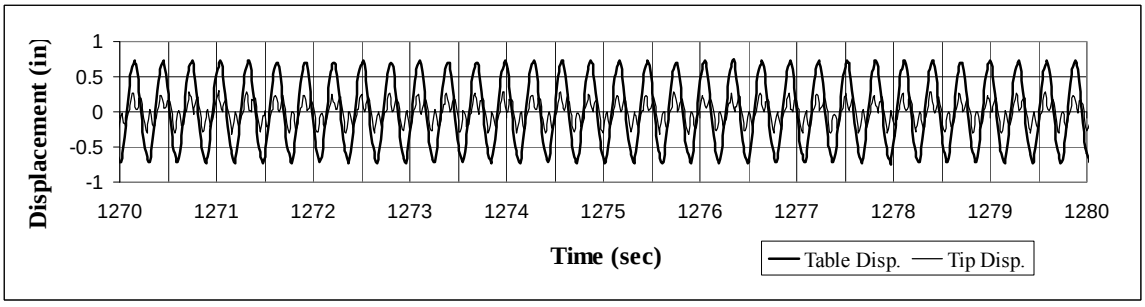
Displacement (in)
1
0.5
0
-0.5
-1
1270 1271 1272 1273 1274 1275 1276 1277 1278 1279 1280
Time (sec)
Table Disp.
Tip Disp.

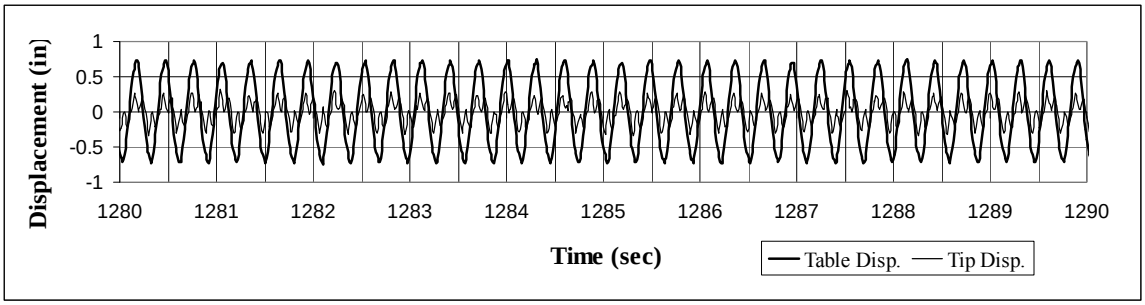
Displacement (in)
1
0.5
0
-0.5
-1
1280 1281 1282 1283 1284 1285 1286 1287 1288 1289 1290
Time (sec)
Table Disp.
Tip Disp.

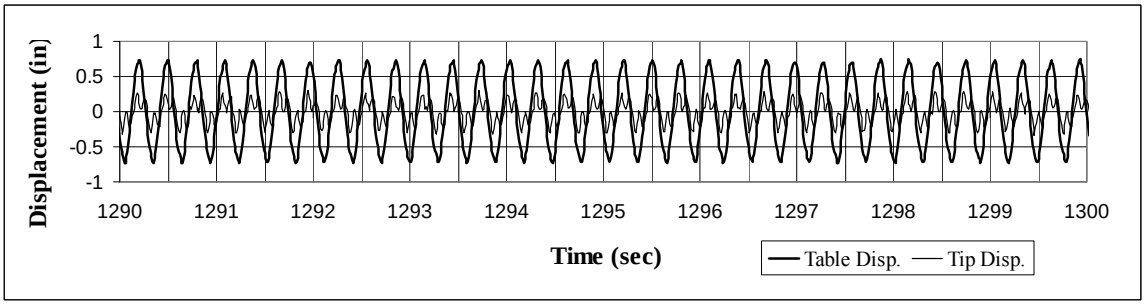
Displacement (in)
1
0.5
0
-0.5
-1
1290 1291 1292 1293 1294 1295 1296 1297 1298 1299 1300
Time (sec)
Table Disp.
Tip Disp.

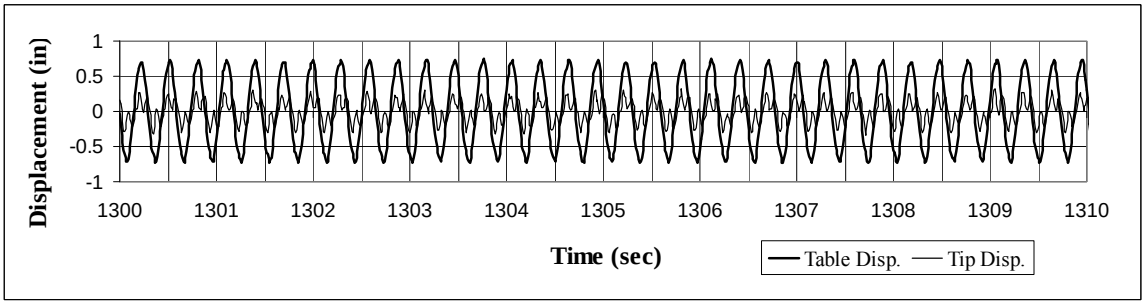
Displacement (in)
1
0.5
0
-0.5
-1
1300 1301 1302 1303 1304 1305 1306 1307 1308 1309 1310
Time (sec)
Table Disp.
Tip Disp.

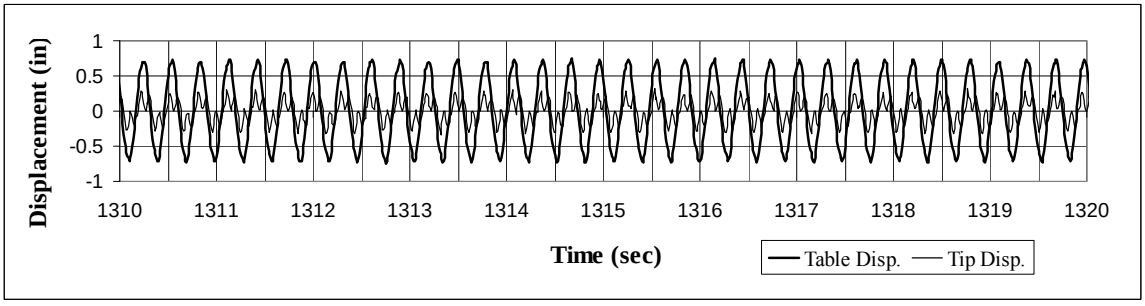
Displacement (in)
1
0.5
0
-0.5
-1
1310 1311 1312 1313 1314 1315 1316 1317 1318 1319 1320
Time (sec)
Table Disp.
Tip Disp.

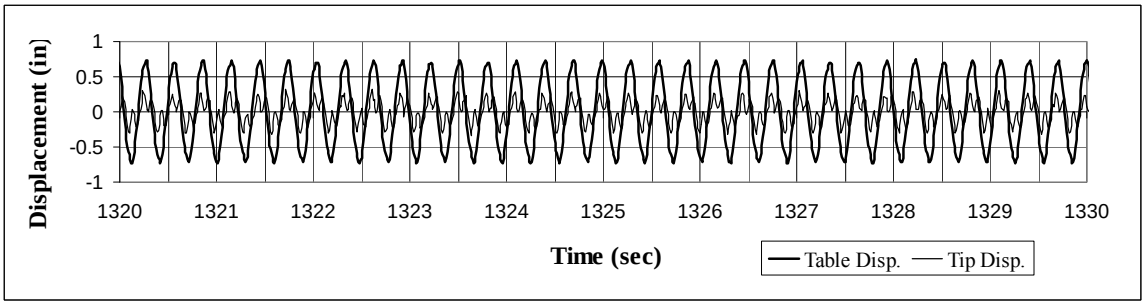
Displacement (in)
1
0.5
0
-0.5
-1
1320 1321 1322 1323 1324 1325 1326 1327 1328 1329 1330
Time (sec)
Table Disp.
Tip Disp.

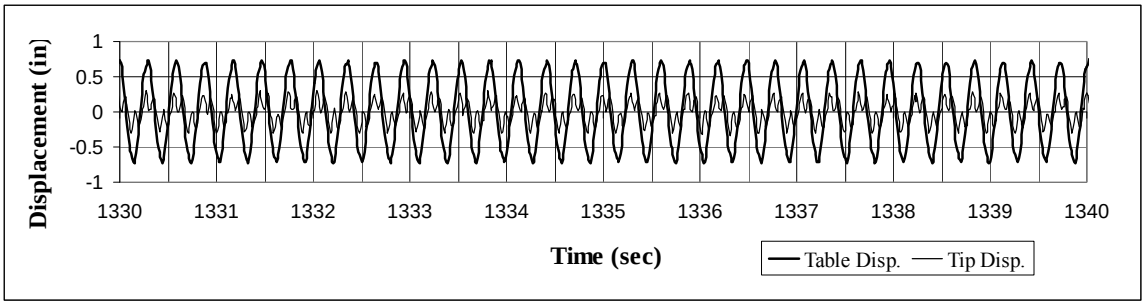
Displacement (in)
1
0.5
0
-0.5
-1
1330 1331 1332 1333 1334 1335 1336 1337 1338 1339 1340
Time (sec)
Table Disp.
Tip Disp.

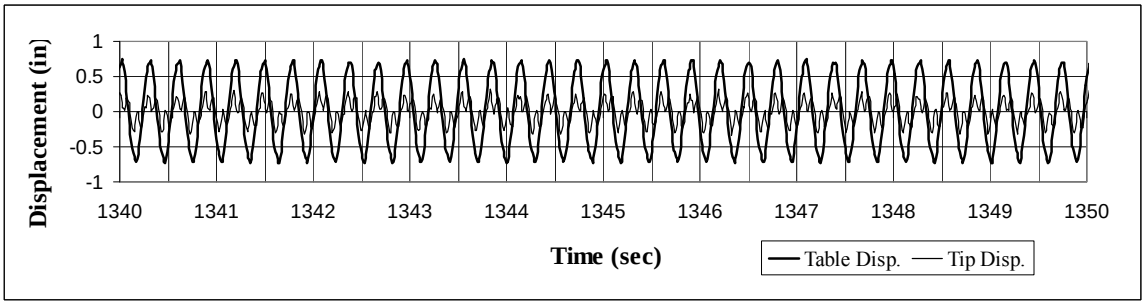
Displacement (in)
1
0.5
0
-0.5
-1
1340 1341 1342 1343 1344 1345 1346 1347 1348 1349 1350
Time (sec)
Table Disp.
Tip Disp.

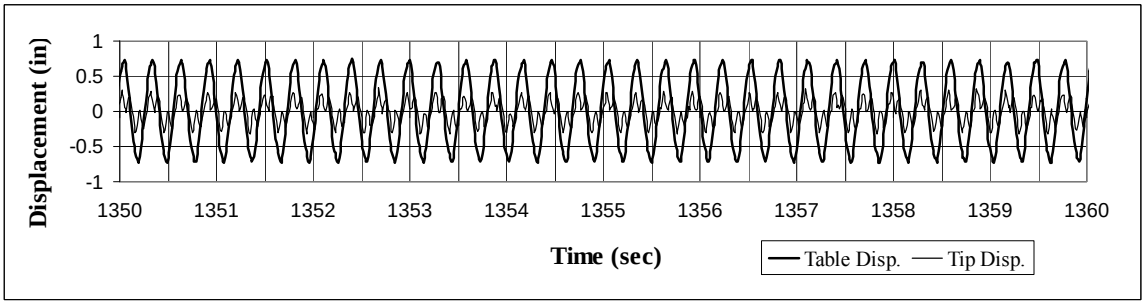
Displacement (in)
1
0.5
0
-0.5
-1
1350 1351 1352 1353 1354 1355 1356 1357 1358 1359 1360
Time (sec)
Table Disp.
Tip Disp.

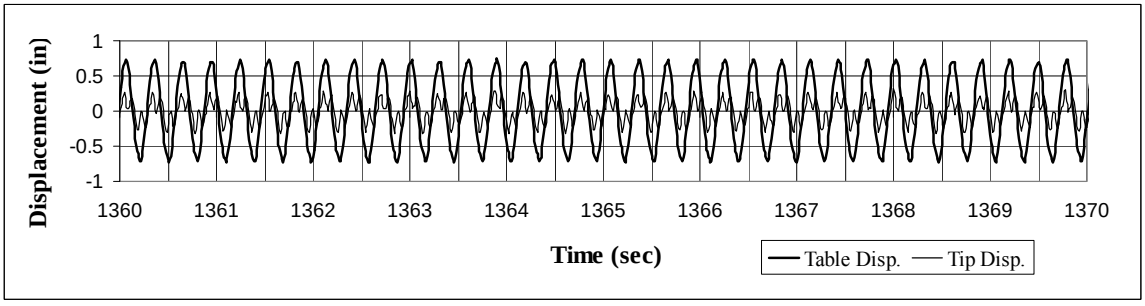
Displacement (in)
1
0.5
0
-0.5
-1
1360 1361 1362 1363 1364 1365 1366 1367 1368 1369 1370
Time (sec)
Table Disp.
Tip Disp.

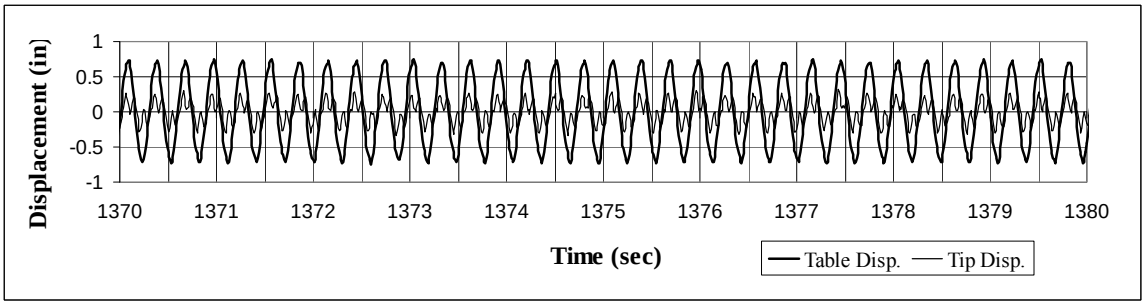
Displacement (in)
1
0.5
0
-0.5
-1
1370 1371 1372 1373 1374 1375 1376 1377 1378 1379 1380
Time (sec)
Table Disp.
Tip Disp.

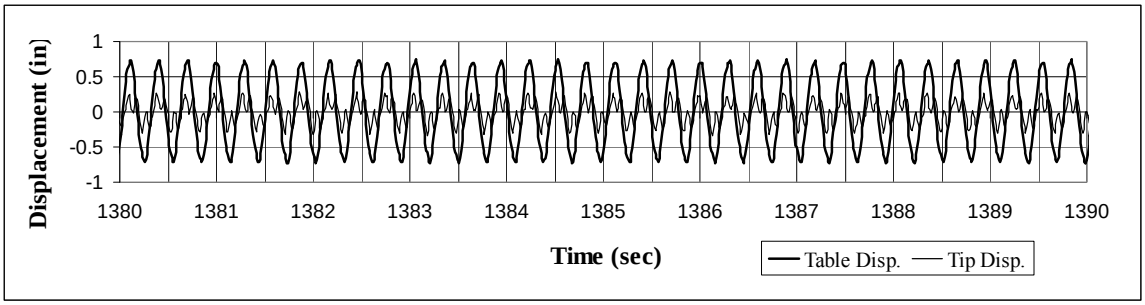
Displacement (in)
1
0.5
0
-0.5
-1
1380 1381 1382 1383 1384 1385 1386 1387 1388 1389 1390
Time (sec)
Table Disp. Tip Disp.

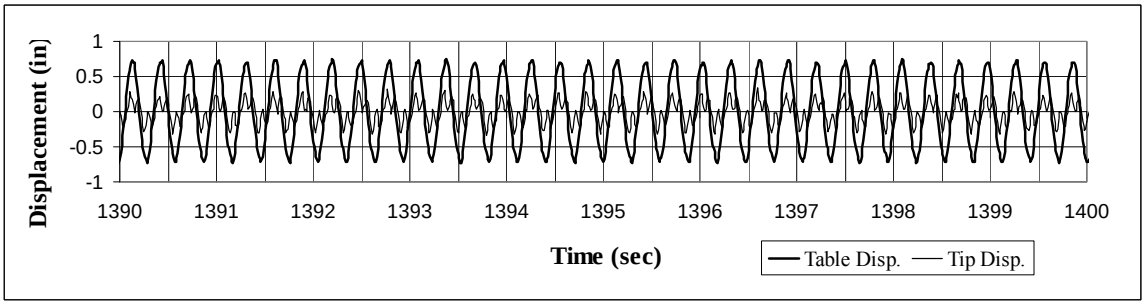
Displacement (in)
1
0.5
0
-0.5
-1
1390 1391 1392 1393 1394 1395 1396 1397 1398 1399 1400
Time (sec)
Table Disp. Tip Disp.

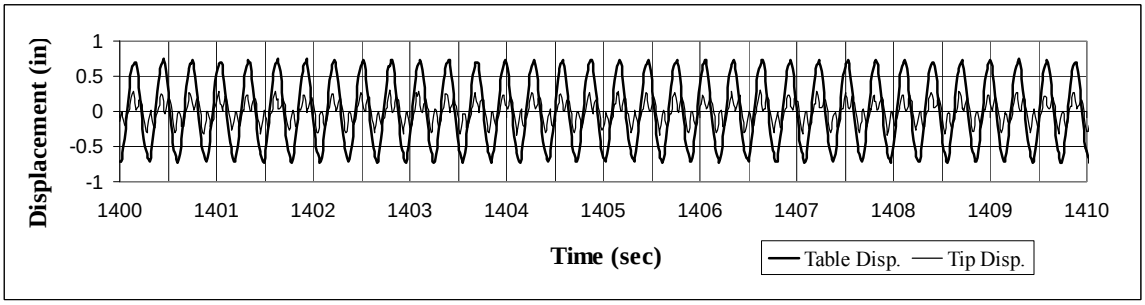
Displacement (in)
1
0.5
0
-0.5
-1
1400 1401 1402 1403 1404 1405 1406 1407 1408 1409 1410
Time (sec)
Table Disp. Tip Disp.

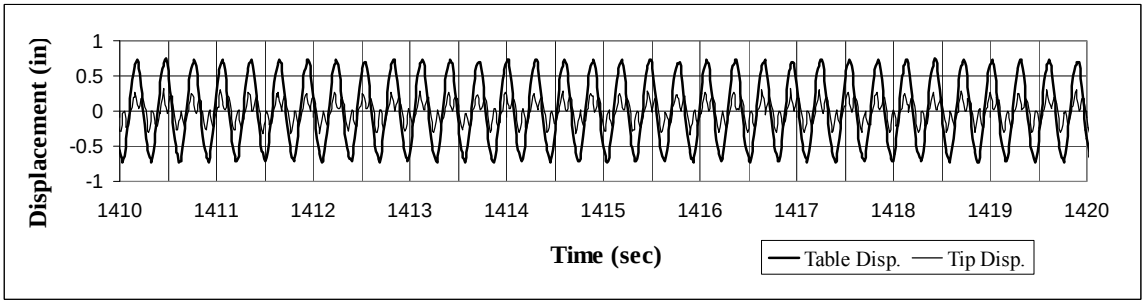
Displacement (in)
1
0.5
0
-0.5
-1
1410 1411 1412 1413 1414 1415 1416 1417 1418 1419 1420
Time (sec)
Table Disp. Tip Disp.

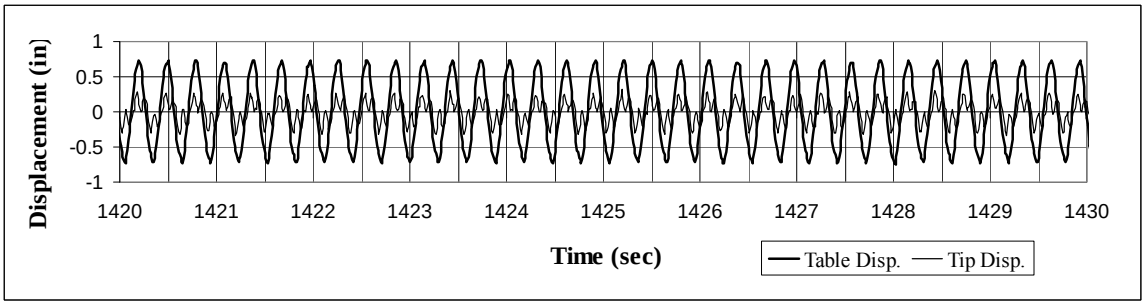
Displacement (in)
1
0.5
0
-0.5
-1
1420 1421 1422 1423 1424 1425 1426 1427 1428 1429 1430
Time (sec)
Table Disp. Tip Disp.

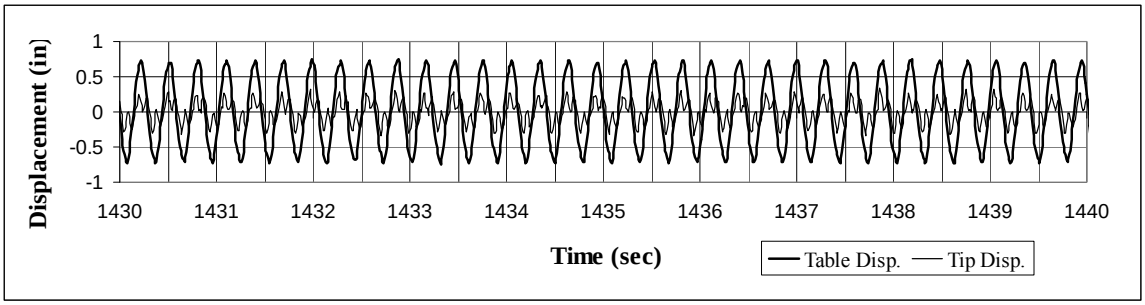
Displacement (in)
1
0.5
0
-0.5
-1
1430 1431 1432 1433 1434 1435 1436 1437 1438 1439 1440
Time (sec)
Table Disp. Tip Disp.

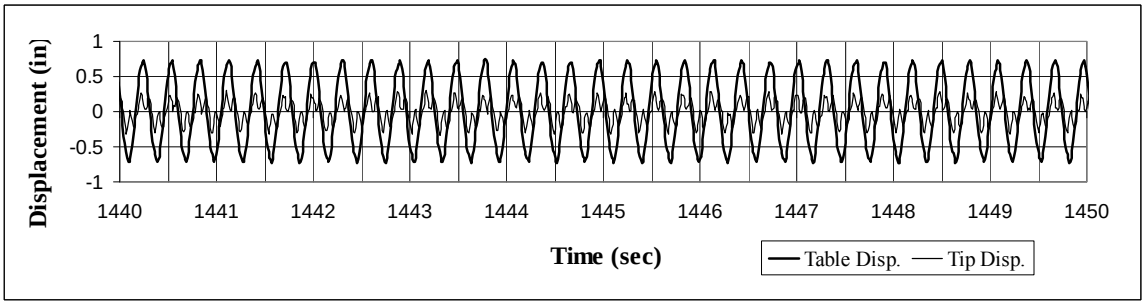
Displacement (in)
1
0.5
0
-0.5
-1
1440 1441 1442 1443 1444 1445 1446 1447 1448 1449 1450
Time (sec)
Table Disp. Tip Disp.

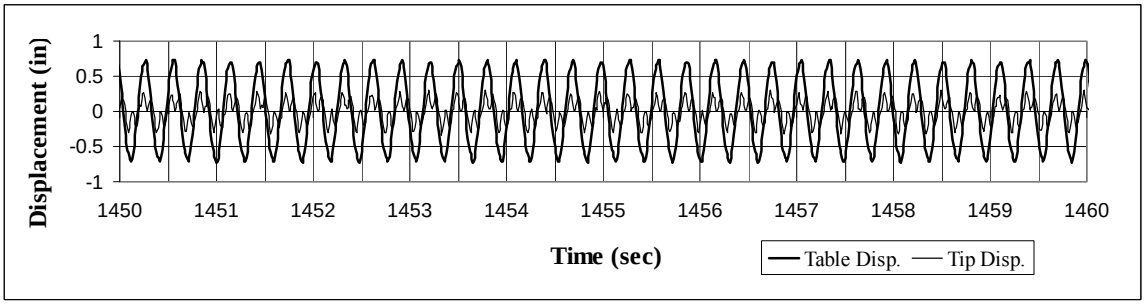
Displacement (in)
1
0.5
0
-0.5
-1
1450 1451 1452 1453 1454 1455 1456 1457 1458 1459 1460
Time (sec)
Table Disp. Tip Disp.

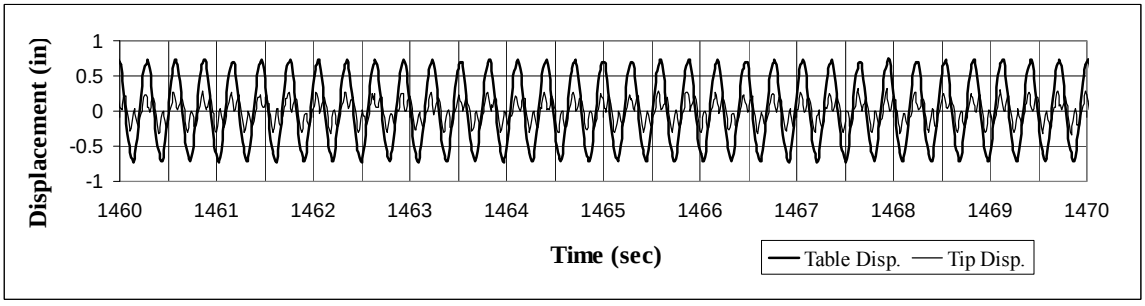
Displacement (in)
1
0.5
0
-0.5
-1
1460 1461 1462 1463 1464 1465 1466 1467 1468 1469 1470
Time (sec)
Table Disp. Tip Disp.

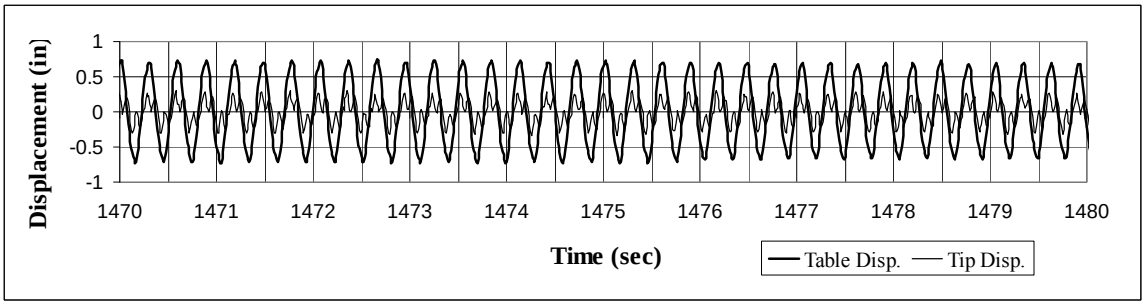
Displacement (in)
1
0.5
0
-0.5
-1
1470 1471 1472 1473 1474 1475 1476 1477 1478 1479 1480
Time (sec)
Table Disp. Tip Disp.